Petroleum Engineering 620 — Fluid Flow in Petroleum Reservoirs
Fundamental Flow Lecture 3 — Material Balance Concepts

Art disturbs, science reassures...
— Georges Braque (1963)

Topic: Material Balance Concepts

Objectives:

- Be able to identify and apply the material balance relations for gas and compressible liquid systems:
  - General Form: (any material balance relation)
    - $q \propto c\frac{d}{dt}[f(p)]$ ($f(p)$= some function of pressure (*e.g.*, $\bar{p}$, $\bar{p}/\bar{z}$, etc.)
  - Gas Material Balance Equations:
    - Dry Gas Case: $\frac{\bar{p}}{\bar{z}}=\frac{p_i}{z_i}\left[1-\frac{G_p}{G}\right]$ (No Influx)
    - General Material Balance Formulation (from Dake[1]): General Form

Withdrawal (rcf)	=	Gas Expansion (rcf)	+	Water Expansion & Pore Compaction (rcf)	+	Water Influx (rcf)

$$G_pB_g+W_pB_w = G(B_g-B_{gi}) + GB_{gi}\frac{(c_wS_{wi}+c_f)}{1-S_{wi}}(p_i-\bar{p}) + W_eB_w$$

    - General Material Balance Formulation (from Dake[1]): $\bar{p}/\bar{z}$ form

$$\frac{\bar{p}}{\bar{z}}=\frac{p_i}{z_i}\left[\frac{1}{1-\frac{(c_wS_{wi}+c_f)}{1-S_{wi}}(p_i-\bar{p})-\frac{(W_e-W_p)B_w}{GB_{gi}}}\right]\left[1-\frac{G_p}{G}\right]$$

  - Oil Material Balance Equations:
    - Constant Compressibility Case: Oil above the Bubble-Point Pressure

$$(p_i-\bar{p})=\frac{1}{Nc_t}\frac{B_o}{B_{oi}}N_p$$

    - Solution Gas Drive Case (from Dake[1]):

$$N_p\left[B_o+(R_p-R_s)B_g\right]+W_pB_w= \quad \text{(Withdrawal (RB))}$$

$$N\left[(B_o-B_{oi})+(R_{si}-R_s)B_g\right] \quad \text{(Oil Expansion (RB))}$$

$$+mNB_{oi}\left[\frac{B_g}{B_{gi}}-1\right] \quad \text{(Gas Cap Expansion (RB))}$$

$$+(1+m)NB_{oi}\frac{(c_wS_{wi}+c_f)}{1-S_{wi}}(p_i-\bar{p}) \quad \text{(Water Exp./Pore Comp.(RB)}$$

$$+W_eB_w \quad \text{(Water Influx (RB))}$$

Petroleum Engineering 620 — Fluid Flow in Petroleum Reservoirs
Fundamental Flow Lecture 3 — Material Balance Concepts

- Be familiar with and be able to apply the "Havlena-Odeh" formulations of the oil and gas material balance equations.
- Be able to compute the following using Cartesian coordinate plots (and the appropriate material balance relations for each case):
  - The wellbore storage coefficient, C_s,
    - $p_{wf} = p_i - \frac{q_{sur}B}{24\,C_s}t$ (p_{wf} vs. t, Drawdown tests)
    - $p_{ws} = p_{wf}(\Delta t=0) + \frac{q_{sur}B}{24\,C_s}\Delta t$ (p_{ws} vs. Δt, Buildup tests)
  - The oil-in-place, N ("slightly compressible" liquid system)

    Average Pressure Formulation:

    - $\bar{p} = p_i - 5.615\frac{N_pB_o}{\phi hAc_t}$ ($\bar{p}$ vs. N_p)

    Wellbore Pressure Formulation:

    - $\frac{p_i - p_{wf}}{q} = b_{pss} + \frac{1}{Nc_t}\frac{B_o}{B_{oi}}\frac{N_p}{q}$ ($\frac{p_i - p_{wf}}{q}$ vs. $\frac{N_p}{q}$)

    or, for a constant flowrate, q, we have

    - $p_{wf} = p_i - qb_{pss} - 0.23395\frac{qB_o}{\phi hAc_t}t$ (p_{wf} vs. t, t in hours)
  - The gas-in-place, G, for a dry gas system
    - $\frac{\bar{p}}{\bar{z}} = \frac{p_i}{z_i}\left[1 - \frac{G_p}{G}\right] = \frac{p_i}{z_i} - \frac{p_i}{z_iG}G_p$ ($\bar{p}/\bar{z}$ vs. G_p)

Lecture Outline:

- Material Balance Relations:
  - Derivation of material balance relations (see attached notes and Dake[1])
  - Oil material balance equation: ($\bar{p}$=psia, p_i=psia, N_p=STB, N=STB, c_t=psia^{-1}, B_o=RB/STB, ϕ=fraction, h=ft, A=reservoir drainage area, ft^2)

    $\bar{p} = p_i - 5.615\frac{N_pB_o}{\phi hAc_t}$ and $N = \frac{\phi hA}{5.615B_{oi}}$, which gives $\bar{p} = p_i - \frac{N_p}{Nc_t}\frac{B_o}{B_{oi}}$.
  - Gas material balance equation: ($\bar{p}$=psia, p_i=psia, $\bar{z}$, z_i=dimensionless, G_p=MSCF, G=MSCF, B_g=RB/MSCF, ϕ=fraction, h=ft, A=reservoir drainage area, ft^2)

    $\frac{\bar{p}}{\bar{z}} = \frac{p_i}{z_i}\left[1 - \frac{G_p}{G}\right] = \frac{p_i}{z_i}\left[1 - 5.615\frac{G_pB_g}{\phi hA}\right]$ where $B_g = 5.02\frac{zT}{p}$, T in °R

Petroleum Engineering 620 — Fluid Flow in Petroleum Reservoirs
Fundamental Flow Lecture 3 — Material Balance Concepts

Lecture Outline: (Continued)

- Wellbore Storage Material Balance Equation:
  - The fundamental material balance equation for wellbore storage is given as:
    - $q_{sf} = q_{sur} + \frac{24C_s}{B}\left[\frac{dp_w}{dt} - \frac{dp_{tbg}}{dt}\right]$ (q_{sf} = sandface rate, q_{sur} = surface rate)
  - Assuming q_{sf} =0 and p_{tbg}=constant, then integrating, we obtain the material balance relation for the *Wellbore Storage Domination* flow regime. In this case all fluid is either produced from (drawdown) or into (buildup) the wellbore.
    - $p_{wf} = p_i - m_{wbs}\, t$ (p_{wf} vs. t, Drawdown tests)
    - $p_{ws} = p_{wf}(\Delta t=0) + m_{wbs}\, \Delta t$ (p_{ws} vs. Δt, Buildup tests)

    where
    - $m_{wbs} = \frac{q_{sur}B}{24\, C_s}$ (p_{wf} vs. t, Drawdown tests)

    and the wellbore storage coefficient terms (C_s variables) are given by:
    - $C_s = V_{wb}c_{wb}$ for a wellbore filled with a compressible fluid
    - $C_s = \frac{144\, A_{wb}}{5.615\, \rho}\frac{g}{g_c}$ for a wellbore with a rising or failing liquid level
- Equation for Boundary-Dominated (or Pseudosteady-State) Flow
  - The material balance equation for this case is given as:
    - $\bar{p} = p_i - 5.615\frac{N_p B_o}{\phi h A c_t}$ (for q constant, N_p=qt)
  - The so-called "pseudosteady-state flow equation" is: (without derivation)
    - $\bar{p} = p_{wf} + qb_{pss}$

    where
    - $b_{pss} = 141.2\frac{\mu B_o}{kh}\left[\ln\left[\frac{r_e}{r_w}\right] - \frac{3}{4} + s\right]$ (for a circular reservoir)

    and
    - $b_{pss} = 141.2\frac{\mu B_o}{kh}\left[\frac{1}{2}\ln\left[\frac{4}{e^{\gamma}C_A}\frac{A}{r_w^2}\right] + s\right]$ (general reservoir (γ=0.577216...))
  - Combining the material balance and pseudosteady-state flow equations gives
    - $\frac{p_i - p_{wf}}{q} = b_{pss} + \frac{1}{Nc_t}\frac{B_o}{B_{oi}}\frac{N_p}{q}$
  - For a constant flowrate, q, the above relation becomes
    - $p_{wf} = p_i - qb_{pss} - 0.23395\frac{qB_o}{\phi h A c_t}t$

    or writing more compactly, we have
    - $p_{wf} = p_{int} - m_{pss}t$, where $m_{pss} = 0.23395\frac{qB_o}{\phi h A c_t}$ and $p_{int} = p_i - qb_{pss}$.

Petroleum Engineering 620 — Fluid Flow in Petroleum Reservoirs
Fundamental Flow Lecture 3 — Material Balance Concepts

References:

1. Dake, L.P.: "*The Practice of Reservoir Engineering*," Elsevier Scientific Publishing Company, 1994 (Chapters 3 and 6).

Reading Assignment:

- Review attached handout notes
  - Appendix A—Development of Material Balance Time Concept
    - Johnston, J.L.: *Variable Rate Analysis of Transient Well Test Data using Semi-Analytical Methods*, M.S. Thesis, Texas A&M University, (August 1992).
  - Appendix A—Development and Use of the Material Balance Time for Boundary Dominated-Liquid Flow
    - Palacio, J.C. and Blasingame, T.A.: "Decline Curve Analysis Using Type Curves—Analysis of Gas Well Production Data," paper SPE 25909 presented at the 1993 Joint Rocky Mountain Regional/Low Permeability Reservoirs Symposium, Denver, CO, 26-28 April 1993.
  - Appendix B—Development, Proof and Use of the Material Balance Pseudotime for Boundary-Dominated Gas Flow
    - Palacio, J.C. and Blasingame, T.A.: "Decline Curve Analysis Using Type Curves—Analysis of Gas Well Production Data," paper SPE 25909 presented at the 1993 Joint Rocky Mountain Regional/Low Permeability Reservoirs Symposium, Denver, CO, 26-28 April 1993.
- Review attached handout notes—"Derivation of Material Balance Relations"
  - Reservoir Oils
    - Undersaturated oil reservoir case ($p>p_b$).
    - Saturated oil reservoir case ($p<p_b$).
  - Natural Gases
    - General case (includes water expansion/pore compaction and water influx).
    - Dry gas case.
- Review attached papers:
  - West, R.D.: "Extensions of the Muskat Depletion Performance Equation," ***Trans.*** AIME, Vol. **213** (1958), 285-291.
  - Havlena, D. and Odeh, A.S.: "The Material Balance as an Equation of a Straight-Line," *JPT* (Aug. 1963), 896-900.
  - Havlena, D. and Odeh, A.S.: "The Material Balance as an Equation of a Straight-Line—Part II, Field Cases," *JPT* (July 1964),815-822.
  - Humphreys, N.V.: "The Material Balance Equation for a Gas Condensate Reservoir With Significant Water Production," paper SPE 21514 presented at the SPE Gas Technology Symposium, Houston, June 23-24, 1991.
  - Fetkovich, M.J., Reese, D.E., and Whitson, C.H.: "Application of a General Material Balance for High-Pressure Gas Reservoirs," *SPEJ*, (March 1998), 3-13.

(Appendix A)

Derivation of "Material Balance" Time (Liquid Flow Case)

From:

Johnston, J.L.: *Variable Rate Analysis of Transient Well Test Data using Semi-Analytical Methods*, M.S. Thesis, Texas A&M University, (August 1992).

From: Johnston, J.L.: *Variable Rate Analysis of Transient Well Test Data using Semi-Analytical Methods*, M.S. Thesis, Texas A&M University, (August 1992).

APPENDIX A

DEVELOPMENT OF MATERIAL BALANCE TIME CONCEPT

In this appendix, we present the pseudosteady-state flow equation for slightly compressible liquids derived from a material balance relation. This derivation rigorously illustrates the necessity for using the material balance time function, t_{mb}, for pseudosteady-state flow.

In words, a material balance based on the amount of oil in a reservoir is given by

Amount of oil originally in reservoir	=	Amount of oil in reservoir at a later time	+	Change in hydrocarbon pore volume due to rock and water expansion.

This can be expressed mathematically as

$$NB_{oi} = (N - N_p)B_o + \Delta V_r + \Delta V_w \quad \cdots\cdots (A\text{-}1)$$

We can express the change in rock and water volume in terms of formation and water compressibility respectively. The general definition of isothermal compressibility is

$$c = -\frac{1}{V}\left[\frac{\partial V}{\partial p}\right]_T$$

We can calculate the slope, $\frac{\partial V}{\partial p}$, by approximating the tangent to the curve (volume versus pressure) by a chord slope, *i.e.*

$$c \approx -\frac{1}{V_i}\left[\frac{V - V_i}{p - p_i}\right]$$

and rearranging this equation to obtain an expression for change in volume gives

$$\Delta V \approx -\, c\, V_i (p - p_i) \quad \cdots\cdots (A\text{-}2)$$

Since the initial volume for rock is the initial pore volume, V_{pi}, Eq. (A-2) can be used to express change in rock volume as

$$\Delta V_r = -\, c_f V_{pi} (p - p_i) \quad \cdots\cdots (A\text{-}3)$$

and since the initial volume for water is given by $V_{pi}S_{wi}$, the change in water volume is

$$\Delta V_w = -\, c_w V_{wi} (p - p_i) = -\, c_w V_{pi} S_{wi} (p - p_i) \quad \cdots\cdots (A\text{-}4)$$

Combining Eqs. (A-3) and (A-4) gives

$$\Delta V_r + \Delta V_w = -\, c_f V_{pi} (p - p_i) - c_w V_{pi} S_{wi} (p - p_i)$$

Grouping terms condenses this equation to

$$\Delta V_r + \Delta V_w = - (c_w S_{wi} + c_f) V_{pi} (p - p_i) \quad \text{(A-5)}$$

We can now substitute Eq. (A-5) into Eq. (A-1), giving

$$N B_{oi} = (N - N_p) B_o - (c_w S_{wi} + c_f) V_{pi} (p - p_i) \quad \text{(A-6)}$$

The original oil in place in reservoir volumes, $N B_{oi}$, can be expressed in terms of pore volume and initial water saturation

$$N B_{oi} = V_{pi} (1 - S_{wi})$$

or

$$V_{pi} = \frac{N B_{oi}}{(1 - S_{wi})} \quad \text{(A-7)}$$

We can substitute Eq. (A-7) for the pore volume term in Eq. (A-6), giving

$$N B_{oi} = (N - N_p) B_o - (c_w S_{wi} + c_f) \frac{N B_{oi}}{(1 - S_{wi})} (p - p_i) \quad \text{(A-8)}$$

We assume the pressure, p, represents the average pressure , $\bar{p}$, in our volumetric system. Rearranging Eq. (A-8) gives

$$N B_{oi} = (N - N_p) B_o + (c_w S_{wi} + c_f) \frac{N B_{oi}}{(1 - S_{wi})} (p_i - \bar{p})$$

or, grouping terms containing N on the left-hand side of the equation, we have

$$N (B_{oi} - B_o) = - N_p B_o + (c_w S_{wi} + c_f) \frac{N B_{oi}}{(1 - S_{wi})} (p_i - \bar{p}) \quad \text{(A-9)}$$

We can express the change in oil volume, $B_{oi} - B_o$, in terms of the isothermal compressibility of oil, c_o. Recall that the definition of c_o is

$$c_o = - \frac{1}{B_o} \left[\frac{\partial B_o}{\partial p} \right]_T$$

As before, we can calculate the slope, $\frac{\partial B_o}{\partial p}$, by approximating the tangent to the curve (formation volume factor versus pressure) by a chord slope, *i.e.*

$$c_o \approx - \frac{1}{B_{oi}} \left[\frac{B_o - B_{oi}}{p - p_i} \right]$$

Rearranging this equation gives the following expression for the change in oil volume, $B_{oi} - B_o$

$$B_o - B_{oi} = - c_o B_{oi} (p - p_i) = c_o B_{oi} (p_i - \bar{p}) \quad \text{(A-10)}$$

We can now substitute Eq. (A-10) into Eq. (A-9) for the change in oil volume, $B_{oi} - B_o$

$$- N c_o B_{oi} (p_i - \bar{p}) = - N_p B_o + (c_w S_{wi} + c_f) \frac{N B_{oi}}{(1 - S_{wi})} (p_i - \bar{p})$$

which can be rearranged to give

$$N_p B_o = N c_o B_{oi} (p_i - \bar{p}) + (c_w S_{wi} + c_f) \frac{N B_{oi}}{(1 - S_{wi})} (p_i - \bar{p})$$

$$N_p B_o = N B_{oi} (p_i - \bar{p}) \left[c_o + \frac{(c_w S_{wi} + c_f)}{(1 - S_{wi})} \right]$$

or finally,

$$N_p B_o = \frac{N B_{oi}}{(1 - S_{wi})} (p_i - \bar{p}) [c_o (1 - S_{wi}) + c_w S_{wi} + c_f] \quad \text{.....(A-11)}$$

If we use the expression derived by Perrine[1] and Martin[2] for total system compressibility, c_t,

$$c_t = c_o (1 - S_{wi}) + c_w S_{wi} + c_f \equiv c_o S_{oi} + c_w S_{wi} + c_f \quad \text{.....(A-12)}$$

we can simplify Eq. (A-11) and write

$$N_p B_o = \frac{N B_{oi}}{(1 - S_{wi})} c_t (p_i - \bar{p}) \quad \text{.....(A-13)}$$

Recall that

$$V_{pi} = \frac{N B_{oi}}{(1 - S_{wi})} \quad \text{.....(A-7)}$$

therefore,

$$N_p = \frac{V_{pi}}{B_o} c_t (p_i - \bar{p}), \text{ where } V_{pi} = \phi h A \text{ , so we can write}$$

$$N_p = \frac{\phi h A}{B_o} c_t (p_i - \bar{p})$$

Rearranging gives

$$(p_i - \bar{p}) \frac{h}{B_o} = \frac{N_p}{\phi c_t A}$$

Multiply through by $\frac{2\pi k}{q\mu}$ to obtain

$$(p_i - \bar{p}) \frac{2\pi k h}{q B_o \mu} = \frac{2\pi k}{\phi \mu c_t A} \frac{N_p}{q} \quad \text{.....(A-14)}$$

The definitions of dimensionless pressure, p_D, and dimensionless time based on drainage area, t_{AD} are

$$p_D = \frac{2\pi k h}{q B_o \mu} (p_i - p_{wf}) \quad \text{.....(A-15)}$$

and

$$t_{AD} = \frac{kt}{\phi\mu c_t A} \quad \text{.....(A-16)}$$

Therefore, if we define a material balance time as $t_{mb}=N_p/q$, Eq. (A-16) becomes

$$2\pi t_{AD,mb} = \frac{2\pi k}{\phi\mu c_t A}\frac{N_p}{q} \quad \text{.....(A-17)}$$

We can now substitute Eq (A-17) into Eq. (A-14) to obtain

$$(p_i - \overline{p})\frac{2\pi kh}{qB_o\mu} = 2\pi t_{AD,mb} \quad \text{.....(A-18)}$$

Eq. A-18 is valid for all flow regimes (transient or pseudosteady-state). We can couple this relationship for $(p_i - \overline{p})$ with the general relationship for $(\overline{p} - p_{wf})$ derived by Camacho[3], which is valid for pseudosteady-state flow and which is given below

$$(\overline{p} - p_{wf})\frac{2\pi kh}{qB_o\mu} = \frac{1}{2}\ln\left[\frac{4}{e^{\gamma}}\frac{A}{C_A r_w^2}\right] + s \quad \text{.....(A-19)}$$

Adding Eqs. A-18 and A-19 eliminates $\overline{p}$, giving

$$(p_i - p_{wf})\frac{2\pi kh}{qB_o\mu} = 2\pi t_{AD,mb} + \frac{1}{2}\ln\left[\frac{4}{e^{\gamma}}\frac{A}{C_A r_w^2}\right] + s \quad \text{.....(A-20)}$$

Substituting the definition of dimensionless pressure, Eq. (A-15), into Eq. (A-20) gives the dimensionless form of the pseudosteady-state flow solution to the diffusivity equation,

$$p_D = 2\pi t_{AD,mb} + \frac{1}{2}\ln\left[\frac{4}{e^{\gamma}}\frac{A}{C_A r_w^2}\right] + s \quad \text{.....(A-21)}$$

This validates the use of the material balance time function, t_{mb}, for pseudosteady-state flow.

REFERENCES used in APPENDIX A

1. Perrine, R.L.: "Analysis of Pressure Buildup Curves," *Drill. and Prod. Prac.*, API, Dallas(1956) 482-509.
2. Martin, J.C.: "Simplified Equations of Flow in Gas Drive Reservoirs and the Theoretical Foundation of Multiphase Pressure Buildup Analyses," *Trans.* AIME(1959) **216**, 309-311.
3. Camacho-V., R.G.: *Well Performance Under Solution Gas Drive*, Ph.D. Dissertation, University of Tulsa, Tulsa, OK (1987).

(Appendix A)

Development and Use of the Material Balance Time for Boundary-Dominated Liquid Flow

From:

Palacio, J.C. and Blasingame, T.A.: "Decline Curve Analysis Using Type Curves—Analysis of Gas Well Production Data," paper SPE 25909 presented at the 1993 Joint Rocky Mountain Regional/Low Permeability Reservoirs Symposium, Denver, CO, 26-28 April 1993.

From: Palacio, J.C. and Blasingame, T.A.: "Decline Curve Analysis Using Type Curves--Analysis of Gas Well Production Data," paper SPE 25909 presented at the 1993 Joint Rocky Mountain Regional/Low Permeability Reservoirs Symposium, Denver, CO, 26-28 April 1993.

APPENDIX A

DEVELOPMENT AND USE OF THE MATERIAL BALANCE TIME FOR BOUNDARY-DOMINATED LIQUID FLOW

DEVELOPMENT

The original material balance approach for boundary-dominated flow (*i.e.*, pseudosteady-state) was developed by Blasingame and Lee,[1] and the following derivation builds upon their developments.

From the definition of liquid compressibility, the following material balance can be derived

$$q_o = -\frac{A\phi h c_t}{5.615 B_o}\frac{d\bar{p}}{dt} \quad \text{..... (A-1)}$$

Since we are considering the single-phase liquid case, the total compressibility, c_t, is assumed to be constant. Therefore, the integration of Eq. A-1 yields

$$\int_0^t q_o\,dt = -\frac{A\phi h c_t}{5.615 B_o}\int_{p_i}^{\bar{p}} d\bar{p}$$

Completing the integration, we have

$$N_p = \frac{A\phi h c_t}{5.615 B_o}(p_i - \bar{p})$$

Solving this relation for the pressure difference, it follows that

$$(p_i - \bar{p}) = \frac{5.615 N_p B_o}{A\phi h c_t} = \frac{1}{N c_t}\frac{B_o}{B_{oi}} N_p \quad \text{..... (A-2)}$$

where Eq. A-2 can also be rearranged to yield

$$(p_i - \bar{p})\frac{h}{B_o} = \frac{5.615 N_p}{A\phi c_t}$$

multiplying through by $\dfrac{k_o}{141.2 q_o \mu_o}$ gives

$$(p_i - \bar{p})\frac{k_o h}{141.2 q_o B_o \mu_o} = \frac{5.615 k_o}{141.2 \phi \mu_o c_t A}\frac{N_p}{q_o}$$

Defining the material balance time function, $\bar{t} = \dfrac{N_p}{q_o}$, it follows that

$$(p_i - \bar{p})\frac{k_o h}{141.2 q_o B_o \mu_o} = \frac{2\pi(0.00633) k_o}{\phi \mu_o c_t A}\bar{t}$$

Redefining the dimensionless time based on drainage area, we have

$$\bar{t}_{DA} = \frac{0.00633 k_o}{\phi \mu_o c_t A}\bar{t} \quad \text{..... (A-3)}$$

Substituting Eq. A-3 into the pressure relation gives us

$$(p_i - \bar{p})\frac{k_o h}{141.2 q_o B_o \mu_o} = 2\pi \bar{t}_{DA} \quad \text{..... (A-4)}$$

The most important characteristic of Eq. A-4 is that this relation is always valid—regardless of time, flow regime, or production scenario—whether the well experiences constant or variable flowing bottomhole pressures, or constant or variable flowrate. This is due to the fact that Eq. A-4 is derived directly from material balance relations and is exact.

It has been shown[2] that for a constant production rate of single-phase liquid, the flow equation for the pressure response under boundary dominated flow can be written as

$$(\bar{p} - p_{wf})\frac{k_o h}{141.2 q_o B_o \mu_o} = \frac{1}{2}\ln\left[\frac{4}{e^{\gamma}}\frac{A}{C_A r_w'^2}\right] \quad \text{..... (A-5)}$$

Although Eq. A-5 was derived for the constant rate case (variable p_{wf}), this relation has been shown[1] to yield a very good approximation for the case where the flowing bottomhole pressure is constant.

The substitution of Eqs. A-4 and A-5 yields

$$(p_i - p_{wf})\frac{k_o h}{141.2 q_o B_o \mu_o} = 2\pi t_{DA} + \frac{1}{2}\ln\left[\frac{4}{e^{\gamma}}\frac{A}{C_A r_w'^2}\right] \quad \text{..... (A-6)}$$

The previous considerations *imply* that Eq. A-6 is valid for the pseudosteady-state flow regime—for any rate or pressure profile. Substituting Eq. A-3 into A-6 gives the following

$$\frac{(p_i - p_{wf})}{q_o} = mt + b_{pss} \quad \text{..... (A-7)}$$

where

$$m = \frac{2\pi(0.00633)k_o}{\phi\mu_o c_t A}\frac{141.2 B_o \mu_o}{k_o h} = \frac{5.615 B_o}{\phi h c_t A} = \frac{1}{N c_t}\frac{B_o}{B_{oi}} \quad \text{..... (A-8)}$$

and

$$b_{pss} = 141.2\frac{B_o \mu_o}{k_o h}\left[\frac{1}{2}\ln\left[\frac{4}{e^{\gamma}}\frac{A}{C_A r_w'^2}\right]\right] \quad \text{..... (A-9)}$$

Rearranging Eq. A-7, we obtain our final form for behavior of a well producing a variable-rate profile during pseudosteady-state (or boundary dominated) flow conditions. This result is given by

$$\frac{q_o}{(p_i - p_{wf})} b_{pss} = \frac{1}{1 + \left[\frac{m}{b_{pss}}\right]\bar{t}} \quad \text{.....(A-10)}$$

USE

The group on the left-hand-side (LHS) of Eq. A-10 is exactly the dimensionless decline rate variable, q_{Dd}, as presented by Fetkovich.[3,4] The second term in the denominator of the right-hand-side (RHS) group in the same equation is defined as, $\bar{t}_{Dd}$, therefore

$$\bar{t}_{Dd} = \left[\frac{m}{b_{pss}}\right]\bar{t} = \frac{2\pi \bar{t}_{DA}}{\frac{1}{2}\ln\left[\frac{4}{e^{\gamma}}\frac{A}{C_A r_w'^2}\right]} + W_e B_w \quad \text{.....(A-11)}$$

The only difference between $\bar{t}_{Dd}$ and the Fetkovich[3,4] dimensionless decline time function, t_{Dd}, is that material balance time, $\bar{t}$, is substituted for production time, t. Fetkovich assumed a circular reservoir, the denominator on the RHS of Eq. A-11 is given by $\ln\left[\frac{r_e}{r_w}\right]-\frac{3}{4}$ which results from using the appropriate C_A value for a circular reservoir. However, Fetkovich actually chose to use 1/2 rather than 3/4 within the argument of the logarithm, as he obtain a better correlation of q_{Dd}-t_{Dd} trends.

Regardless, Eq. A-10 can be reduced to

$$q_{Dd}=\frac{1}{1+\bar{t}_{Dd}} \qquad \text{.....(A-12)}$$

Eq. A-12 is a harmonic decline type of equation where the decline exponent is unity. This is evident by comparing Eq. A-12 to Arps[5] original definition of a hyperbolic decline which in dimensionless form is

$$q_{Dd}=\frac{1}{(1+bt_{Dd})^{1/b}} \qquad \text{.....(A-13)}$$

When the decline exponent, b, is taken as unity in the Arps[5] equations we call this a harmonic decline. Given b=1, Eqs. A-12 and A-13 have exactly the same form.

Therefore if $\bar{t}$ is correctly calculated, a scaled log-log plot of $\frac{q_o}{(p_i-p_{wf})}$ versus $\bar{t}$ will overlay the q_{Dd} versus $\bar{t}_{Dd}$ trend for a *harmonic decline* on Fetkovich's[3,4] type curve. Once the match has been obtained, the "match point" relations for m , b_{pss}, and N are:

$$b_{pss}=\frac{[q_{Dd}]_{MP}}{\left[\frac{q_o}{(p_i-p_{wf})}\right]_{MP}} \qquad \text{.....(A-14)}$$

$$m=\frac{1}{Nc_t}\frac{B_o}{B_{oi}}=b_{pss}\frac{[t_{Dd}]_{MP}}{[\bar{t}]_{MP}} \qquad \text{.....(A-15)}$$

$$N=\frac{1}{c_{ti}}\frac{B_o}{B_{oi}}\frac{[\bar{t}]_{MP}}{[t_{Dd}]_{MP}}\frac{\left[\frac{q_o}{(p_i-p_{wf})}\right]_{MP}}{[q_{Dd}]_{MP}} \qquad \text{.....(A-16)}$$

where MP denotes a match point value.

REFERENCES used in APPENDIX B

1. Blasingame, T.A. and Lee, W.J.: "The Variable-Rate Reservoir Limits Testing," paper SPE 15028 presented at the SPE Permian basin Oil & Gas Recovery Conference, Midland, March 13-14, 1986.
2. Dake, L.P.: "*Fundamentals of Reservoir Engineering*," Elsevier Scientific Publishing Company , 1978, 145-150.
3. Fetkovich, M.J.: "Decline Curve Analysis Using Type Curves," *JPT* (June 1980) 1065-77.
4. Fetkovich, M.J., *et al*: "Decline-Curve Analysis Using Type Curves--Case Histories," *SPEFE* (Dec. 1987) 637-56.
5. Arps, J.J.: "Analysis of Decline Curves," ***Trans***. AIME (1945) 160, 228-247.

(Appendix B)

Development, Proof and use of the Material Balance Pseudotime for Boundary-Dominated Gas Flow

From:

Palacio, J.C. and Blasingame, T.A.: "Decline Curve Analysis Using Type Curves—Analysis of Gas Well Production Data," paper SPE 25909 presented at the 1993 Joint Rocky Mountain Regional/Low Permeability Reservoirs Symposium, Denver, CO, 26-28 April 1993.

From: Palacio, J.C. and Blasingame, T.A.: "Decline Curve Analysis Using Type Curves--Analysis of Gas Well Production Data," paper SPE 25909 presented at the 1993 Joint Rocky Mountain Regional/Low Permeability Reservoirs Symposium, Denver, CO, 26-28 April 1993.

APPENDIX B

DEVELOPMENT, PROOF AND USE OF THE MATERIAL BALANCE PSEUDOTIME FOR BOUNDARY-DOMINATED GAS FLOW

DEVELOPMENT

Blasingame and Lee[1] proposed a gas flow equation based on a modified pseudotime function to model the general variable-rate/variable pressure drop gas flow case. This was done on an empirical basis using numerical simulation as validation.

Analytical proofs are given below to provide the theoretical background for the modified gas flow equation proposed by Blasingame and Lee. Beginning with the material balance equation for a liquid, we have:

$$\frac{(p_i - p_{wf})}{q_o} = \frac{1}{Nc_t}\frac{B_o}{B_{oi}}\frac{N_p}{q_o} = \frac{1}{Nc_t}\frac{B_o}{B_{oi}}\bar{t} \quad \text{..... (B-1)}$$

Blasingame and Lee proposed a relation similar in form to Eq. B-1 for the gas flow case, this result is given by:

$$\frac{(p_{pi} - \bar{p}_p)}{q_g} = \frac{1}{Gc_t}\bar{t}_a \quad \text{..... (B-2)}$$

Eq. B-2 is *assumed* to be valid when the pseudotime function is defined by

$$\bar{t}_a = \frac{\mu_{gi}c_{ti}}{q_g}\int_0^t \frac{q_g}{\mu_g(\bar{p})c_t(\bar{p})}dt \quad \text{..... (B-3)}$$

The pseudopressure functions in Eq. B-2 are normalized variables,[2] which are defined by

$$p_{pi} = \left[\frac{\mu_{gi}z_i}{p_i}\right]\int_{p_{base}}^{p_i}\frac{p}{\mu_g z}dp$$

and

$$\bar{p}_p = \left[\frac{\mu_{gi}z_i}{p_i}\right]\int_{p_{base}}^{\bar{p}}\frac{p}{\mu_g z}dp$$

The pseudosteady-state gas flow equation (given by Al Hussainy, *et al.*[3,4]) is given by:

$$\frac{(\bar{p}_p - p_{pwf})}{q_g} = 141.2\frac{\mu_{gi}B_{gi}}{k_g h}\left[\frac{1}{2}\ln\left[\frac{4}{e^{\gamma}}\frac{A}{C_A r_w'^2}\right]\right] \quad \text{..... (B-4)}$$

The addition of Eqs. B-3 and B-4 yields the following generalized relation for the variable-rate flow of gas in a reservoir during boundary-dominated flow conditions. This result is:

$$\frac{\Delta p_p}{q_g} = m_a\bar{t}_a + b_{a,pss} \quad \text{..... (B-5)}$$

where

$$\Delta p_p=(p_{pi}-p_{pwf}) \quad \text{(B-6)}$$

$$m_a=\frac{1}{Gc_{ti}} \quad \text{(B-7)}$$

$$b_{a,pss}=141.2\frac{\mu_{gi}B_{gi}}{k_g h}\left[\frac{1}{2}\ln\left[\frac{4}{e^{\gamma}}\frac{A}{C_A r_w'^2}\right]\right] \quad \text{(B-8)}$$

PROOF

In this section we will provide the analytical proof of Eq. B-2. This process begins by using the definition of gas compressibility, which is given by:

$$c_g=\frac{1}{\rho_g}\frac{d}{dp}(\rho_g)$$

The density of a real gas is given as:

$$\rho_g=\frac{M}{RT}\frac{p}{z}$$

Substituting the gas density identity into the gas compressibility definition, we obtain:

$$c_g=\frac{1}{\rho_g}\frac{d}{dp}(\rho_g)=\frac{1}{\frac{M}{RT}\frac{p}{z}}\frac{d}{dp}\left[\frac{M}{RT}\frac{p}{z}\right]=\frac{1}{\frac{p}{z}}\frac{d}{dp}\left[\frac{p}{z}\right] \quad \text{(B-9)}$$

Evaluating Eq. B-9 at the average reservoir pressure, then solving for the pressure derivative expression, we have:

$$\frac{d}{d\bar{p}}\left[\frac{\bar{p}}{\bar{z}}\right]=\frac{\bar{p}}{\bar{z}}\bar{c}_g \quad \text{(B-10)}$$

Recalling the gas material balance equation, we have:

$$\frac{\bar{p}}{\bar{z}}=\frac{p_i}{z_i}\left[1-\frac{G_p}{G}\right]$$

Taking the time derivative of the gas material balance equation, then solving for the gas flowrate gives

$$q_g=\frac{dG_p}{d\bar{p}}=-\frac{Gz_i}{p_i}\frac{d}{dt}\left[\frac{\bar{p}}{\bar{z}}\right] \quad \text{(B-11)}$$

Applying the chain rule to Eq. B-11, we obtain

$$q_g=\frac{dG_p}{d\bar{p}}=-\frac{Gz_i}{p_i}\frac{d}{d\bar{p}}\left[\frac{\bar{p}}{\bar{z}}\right]\frac{d\bar{p}}{dt} \quad \text{(B-12)}$$

Substituting Eq. B-10 into Eq. B-12 yields

$$q_g=-\frac{Gz_i}{p_i}\frac{\bar{p}}{\bar{z}}\bar{c}_g\frac{d\bar{p}}{dt} \quad \text{(B-13)}$$

Substituting Eq. B-13 into Eq. B-3, we obtain

$$\bar{t}_a=\frac{\mu_{gi}c_{ti}}{q_g}\left[-\frac{Gz_i}{p_i}\right]\int_0^t\frac{\bar{p}}{\bar{z}}\bar{c}_g\frac{1}{\mu_g\bar{c}_t}\frac{d\bar{p}}{dt}dt \quad \text{(B-14)}$$

We can assume that the formation compressibility is negligible compared to the fluid compressibility (*i.e.*, $\bar{c}_t\cong\bar{c}_g$). Making this assumption, changing the variable of integration from time to pressure, and rearranging terms, Eq. B-14 becomes

$$\bar{t}_a = -\frac{Gc_{ti}}{q_g}\left[\frac{\mu_{gi}z_i}{p_i}\right]\int_{p_i}^{\bar{p}} \frac{\bar{p}}{\mu_g \bar{z}} d\bar{p} \quad \text{.....(B-15)}$$

Recalling the definition of normalized pseudopressure, Eq. B-15 may be re-written as

$$\bar{t}_a = Gc_t \frac{(p_{pi} - \bar{p}_p)}{q_g}$$

where this result can be rearranged to yield

$$\frac{(p_{pi} - \bar{p}_p)}{q_g} = \frac{1}{Gc_t}\bar{t}_a \quad \text{.....(B-16)}$$

Eq. B-16 is identical to Eq. B-2—where this result provides the proof that Eq. B-3 is the exact definition of the pseudotime function for boundary-dominated gas flow.

USE

The pseudopressure-pseudotime relations developed above for the decline curve analysis of gas reservoir systems can also be written as "Fetkovich"-style variables. More specifically, we can rearrange Eq. B-5 to yield:

$$\frac{q_g}{\Delta p_p} b_{a,pss} = \frac{1}{1 + \left[\frac{m_a}{b_{a,pss}}\right]\bar{t}_a} \quad \text{.....(B-17)}$$

Eq. B-17 and the liquid flow relation (Eq. A-10) have identical forms and as such, Eq. B-17 can be written as

$$q_{Dd} = \frac{1}{1 + \bar{t}_{a,Dd}} \quad \text{.....(B-18)}$$

where the dimensionless decline rate function, q_{Dd}, is given by:

$$q_{Dd} = \frac{q_g}{\Delta p_p} b_{a,pss} \quad \text{.....(B-19)}$$

and the dimensionless decline time function, $\bar{t}_{a,Dd}$, is given by:

$$\bar{t}_{a,Dd} = \left[\frac{m_a}{b_{a,pss}}\right]\bar{t}_a \quad \text{.....(B-20)}$$

Eq. B-18 (the gas flow identity) and the liquid flow (Eq. A-12) are identical in form, as is expected—therefore, all of the comments regarding the comparison of Eq. A-12 to the Arps[5] relations (in particular, the harmonic decline case) apply for the gas case as well.

These results prove that when pseudopressure and the material balance pseudotime are used to model gas flow, the data trend *must decline along the harmonic stem* on the Fetkovich[6,7] (liquid flow) type curve. If $\bar{t}_a$ is correctly calculated, then a scaled log-log plot of $q_g/(p_{pi} - p_{pwf})$ versus $\bar{t}_a$ will overlay the q_{Dd} versus t_{Dd} trend on the Fetkovich[6,7] type curve—exactly on the b=1 stem.

The "match point" relations are used to estimate the gas-in-place and formation properties are given by:

$$b_{a,pss}=\frac{\left[q_{Dd}\right]_{\mathrm{MP}}}{\left[\dfrac{q_g}{(p_{pi}-p_{pwf})}\right]_{\mathrm{MP}}} \quad \text{.....(B-21)}$$

$$m_a=\frac{1}{Gc_{ti}}=b_{a,pss}\frac{\left[t_{Dd}\right]_{\mathrm{MP}}}{\left[\bar{t}_a\right]_{\mathrm{MP}}} \quad \text{.....(B-22)}$$

$$G=\frac{1}{c_{ti}}\frac{\left[\bar{t}_a\right]_{\mathrm{MP}}}{\left[t_{Dd}\right]_{\mathrm{MP}}}\frac{\left[\dfrac{q_g}{(p_{pi}-p_{pwf})}\right]_{\mathrm{MP}}}{\left[q_{Dd}\right]_{\mathrm{MP}}} \quad \text{.....(B-23)}$$

where MP denotes a match point value.

REFERENCES used in APPENDIX B

1. Blasingame, T.A- and Lee, W.J.: "The Variable-Rate Reservoir Limits Testing of Gas Wells," paper SPE 17708 presented at the 1988 SPE Gas Technology Symposium, Dallas, TX, June 13-15, 1988.
2. Meunier, D.F., Kabir, C.S., Wittmann, M.J.: "Gas Well Test Analysis: Use of Normalized Pseudovariables," *SPEFE* (Dec. 1987) 629-636.
3. Al-Hussainy, R., Ramey, H.J. Jr. and Crawford, P.B. : "The Flow of Real Gases through Porous Media," *JPT* (May 1966) 624-636; ***Trans.*** AIME, **237**.
4. Al-Hussainy, R. and Ramey, H.J. Jr. : "Application of Real Gas Flow Theory to Well Testing and Deliverability Forecasting," *JPT* (May 1966) 637-642; ***Trans.*** AIME, **237**.
5. Arps, J.J.: "Analysis of Decline Curves," ***Trans.*** AIME (1945) 160, 228-247.
6. Fetkovich, M.J.: "Decline Curve Analysis Using Type Curves," *JPT* (June 1980) 1065-77.
7. Fetkovich, M.J., *et al*: "Decline-Curve Analysis Using Type Curves--Case Histories," *SPEFE* (Dec. 1987) 637-56.

Material Balance Notes

(from Department of Petroleum Engineering Course Notes — 1984)

- Black Oil Cases
  - Undersaturated Oil
  - Solution Gas Drive
- Dry Gas Case

Petroleum Engineering 620
Fluid Flow in Reservoirs

VOLUMETRIC OIL RESERVOIRS

I. UNDERSATURATED RESERVOIR

OBJECTIVE: TO DERIVE A MATERIAL BALANCE EQUATION FOR AN UNDERSATURATED RESERVOIR

A. ASSUMPTIONS

1. $P > P_B$
2. NO ORIGINAL OR FINAL GAS CAP
3. NO WATER INFLUX OR PRODUCTION

B. DERIVATION OF MATERIAL BALANCE EQUATION

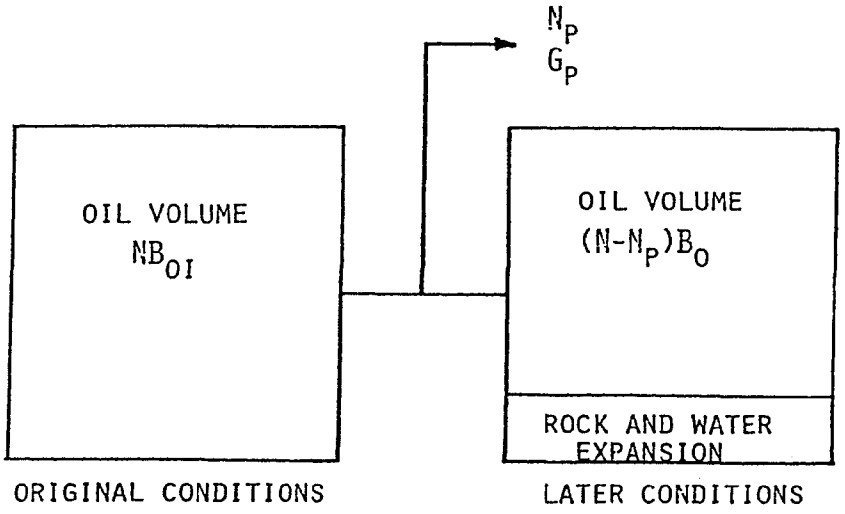

BY VOLUMETRIC BALANCE

ORIGINAL VOLUME = FINAL VOLUME

ORIGINAL VOLUME = NB_{OI}

FINAL VOLUME = $(N-N_P)B_O$ + VOLUME OCCUPIED BY WATER AND ROCK EXPANSION AS PRESSURE DECLINES

- ROCK AND WATER EXPANSION IMPORTANT IN UNDERSATURATED RESERVOIRS

FROM DEFINITION OF COMPRESSIBILITY

$$c_W = -\frac{1}{V_W}\left(\frac{dV_W}{dP}\right) \cong -\frac{1}{V_{WI}}\frac{\Delta V_W}{\Delta P}$$

THUS, CHANGE IN RESERVOIR WATER VOLUME DUE TO PRESSURE CHANGE:

$$\Delta V_W = -c_W V_{WI} \Delta P$$

AS PRESSURE DECREASES, MATRIX SUPPORTING STRUCTURE COLLAPSES INTO PORE SPACE

$$c_F = -\frac{1}{V_P}\left(\frac{dV_P}{dP}\right) \cong -\frac{1}{V_{PI}}\frac{\Delta V_P}{\Delta P}$$

THUS, CHANGE IN PORE VOLUME DUE TO PRESSURE CHANGE:

$$\Delta V_P = -c_F V_{PI} \Delta P$$

TOTAL CHANGE IN WATER VOLUME AND PORE VOLUME:

$$\Delta V_W + \Delta V_P = -\left[c_W V_{WI} + c_F V_{PI}\right]\Delta P$$

$$= \Delta V_{TOTAL}$$

NOTE THAT

$$V_W = S_W V_P$$

$$V_{WI} = S_{WI} V_{PI}$$

THUS

$$\Delta V_{TOTAL} = -\left[c_W S_{WI} + c_F\right] V_{PI} \Delta P$$

ALSO

$$V_{PI} = \frac{NB_{OI}}{1-S_{WI}}$$

THUS

$$\Delta V_{TOTAL} = -\frac{NB_{OI}}{1-S_{WI}} \left[c_W S_{WI} + c_F\right] \Delta P$$

THE VOLUMETRIC BALANCE BECOMES:

$$NB_{OI} = (N-N_P)B_O - \frac{NB_{OI}}{1-S_{WI}}\left[c_W S_{WI} + c_F\right]\Delta P$$

SOLVING FOR N:

$$N = \frac{N_P B_O}{B_O + B_{OI}\left(\frac{c_W S_{WI} + c_F}{1-S_{WI}}\right)(P_I-P) - B_{OI}} \qquad (V\text{-}1)$$

TO SIMPLIFY, NOTE:

$$c_O = -\frac{1}{V}\left(\frac{DV}{DP}\right) \cong -\frac{1}{V}\left(\frac{\Delta V}{\Delta P}\right)$$

IF V_{SC} IS VOLUME OF OIL IN STOCK TANK (STANDARD CONDITIONS)

$$-\frac{1}{V}\left(\frac{\Delta V}{\Delta P}\right) \cong -\frac{1}{V_I/V_{SC}}\,\frac{(V/V_{SC} - V_I/V_{SC})}{(P-P_I)}$$

$$= -\frac{1}{B_{OI}}\,\frac{(B_O-B_{OI})}{(P-P_I)}$$

THEN

$$B_O-B_{OI} = c_O B_{OI}(P_I-P)$$

SUBSTITUTING INTO EQUATION V-1

$$N = \frac{N_P B_O}{B_{OI}\left[c_O + \frac{c_W S_{WI} + c_F}{1-S_{WI}}\right](P_I - P)}$$

DEFINE

$$c_E = c_O + \frac{c_W S_{WI} + c_F}{1-S_{WI}} = \frac{c_O S_{OI} + c_W S_{WI} + c_F}{(1-S_{WI})}$$

THUS

$$N = \frac{N_P B_O}{B_{OI} c_E (P_I - P)} \qquad (V\text{-}2)$$

C. CONSIDERATIONS

1. EQS. V-1 OR V-2 SHOULD BE USED FOR ESTIMATING OOIP ABOVE BUBBLE POINT WHERE ROCK AND WATER EXPANSION NOT NEGLIGIBLE

2. DIFFICULTY IN MEASURING c_F AND c_W MAY LIMIT ACCURACY

D. Example - Use of Material Balance to Determine Original Oil in Place in Undersaturated Reservoir

Problem

DETERMINE THE ORIGINAL OIL IN PLACE FOR THE UNDERSATURATED RESERVOIR FOR WHICH DATA ARE SUMMARIZED BELOW.

$N_P = 1.4 \times 10^6$ STB
$B_O = 1.46$ RB/STB
$B_{OI} = 1.39$ RB/STB
$c_W = 3.71 \times 10^{-6}$ PSI^{-1}
$c_F = 3.52 \times 10^{-6}$ PSI^{-1}
$S_{WI} = 32\%$

THE RESERVOIR WAS DISCOVERED AT AN INITIAL PRESSURE OF 4300 PSI. PRESSURE HAS DECLINED TO 2450 PSI.

Solution

FROM EQUATION V-1

$$N = \frac{N_P B_O}{B_O + B_{OI}\left[\frac{c_W S_{WI} + c_F}{1-S_{WI}}\right](P_I - P) - B_{OI}}$$

$$N = \frac{1.4 \times 10^{6}(1.46)}{1.46+1.39\left[\frac{3.71 \times 10^{-6}(0.32)+3.52 \times 10^{-6}}{1-0.32}\right](4300-2450)-1.39}$$

$= 2.33 \times 10^{7}$ STB

NOTE:

IF C_F IS ASSUMED TO BE 0:

$$N = \frac{1.4 \times 10^{6}(1.46)}{1.46 + 1.39\left[\frac{3.71 \times 10^{-6}(0.32) + 0}{1-0.32}\right](4300-2450)-1.39}$$

$= 2.74 \times 10^{7}$ STB

CALCULATED VALUE OF N IS SIGNIFICANTLY INCREASED IF C_F NEGLECTED

I. Saturated Reservoir - Solution Gas Drive

OBJECTIVE: TO DERIVE A MATERIAL BALANCE EQUATION FOR A SOLUTION GAS DRIVE RESERVOIR AND TO APPLY IT TO ESTIMATE ORIGINAL OIL IN PLACE (OOIP)

A. Assumptions

1. $P \leq P_B$
2. No original gas cap
3. No water influx or production
4. Negligible rock and water expansion

B. Derivation of Material Balance Equation

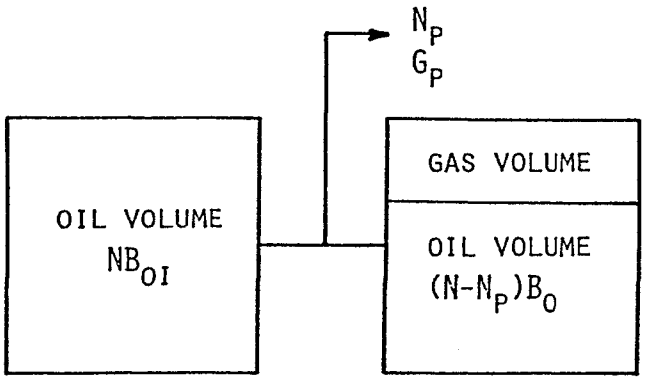

ORIGINAL CONDITIONS LATER CONDITIONS

BY VOLUMETRIC BALANCE

ORIGINAL VOLUME = FINAL VOLUME

ORIGINAL OIL VOLUME = NB_{OI}

ORIGINAL FREE GAS VOLUME = 0

FINAL OIL VOLUME = $(N-N_P)B_O$

- DETERMINE FINAL FREE GAS VOLUME BY PERFORMING A GAS BALANCE

ORIGINAL DISSOLVED GAS = NR_{SI}

FINAL DISSOLVED GAS = $(N-N_P)R_S$

GAS PRODUCED = G_P

THEREFORE,

FINAL FREE GAS = $NR_{SI} - (N-N_P)R_S - G_P$

- CONVERT TO RESERVOIR CONDITIONS

FINAL FREE GAS = $\{NR_{SI} - (N-N_P)R_S - G_P\}B_G/5.61$

THE VOLUMETRIC BALANCE BECOMES:

$$NB_{OI} = (N-N_P)B_O + \{NR_{SI}-(N-N_P)R_S-G_P\}B_G/5.61$$

SOLVING FOR N

$$N = \frac{N_P B_O - (N_P R_S - G_P)B_G/5.61}{B_O + (R_{SI}-R_S)B_G/5.61 - B_{OI}} \qquad (V\text{-}3)$$

TO SIMPLIFY, NOTE THAT

$$B_T = B_O + (R_{SI}-R_S)B_G/5.61$$

$$R_P = G_P/N_P$$

ALSO,

$$B_{OI} = B_{TI} \qquad \text{(NO GAS EVOLVED AT } P_B\text{)}$$

SUBSTITUTING INTO EQUATION V-3

$$N = \frac{N_P\{B_T + (R_P-R_{SI})B_G/5.61\}}{B_T-B_{TI}} \qquad \text{(V-4)}$$

SUBSTITUTING FOR B_O IN THE NUMERATOR ONLY, AN ALTERNATIVE FORM IS

$$N = \frac{N_P\{B_O + (R_P-R_S)B_G/5.61\}}{B_T-B_{TI}} \qquad \text{(V-5)}$$

III. Derivation of Material Balance Equation

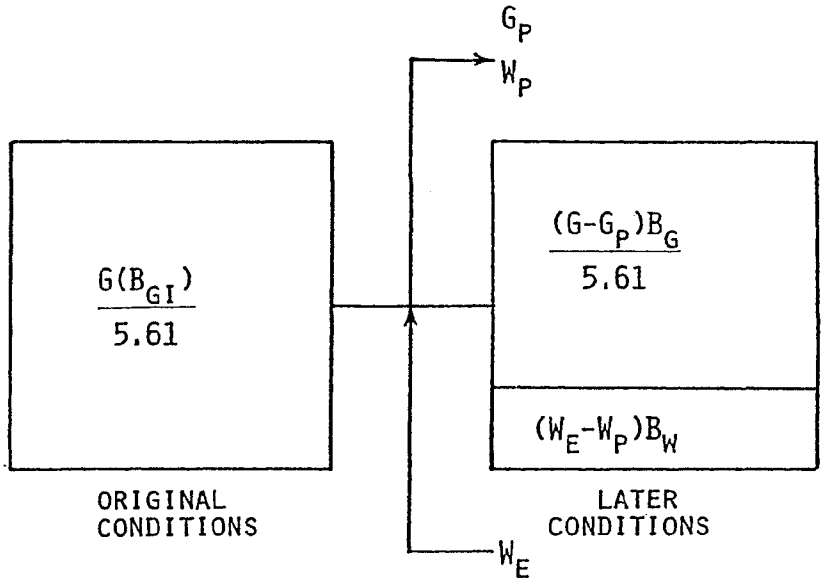

- From Volumetric Balance

INITIAL VOLUME = FINAL VOLUME

$$G(B_{GI})/5.61 = (G-G_P)(B_G/5.61) + (W_E-W_P)(B_W)$$

WHERE B_G = GAS FORMATION VOLUME FACTOR, RCF/SCF

$$G(B_{GI})/5.61 = (G-G_P)(B_G/5.61) - W_P(B_W) + W_E(B_W)$$

THIS CAN BE REARRANGED TO BE

$$G(B_G-B_{GI})/5.61 = (G_P(B_G)/5.61) + W_P(B_W) - W_E(B_W)$$

THE GENERALIZED FORM OF THE MATERIAL BALANCE EQUATION

$$\frac{G_P(B_G)/5.61 + W_P(B_W)}{(B_G-B_{GI})/5.61} = G + \frac{W_E(B_W)}{(B_G-B_{GI})/5.61} \qquad (X\text{-}6)$$

A. PRESSURE DEPLETION CASE - NO WATER INFLUX

$W_E = W_P = 0$

THEREFORE:

$$G(B_G-B_{GI})/5.61 = G_P(B_G)/5.61$$

OR

$$G_P = G(1-B_{GI}/B_G) \qquad (X\text{-}7)$$

SINCE $B_G = \frac{V_{R.C.}}{V_{S.C.}} = \frac{P_{S.C.}}{} \frac{T_{R.C.}}{P_{R.C.}} Z_{R.C.}$

$$B_G/B_{GI} = (P_I/z_I)(z/P) = \text{CONSTANT}$$

THEN $$G_P = G(1 - (P/z)(z_I/P_I))$$

THIS CAN BE REARRANGED TO BE

$$(P_I/z_I)(1-G_P/G) = P/z \qquad (X\text{-}8)$$

THIS SUGGESTS A PLOT OF (P/z) VS. G_P

WHEN $(P/z) = 0$, NOTE THAT

$$P_I/z_I\ (1-G_P/G) = 0$$

OR

$$G_P = G$$

ALSO, THE PLOT SHOULD BE LINEAR AND THUS READILY EXTRAPOLATED TO $P/z = 0$.

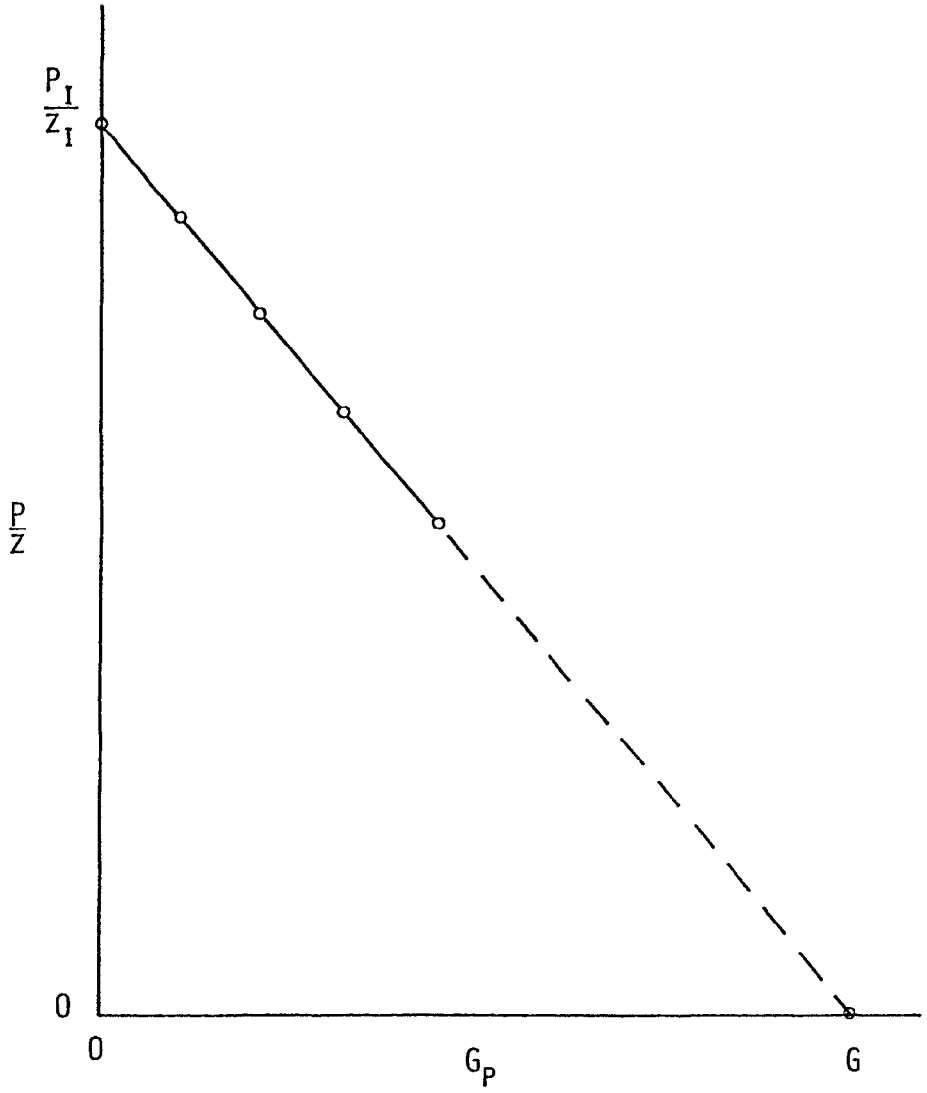
$\frac{P_I}{Z_I}$
$\frac{P}{Z}$
0
0
G_P
G

B. Example Problem - Determination of OGIP and Drive Mechanism Using a P/z Plot

Problem

An isopach map of the "Zapata Sand" in the Woodford Field in Atascosa County, Texas indicated an original gas in place of 44 mmscf. Production from the field has resulted in the following:

Reservoir Pressure (psia)	G_p (mmscf)	z
4000	0.00	0.80
3500	2.46	0.73
3000	4.92	0.66
2500	7.88	0.60
2000	11.20	0.55
200	---	0.94

The z factors were derived from fluid analysis data. A volumetric type depletion is suspected.

Perform a P/z plot to confirm original gas in place estimates and the suspected drive mechanisms.

SOLUTION

G_P (MMSCF)	P/z (PSIA)
0.00	5000
2.46	4795
4.92	4545
7.88	4167
11.20	3636

(SEE GRAPH)

THE CHARACTERISTICS OF THE BEST STRAIGHT LINE FIT OF THE DATA SET ARE:

A) G = 43.6 MMSCF (BY EXTRAPOLATION)

B) THE CURVE GIVES SOME INDICATION OF NONLINEARITY BUT STILL FITS THE EXPECTED GAS-IN-PLACE ESTIMATE

C) THE STRAIGHT LINE AND GOOD AGREEMENT WITH ORIGINAL GAS-IN-PLACE ESTIMATE CONFIRM THE VOLUMETRIC DEPLETION CHARACTERISTICS

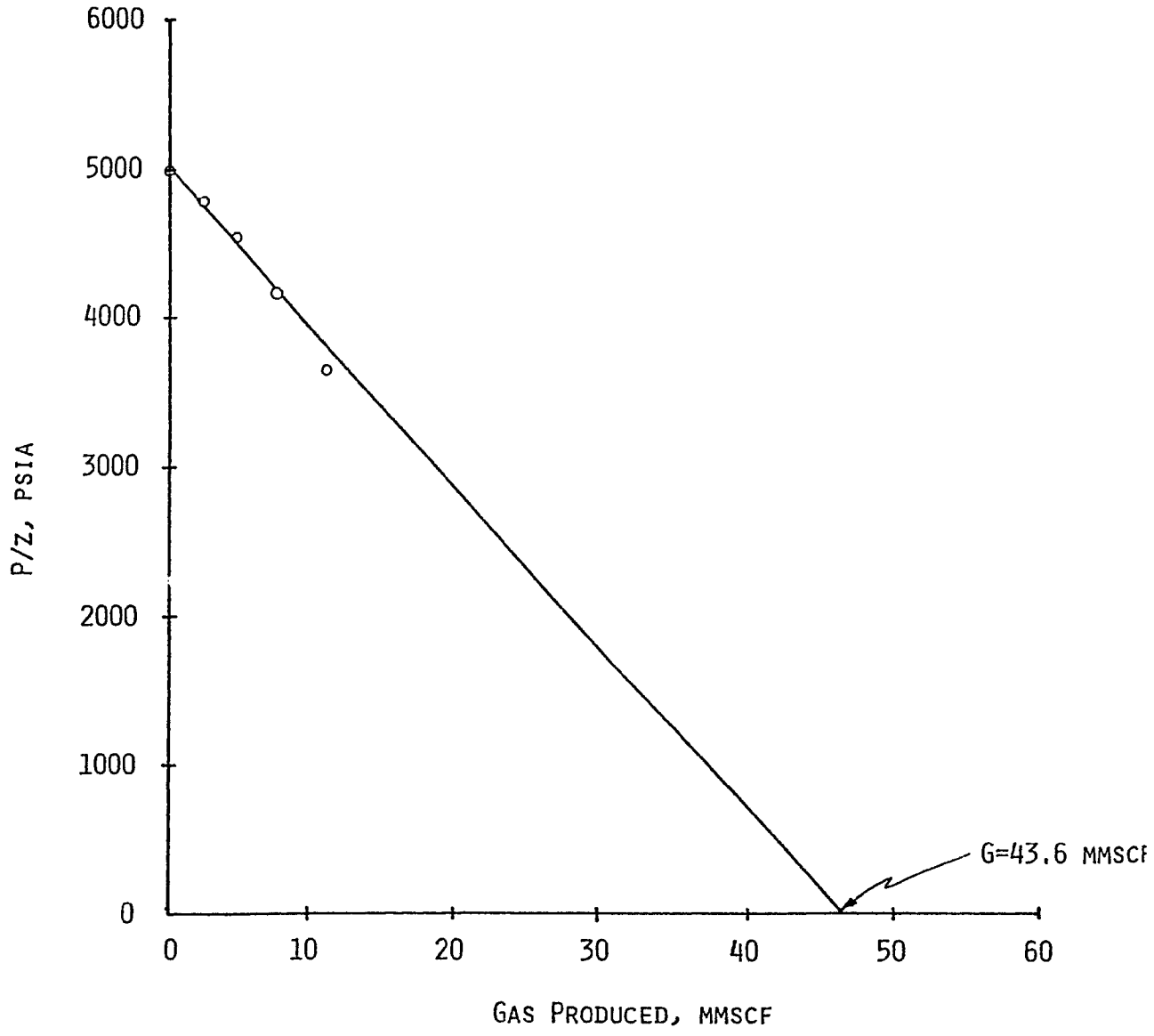
6000
5000
4000
3000
2000
1000
0
P/Z, PSIA
0
10
20
30
40
50
60
GAS PRODUCED, MMSCF
G=43.6 MMSCF

Reference(s):

- West, R.D.: "Extensions of the Muskat Depletion Performance Equation," ***Trans.*** AIME, Vol. **213** (1958), 285-291.
- Havlena, D. and Odeh, A.S.: "The Material Balance as an Equation of a Straight-Line," *JPT* (Aug. 1963), 896-900.
- Havlena, D. and Odeh, A.S.: "The Material Balance as an Equation of a Straight-Line—Part II, Field Cases," *JPT* (July 1964),815-822.
- Humphreys, N.V.: "The Material Balance Equation for a Gas Condensate Reservoir With Significant Water Production," paper SPE 21514 presented at the SPE Gas Technology Symposium, Houston, June 23-24, 1991.
- Fetkovich, M.J., Reese, D.E., and Whitson, C.H.: "Application of a General Material Balance for High-Pressure Gas Reservoirs," *SPEJ*, (March 1998), 3-13.

Extensions of the Muskat Depletion Performance Equation

R. D. WEST
MEMBER AIME

MENE GRANDE OIL CO.
MARACAIBO, VENEZUELA

ABSTRACT

Muskat's depletion performance equation is here derived considering the expansion behavior of the reservoir hydrocarbon system and a simple fractional-flow equation. This method of derivation leads logically to the two extensions that follow. The first of these is concerned with gravity segregation in a depletion-drive reservoir. The second is concerned with including an empirically determined term for water influx in the performance equation. The more general equation for gravity segregation when there is a primary gas cap and empirically-determined water influx is stated for completeness. These equations have been found useful in reservoir performance calculations in Eastern Venezuela.

A discussion on the methods of solving these equations follows, and considers firstly the effect of taking finite intervals in the numerical integration, and secondly, methods of incorporating the time functions involved in segregation in with the expansion behavior. The paper concludes with a brief general discussion on further extensions to the depletion performance equation.

INTRODUCTION

The two fundamental sources of energy by which oil is produced from a reservoir result from pressure depletion inside the boundaries of the reservoir and fluid encroachment across the boundaries of the reservoir. The wells in either case form low pressure outlets through which oil and gas may be produced by the expansive force of the reservoir fluids and associated encroaching fluids.

When the reservoir pressure is higher than the bubble-point pressure of the oil, so that there is no free gas in the reservoir, these expansive forces are the only ones available for the production of oil. However, when the reservoir pressure is less than the bubble-point pressure of the oil, free gas is vaporized as the pressure falls. With both oil and free-gas phases present, the additional forces of gravity and capillarity may operate on the gas-oil system, as they have previously operated on the oil-interstitial water system. Gravity tends to segregate the free gas from the oil due to their density difference. Capillarity opposes and eventually balances gravity as the more extreme free gas and oil saturations are reached, preventing the independent movement of free gas until it is above a certain saturation, and the independent movement of oil when it is below a certain saturation.

The type of depletion performance equation chosen for predicting the future performance of a reservoir depends on the amount of past history available. When the reservoir is somewhere past the halfway mark in depletion, some form of decline curve is often used. With less past history, material balance equations which incorporate empirical factors based on the past performance are often used. When, however, the amount of past history is small, the Muskat depletion performance equation will usually be used. The distinguishing feature of this type of equation is that empirical factors based on the over-all or macroscopic reservoir behavior are almost or entirely absent. Each parameter affecting the reservoir performance is ascribed an independent set of values based on measurements made on laboratory samples; that is, incorporating microscopic empirical factors.

In establishing Muskat-type depletion performance equations, it is necessary to consider the reservoir as consisting of a number of associated blocks, in each of which the saturations and pressures may be considered uniform, and in each of which all substances have uniform pressure-volume characteristics. Thus, a primary gas cap can usually be considered as one block and an aquifer as another. Gravity segregation may be negligible for practical purposes when the rock and oil properties are adverse and/or the dip or thickness of the reservoir is too small. In this case the whole oil leg may be considered as one block, except in very large reservoirs.

In very large reservoirs the fluid and rock properties may vary enough, particularly in the dip direction, for it to be necessary to divide the oil leg into a number of blocks, in each of which the relevant quantities may be considered uniform. When gravity segregation of the oil and free gas is not negligible, it is necessary to consider the space occupied by the initial oil leg as divided into two blocks, a secondary gas cap and an effective oil leg, in each of which saturations may be considered to be uniform. The total volume of these two blocks is thus constant, but the secondary gas cap grows continuously at the expense of the oil leg.

Muskat[1] derived depletion performance equations for the basic case of an oil reservoir with closed boundaries and without segregation, and for the case of an oil

Original manuscript received in Society of Petroleum Engineers office July 2, 1957. Revised manuscript received Oct. 15, 1958. Paper presented at 32nd Annual Fall Meeting of Society of Petroleum Engineers in Dallas, Tex., Oct. 6-9, 1957.

[1]References given at end of paper.

reservoir with a boundary open to a primary gas cap. These two cases are rederived in this paper using a different approach, because this serves as an introduction to the method used to develop equations for the extensions that follow. This approach also enables those meeting these equations for the first time to see the exact relationship between this differential form of the material balance equation and the other forms in use. The mathematical treatment is simple but it is felt that it gains more, in that physical significance of the terms is readily obtained, than it loses by being non-rigorous.

EXPANSION BEHAVIOR OF THE RESERVOIR SUBSTANCES

The expansibility of a reservoir fluid or solid is here defined as the rate of increase in volume of the substance with pressure decrease. If the standard volume of the substance (that is, its volume in any units whatever corrected to standard temperature and pressure) is V_s, and its volume factor at the reservoir temperature is B_s, the reservoir volume is $V_s \cdot B_s$. If the pressure falls by a small interval, Δp, and the volume factor increases to $(B_s + \Delta B_s)$, the rate of increase in volume of the substance with pressure decrease is

$$\frac{V_s (B_s + \Delta B_s) - V_s \cdot B_s}{\Delta p}$$

or $V_s \cdot \Delta B_s/\Delta p$. In the limit, as $\Delta p \to 0$, this expansibility is equal to $V_s \cdot dB_s/dp$. The expansibility of a reservoir substance is therefore equal to the standard volume of the substance multiplied by the rate of change of its volume factor with pressure.

The standard volume of the free gas in any block of the reservoir is equal to $\frac{V_p \cdot S_g}{B_g}$. The free gas expands as the pressure decreases and its expansibility is therefore $\frac{V_p \cdot S_g}{B_g} \cdot \frac{dB_g}{dp}$.

The standard volume of the oil in any block of the reservoir is equal to $\frac{V_p \cdot S_o}{B_o}$. As the pressure on the oil is decreased the oil itself shrinks, but gas is vaporized, and this gas causes an increase in total volume. The expansibility due to the oil shrinkage is $-\frac{V_p \cdot S_o}{B_o} \cdot \frac{dB_o}{dp}$ and that due to the liberation of solution gas is $\frac{V_p \cdot S_o}{B_o} \cdot B_g \cdot \frac{dR_s}{dp}$. The former expression may be referred to as the expansibility of the oil, and the latter as that of the solution gas.

The over-all expansibility of the hydrocarbon system in any block of the reservoir is therefore the sum of these three components,

$$V_p\left[S_g \cdot \frac{1}{B_g} \cdot \frac{dB_g}{dp} + S_o \cdot \frac{B_g}{B_o} \cdot \frac{dR_s}{dp} - S_o \cdot \frac{1}{B_o} \frac{dB_o}{dp}\right].$$

In addition to the hydrocarbon system, the reservoir system contains interstitial water and rock. The standard volume of the interstitial water is $\frac{V_p \cdot S_{wi}}{B_w}$, and its expansibility is therefore, $\frac{V_p \cdot S_{wi}}{B_w} \cdot \frac{dB_w}{dp}$. As the rock volume factor has been defined in terms of pore space and not in terms of the rock itself, the standard volume of the rock is therefore in effect, V_p, and the expansibility of the rock is $V_p \cdot \frac{dB_r}{dp}$.

The over-all expansibility of the fluids and solid in any block is therefore equal to

$$V_p\left[S_g \cdot \frac{1}{B_g} \cdot \frac{dB_g}{dp} + S_o \cdot \frac{B_g}{B_o} \cdot \frac{dR_s}{dp} - S_o \cdot \frac{1}{B_o} \cdot \frac{dB_o}{dp} + S_w \cdot \frac{1}{B_w} \cdot \frac{dB_w}{dp} + \frac{dB_r}{dp}\right]$$

However, below bubble-point pressure, the interstitial water and rock terms will usually be negligible, except in an aquifer.

PERFORMANCE OF ONE-BLOCK OIL RESERVOIR

In the simple one-block oil reservoir with closed boundaries, all of the fluid represented by the expansion for any pressure interval must be produced through the wells. By definition, the pressure and saturations are assumed to be uniform throughout the block, and segregation is therefore implicitly excluded. It is therefore possible to obtain a theoretical performance below bubble-point pressure in terms of oil desaturation as follows.

The rate at which the oil in the reservoir shrinks is $V_{p \cdot oi} \cdot \frac{S_o}{B_o} \cdot \frac{dB_o}{dp}$, as previously shown. The rate at which oil is produced from the wells is equal to the expansibility of the hydrocarbon system (thus, neglecting interstitial water and rock terms) multiplied by the fraction of oil in the total hydrocarbon flow. Since the absence of segregation implies the ignoring of gravity effects, the fraction of oil in the mixed oil and gas flow is given by

$$f_o = \frac{1}{1 + \frac{\mu_o}{\mu_g} \cdot \frac{k_{rg}}{k_{ro}}}.$$

The rate at which oil is produced from the wells is therefore,

$$V_{p \cdot oi} \cdot \frac{1}{1 + \frac{\mu_o}{\mu_g} \cdot \frac{k_{rg}}{k_{ro}}}\left[S_g \cdot \frac{1}{B_g} \cdot \frac{dB_g}{dp} + S_o \cdot \frac{B_g}{B_o} \cdot \frac{dR_s}{dp} - S_o \cdot \frac{1}{B_o} \cdot \frac{dB_o}{dp}\right].$$

This equation ignores any special effects due to radial-flow distribution around wells, unless the relative permeability ratio is adjusted to allow for them.

The rate of oil desaturation with pressure decrease, $V_{p \cdot oi} \cdot \frac{dS_o}{dp}$, is therefore equal to the sum of these two quantities, i.e.,

$$V_{p \cdot oi} \cdot \frac{dS_o}{dp} = V_{p \cdot oi} \frac{1}{1 + \frac{\mu_o}{\mu_g} \cdot \frac{k_{rg}}{k_{ro}}}\left[S_g \cdot \frac{1}{B_g} \cdot \frac{dB_g}{dp} + S_o \frac{B_g}{B_o} \cdot \frac{dR_s}{dp} - S_o \cdot \frac{1}{B_o} \cdot \frac{dB_o}{dp}\right] + V_{p \cdot oi}\, S_o \cdot \frac{1}{B_o} \cdot \frac{dB_o}{dp}.$$

Thus,

$$\frac{dS_o}{dp} = \frac{1}{1 + \frac{\mu_o}{\mu_g} \cdot \frac{k_{rg}}{k_{ro}}}\left[S_g \cdot \frac{1}{B_g} \frac{dB_g}{dp} + S_o \cdot \frac{B_g}{B_o} \cdot \frac{dR_s}{dp}\right.$$

$$- S_o \cdot \frac{1}{B_o} \cdot \frac{dB_o}{dp} + S_o \cdot \frac{1}{B_o} \cdot \frac{dB_o}{dp} + S_o \cdot \frac{\mu_o}{\mu_g} \frac{k_{rg}}{k_{ro}} \frac{1}{B_o} \frac{dB}{dp} \Bigg],$$

or

$$\frac{dS_o}{dp} = \frac{1}{1 + \frac{\mu_o}{\mu_g} \cdot \frac{k_{rg}}{k_{ro}}} \Bigg[S_g \cdot \frac{1}{B_g} \frac{dB_g}{dp} + S_o \cdot \frac{B_g}{B_o} \cdot \frac{dR_s}{dp} + S_o \cdot \frac{\mu_o}{\mu_g} \cdot \frac{k_{rg}}{k_{ro}} \cdot \frac{1}{B_o} \cdot \frac{dB_o}{dp} \Bigg].$$

This is, of course, the same as the equation developed by Muskat[1], except that he has $B_g \cdot \frac{d\frac{1}{B_g}}{dp}$ instead of $\frac{1}{B_g} \cdot \frac{dB_g}{dp}$. Numerically, these two terms are equal, but they are opposite in sign. The difference arises because of the non-rigorous development of the above equation.

PERFORMANCE OF TWO-BLOCK OIL RESERVOIR WITH PRIMARY GAS CAP

When a reservoir has a primary gas cap it must be considered as consisting of two blocks, the primary gas cap and the oil leg, in each of which the saturations are assumed to be uniform. Furthermore, it must be assumed that none of the fluids in the gas-cap block are produced through wells. In this case, all fluid represented by the expansion of the gas cap in any pressure interval is transferred into the oil-leg block.

The expansibility of the gas cap is,

$$V_{p \cdot oi} \cdot m_p \cdot \Bigg[S_{gp} \cdot \frac{1}{B_g} \cdot \frac{dB_g}{dp} + S_{op} \cdot \frac{B_g}{B_o} \cdot \frac{dR_s}{dp} - S_{op} \cdot \frac{1}{B_o} \cdot \frac{dB_o}{dp} \Bigg].$$

Adding this expansibility to that of the oil leg, and using the procedure just cited, the rate of oil desaturation for this type of reservoir mechanism is given by

$$\frac{dS_o}{dp} = \frac{1}{1 + \frac{\mu_o}{\mu_g} \cdot \frac{k_{rg}}{k_{ro}}} \Bigg[\Bigg[S_g \cdot \frac{1}{B_g} \cdot \frac{dB_g}{dp} + S_o \cdot \frac{B_g}{B_o} \cdot \frac{dR_s}{dp} + S_o \cdot \frac{\mu_o}{\mu_g} \cdot \frac{k_{rg}}{k_{ro}} \cdot \frac{1}{B_o} \cdot \frac{dB_o}{dp} \Bigg] + m_p \Bigg[S_{gp} \cdot \frac{1}{B_g} \cdot \frac{dB_g}{dp} + S_{op} \cdot \frac{B_g}{B_o} \cdot \frac{dR_s}{dp} - S_{op} \cdot \frac{1}{B_o} \cdot \frac{dB}{dp} \Bigg] \Bigg]$$

This equation is also the same as the one developed by Muskat[1], but with the same qualification mentioned earlier regarding the free gas term. One further assumption in this equation is that the expansibility of the gas cap is freely available to the oil leg; that is, it is not restricted by permeability or any other factor to any definite transference rate. This assumption is considered not unreasonable because of the low viscosity of gas and the fact that gas caps are often not bigger than the same order of magnitude as the oil leg.

SEGREGATION

Before considering the depletion performance equation for a reservoir with segregation, it is convenient to review the basic principles of segregation.

The forces of gravity and capillarity control the segregation of free gas and oil in the reservoir. Gravity is the force which initiates and maintains the segregation by virtue of the difference in density of the two fluids concerned. Capillarity opposes this segregation, and eventually balances it, at extreme free gas and oil saturations.

Since the reservoir oil is heavier than the free gas, it always tends to flow down-dip relative to the gas under the action of gravity. However, an equal reservoir volume of gas must flow up-dip relative to the oil, and the rate of segregation is therefore determined by whichever has the low mobility. Assuming that the reservoir is thin in relation to its length in the dip direction, the effective direction of segregation may be assumed to be along the dip direction. The gravitational force causing segregation in this direction is $(\rho_o - \rho_g) \cdot g \cdot \sin D$, and the segregation rate is therefore,

$$q_m = \left[\text{lower of } \frac{k_o}{\mu_o} \text{ and } \frac{k_g}{\mu_g} \right] \cdot A \cdot (\rho_o - \rho_g) \cdot g \cdot \sin D$$

In view of the assumption that the reservoir is thin in relation to its length in the dip direction, and that the effective direction of segregation is therefore along the dip direction, the cross-sectional area, A, through which segregation takes place is the slant height area of the reservoir. It is further assumed that in thin reservoirs the mobilities based on uniform saturations throughout the sand thickness will decide the segregation rates of the oil and gas phases. These assumptions are not true for thick reservoirs as described by Martin[2]. Since during depletion the reservoir pressure falls throughout the oil leg, solution gas is vaporized throughout the oil leg and is all involved in segregation. The effective area through which segregation takes place is therefore considered to be the average slant height area between the gas-oil contact at any time and the bottom of the oil leg.

While capillarity is at all times modifying the segregation of gas and oil, it can be shown that capillary pressures and their gradients are usually negligible in field-sized systems. However, there are circumstances in which the capillary pressure is not negligible, and other circumstances in which the capillary pressure gradient is not negligible, and the practical effects of capillarity may be considered under these two heads.

In a field-sized system, the capillary pressures are important in determining the threshold values of mobility at extreme saturations. Due to the capillary pressure, gas has no mobility independent of the oil below a certain gas saturation, and this saturation thus identifies the point at which segregation can begin. At the other extreme oil has no mobility below a certain oil saturation, and this saturation thus identifies the point at which segregation ceases. However, here a time element is involved, because as this oil saturation is approached the oil mobility becomes very small, although greater than zero. Thus, in practice, it has been found convenient to identify the oil saturation at which segregation ceases by that corresponding to a small but arbitrary value of oil flow measured as a fraction of the total flow. A limiting value of $f_o = 0.001$ has been found suitable. Using such a value to identify the point at which segregation ceases, a residual oil saturation in the secondary gas cap of 25 to 35 per cent commonly results, as opposed to the value of 5 to 15 per cent commonly quoted for primary gas caps. This latter range of values may be taken as an indication of possible ultimate residual oil values.

It can be shown that the capillary pressure gradients are important only when the gas and oil saturations change rapidly in a short distance. In a depletion-drive reservoir with gravity segregation, this is at the interface between the secondary gas cap and the oil leg. Terwilliger, *et al*[3], working on an air-brine system, have shown that while there is no sharp interface between the two fluids in a gravity-drained sand column, the greater part of the saturation change occurs in a stabilized zone in which all saturations maintain a constant relative position to one another. Work by Stahl, *et al*[4], on an air-Wilcox crude system also shows the formation of a stabilized zone (see Fig. 3 of their paper). This stabilized zone appears to be the product of capillary pressure gradients. The important point about it for field-sized systems is its length in relation to the production rate from the oil leg.

Both Terwilliger, *et al*[3], and Stahl, *et al*[4], showed that stabilized zones from 1- to 3-ft thick were formed as long as the drainage rate did not exceed the so-called "maximum rate of gravity drainage". This latter quantity is defined as the rate of segregation obtained from the equation given above when $S_o = 100$ per cent. These investigators used systems with liquid mobilities in the range of 2 to 3 darcy/cp. The length of the stabilized zone for higher production rates has not been adequately examined, nor has the problem of when a stabilized zone is no longer formed. However, in practice, the production rate from the oil leg will often not exceed the maximum rate of gravity drainage, and in these cases a relatively short stabilized zone may be expected to form, the thickness of which may be considered negligible in a field-sized system.

To summarize on segregation, the mobility and area through which it operates may be designated, and a sharp interface between the secondary gas cap may be assumed unless the oil production rate is very high.

PERFORMANCE OF TWO-BLOCK OIL RESERVOIR WITH SEGREGATION

The simplest case of an oil reservoir with segregation involves two blocks; a secondary gas cap and an oil leg. For the purpose of this paper it is assumed that the production rate is such that a sharp interface between the two blocks may be considered to exist, and that all production is from the oil leg. The secondary gas cap expands continuously at the expense of the oil leg, although the two blocks taken together have a fixed total size. The basic principle involved in establishing the depletion performance equation for this type of reservoir is that the whole system is considered to obey the expansion behavior previously given, with the sizes of the blocks changing in accordance with the segregation behavior previously given.

The expansibility of the secondary gas cap is

$$V_{p\cdot o1}\, m_s \cdot \left[S_{o1} \cdot \frac{1}{B_g} \cdot \frac{dB_g}{dp} + S_{o1} \cdot \frac{B_g}{B_o} \cdot \frac{dR_s}{dp} - S_{o1} \cdot \frac{1}{B_o} \cdot \frac{dB_o}{dp} \right],$$

and since it is assumed that there is no production from this block, this is the rate of fluid transfer into the oil-leg block. Proceeding as before, the equation relating the oil desaturation rate with pressure decline is

$$\frac{dS_o}{dp} = \frac{1}{1 + \frac{\mu_o}{\mu_g} \cdot \frac{k_{rg}}{k_{ro}}} \left[\left[S_g \cdot \frac{1}{B_g} \cdot \frac{dB_g}{dp} + S_o \cdot \frac{B_g}{B_o} \cdot \frac{dR_s}{dp} + S_o \cdot \frac{\mu_o}{\mu_g} \cdot \frac{k_{rg}}{k_{ro}} \cdot \frac{1}{B_o} \cdot \frac{dB_o}{dp} \right] + m_s \left[S_{o1} \cdot \frac{1}{B_g} \cdot \frac{dB_g}{dp} + S_{o1} \cdot \frac{B_g}{B_o} \cdot \frac{dR_s}{dp} - S_{o1} \cdot \frac{1}{B_o} \cdot \frac{dB_o}{dp} \right] \right]$$

It will be noticed that this equation is similar to the equation for an oil reservoir without segregation, but with a primary gas cap, except that a varying term, m_s, is used to relate the size of the secondary gas cap to that of the oil leg. The subordinate equations used to calculate the change in m_s from the segregation behavior are given later.

WATER INFLUX IN A COMBINATION-DRIVE RESERVOIR

When a reservoir has an aquifer associated with it, it must again be considered in two blocks — the oil leg and the aquifer — in each of which saturations are assumed to be uniform. If none of the aquifer water is produced from the aquifer block, the fluid represented by the expansion of the aquifer for any interval is transferred into the oil-leg block. Using the same procedure as cited the expansibility of the aquifer is

$$V_{p\cdot o1} \cdot m_s \cdot \left[\frac{1}{B_w} \cdot \frac{dB_w}{dp} + \frac{dB_r}{dp} \right],$$

and a depletion performance equation could be established as

$$\frac{dS_o}{dp} = \frac{1}{1 + \frac{\mu_o}{\mu_g} \cdot \frac{k_{rg}}{k_{ro}}} \cdot \left[\left[S_g \cdot \frac{1}{B_g} \cdot \frac{dB_g}{dp} + S_o \cdot \frac{B_g}{B_o} \cdot \frac{dR_s}{dp} + S_o \cdot \frac{\mu_o}{\mu_g} \cdot \frac{k_{rg}}{k_{ro}} \cdot \frac{1}{B_o} \cdot \frac{dB_o}{dp} \right] + m_s \left[\frac{1}{B_w} \cdot \frac{dB_w}{dp} + \frac{dB_r}{dp} \right] \right].$$

However, as with the gas cap, this equation includes the assumption that the expansion capacity is freely available to the oil leg. But whereas the assumption is often considered reasonable in the gas-cap case, it is not considered reasonable with an aquifer since the aquifer is usually much larger than the oil leg and the water viscosity is considerably higher than gas viscosity. One approach might be to consider incorporating a pressure lag factor in the term including the expansibility of the aquifer. Here it is intended to discuss one way of another approach, an empirical one, that has been found useful. In this method the water influx is determined empirically using the material balance equation and volumetric determinations of the oil leg. The influx rate against pressure decline, dE/dp, is then determined, and this influx rate is then plotted against pressure. If this plot of dE/dp against pressure is a straight line, dE/dp may be assumed to be constant. If not, the relationship between dE/dp and pressure may be found by standard regression techniques. In either case values of dE/dp may now be predicted for future performance, providing the oil off-take rate is not changed rapidly.

This quantity, dE/dp, is used by noting that it is the *effective* expansibility of the aquifer, and is therefore equal to

$$V_{p\cdot o1} \cdot m_s \cdot \left[\frac{1}{B_w} \cdot \frac{dB_w}{dp} + \frac{dB_r}{dp} \right]$$

times its lag correction factor. The depletion performance equation therefore becomes

$$\frac{dS_o}{dp} = \frac{1}{1 + \frac{\mu_o}{\mu_g} \cdot \frac{k_{rg}}{k_{ro}}} \cdot \left[S_g \cdot \frac{1}{B_g} \cdot \frac{dB_g}{dp} + S_o \cdot \frac{B_g}{B_o} \cdot \frac{dR_s}{dp} + S_o \cdot \frac{\mu_o}{\mu_g} \cdot \frac{k_{rg}}{k_{ro}} \cdot \frac{1}{B_o} \cdot \frac{dB_o}{dp} + \frac{1}{V_{p \cdot oi}} \cdot \frac{dE}{dp} \right].$$

There are two ways of using the equation when it is obtained. When the influx rate is small in relation to the production rate, and/or for relatively short prediction periods, the cumulative water influx may be converted to a water saturation averaged over the reservoir, and the gas saturation and hence the relative permeability ratio changed accordingly. With larger influx rates and/or longer prediction periods, a third block, an invaded oil-leg block, must be considered which grows continuously at the expense of the oil-leg block. An average oil saturation can be ascribed to this block from fractional-flow curve considerations, and a sharp interface between this and the oil leg itself can be assumed. The variation of the ratio of the pore volume of this invaded block to that of the oil leg can therefore be calculated and incorporated in the performance equation.

GRAVITY SEGREGATION IN A COMBINATION-DRIVE RESERVOIR

Putting together the results of the last two sections, the depletion performance equation for a combination-drive reservoir considered in four blocks (primary gas cap, secondary gas cap, oil leg and aquifer) may be stated as follows.

$$\frac{dS_o}{dp} = \frac{1}{1 + \frac{\mu_o}{\mu_g} \cdot \frac{k_{rg}}{k_{ro}}} \left[\left[S_g \cdot \frac{1}{B_g} \cdot \frac{dB_g}{dp} + S_o \cdot \frac{B_g}{B_o} \cdot \frac{dR_s}{dp} + S_o \cdot \frac{\mu_o}{\mu_g} \cdot \frac{k_{rg}}{k_{ro}} \cdot \frac{1}{B_o} \cdot \frac{dB_o}{dp} + \frac{1}{V_{p \cdot oi}} \cdot \frac{dE}{dp} \right] + m_p \left[S_{gp} \cdot \frac{1}{B_g} \cdot \frac{dB_g}{dp} + S_{op} \cdot \frac{B_g}{B_o} \cdot \frac{dR_s}{dp} - S_{op} \cdot \frac{1}{B_o} \cdot \frac{dB_o}{dp} \right] + m_i \left[S_{gi} \cdot \frac{1}{B_g} \cdot \frac{dB_g}{dp} + S_{oi} \cdot \frac{B_g}{B_o} \cdot \frac{dR_s}{dp} - S_{oi} \cdot \frac{1}{B_o} \cdot \frac{dB_o}{dp} \right] \right]$$

The same segregation equation as before is used to obtain the variations in m_i.

NUMERICAL SOLUTION OF DEPLETION PERFORMANCE EQUATIONS

These depletion performance equations cannot be integrated formally, and it is therefore necessary to integrate them numerically. In this numerical integration a sequence of relatively small but nonetheless finite pressure decrements is considered; 100 psi being a suitable interval in many cases. These numerical integration procedures are well known, and it is intended to mention only those points special to the equations developed here. It is convenient to consider these points under the two heads of solving for the expansibilities and solving for the segregation variables.

SOLVING FOR THE EXPANSIBILITIES

The expansibility applied to a finite pressure interval becomes a finite expansion, and it is necessary to convert the expansibilities in the depletion performance equation to forms applicable to finite intervals.

Each pressure decrement involves a fall from an initial pressure to a final pressure. The amount of material involved in the expansion is identified by the standard volumes present at the beginning of the interval. Since the expansion is the difference between the initial and final volume, corresponding to the initial and final pressures, the solution gas vaporized during the interval and the oil and gas produced during the interval are involved as their volumes at the final pressure. The viscosity ratio, and the rates of change of the volume factors with pressure, are involved as the average values for the interval (because, for instance, $\Delta B_o = [dB_o/dp]_{av} \cdot \Delta p$). Similarly, the relative permeability ratio should be that corresponding to the average saturations during the interval (*not* the average ratio itself).

The basic depletion performance equation therefore becomes, for a finite pressure decrement,

$$\Delta S_o = \frac{1}{1 + \left(\frac{\mu_o}{\mu_g}\right)_{av} \left(\frac{k_{rg}}{k_{ro}}\right)_{\bar{S}_g}} \left[S_{gi} \cdot \frac{1}{B_{gi}} \cdot \left(\frac{dB_g}{dp}\right)_{av} + S_{oi} \cdot \frac{B_g f}{B_{oi}} \cdot \left(\frac{dR_s}{dp}\right)_{av} + S_{oi} \cdot \left(\frac{\mu_o}{\mu_g}\right)_{av} \cdot \left(\frac{k_{rg}}{k_{ro}}\right)_{\bar{S}_g} \frac{1}{B_{oi}} \cdot \left(\frac{dB_o}{dp}\right)_{av} \right] \Delta p.$$

The other equations are modified in a similar way.

In the equation just cited, all values except the average gas saturation, on which the relative permeability ratio is based, are determined directly. It is possible to consider each term in the equation as consisting of a pressure function multiplied by a saturation function. Values may be assigned to the pressure functions in advance, but the saturation functions must be calculated for each decrement in turn. The average gas saturation, which is not determined directly, may be predicted as follows. The values of ΔS_o for equal pressure decrements, increase smoothly until at some point beyond where the equilibrium gas saturation is reached. At this point the term,

$$S_{oi} \cdot \left(\frac{\mu_o}{\mu_g}\right)_{av} \cdot \left(\frac{k_{rg}}{k_{ro}}\right)_{\bar{S}_g} \cdot \frac{1}{B_{oi}} \cdot \left(\frac{dB_o}{dp}\right)_{av}$$

increases less than

$$1 + \left(\frac{\mu_o}{\mu_g}\right)_{av} \cdot \left(\frac{k_{rg}}{k_{ro}}\right)_{\bar{S}_g},$$

and the values of ΔS_o pass through a maximum near this point and thereafter start decreasing smoothly. A plot of ΔS_o against pressure enables a prediction of the average gas saturation for the next interval to be made, and with experience the prediction can be done very close. In any case, if the predicted value is too much in error a more accurate average saturation may be determined using the final value calculated using the predicted average, and the line of calculation repeated.

Using the values as identified, and not all initial or final values as has often been done, no more complex method of numerical integration is required. This point has been confirmed using machine computations with pressure decrements as small as 10 psi.

SOLVING FOR THE SEGREGATION VARIABLES

Segregation cannot begin until the equilibrium gas saturation is reached, since this is the saturation at which the gas has a mobility independent of the oil.

This is not necessarily the point at which k_{rg}/k_{ro} becomes greater than zero, since it may be argued that some gas is carried along entrained in the oil at lower saturations. Segregation requires the gas to have an independent mobility. The equilibrium gas saturation will not be known with any great accuracy, and unnecessary calculation may often be saved by making it coincide with the gas saturation at the end of a convenient pressure interval. The calculation to this point is the same with or without segregation. The procedure for the next pressure decrement is as follows.

1. Calculate ΔS_o for the next interval as if there were no segregation, and knowing the off-take rate, obtain the time, Δt, taken to produce this pressure decrement.

2. Calculate k_o/μ_o and k_g/μ_g corresponding to the average gas and oil saturation for the interval, and find out which is the lesser; the lesser is used.

3. Plot the slant height cross-sectional area of the reservoir at different structural positions in the reservoir as a curve against position. Whence obtain a plot of the average cross-sectional area between any structural position and the bottom of the reservoir against the position of the upper limit.

4. Compute q_m and Q_m according to the following.

$$q_m = \left[\text{lesser of } \frac{k_o}{\mu_o} \text{ and } \frac{k_g}{\mu_g}\right] \cdot A \cdot (\rho_o - \rho_g) \cdot g \cdot \sin D \cdot \frac{1}{B_o}, \text{ and } Q_m = q_m \cdot \Delta t,$$

where the appropriate value for A is used from the plot obtained in Step 3.

5. Compute m, and the increase in oil saturation in the oil leg, ΔS_{om}, from the following sequence of equations.

$$\Delta V_p = \frac{Q_m \cdot B_o f}{S_o f - S_{or}}$$

$$V_p = \Sigma \Delta V_p$$

$$V_{p\cdot or} = \text{initial } V_{p\cdot or} - V_p$$

$$m = \frac{V_p}{V_{p\cdot or}\text{ final}}$$

$$\Delta S_{om} = \frac{Q_m B_o f}{V_{p\cdot or}\text{ final}}$$

6. Return to the table in which the gas-cap term is calculated and insert the values of m corresponding to the average of the one previously used (zero in this first line) and the one just determined. Calculate a revised secondary gas-cap term.

7. Return to the table in which ΔS_o is calculated and add ΔS_{om} to the value of S_o for the end of the interval. Using this value of $(S_o + \Delta S_{om})$ and the value of S_o for the beginning of the interval, determine a revised value of K_{rg}/K_{ro} corresponding to the revised average gas saturation during the interval.

8. Using the new value of S_o without ΔS_{om} being added for the interval, recalculate the time taken for the interval.

9. Using the new value of S_o with ΔS_{om} being added for the interval, recalculate k_g/μ_g, k_o/μ_o, thence the revised segregation rate q_m, and thence revised values to $V_{p\cdot or}$, m, and S_{om}. These revised values are now inserted and used in starting the calculation for the next interval.

The calculations for the intervals from now on follow the same general pattern but are greatly facilitated by keeping running plots of ΔS_o, ΔS_{om}, V_p, m, and the other variables against pressure. After the first interval, predicted values may be used from these plots, and the derivation of the second approximation as just described is made considerably more accurate, if not unnecessary in some cases.

OTHER EXTENSIONS TO THE MUSKAT EQUATION

It will be noted that the basic depletion performance equation consists of a simple expansibility multiplied by a simple fractional-flow equation. The extensions just given use the same fractional-flow equation but include extensions to the expansibility. It might be deduced from this that the most general depletion performance equation should be in the nature of the most general expansibility multiplied by the most general fractional-flow equation, and that in general specific extensions should involve the extension of either the one or the other part. This appears to be true providing production is only from one block. For instance, the given segregation case was derived by considering an extension to the expansibility and using subsidiary equations to identify the change in saturation due to the segregation itself. In general, it appears that extending the expansibility terms offers the more useful approach to extending the basic depletion performance equation.

It was mentioned earlier that with more than one block the treatment given includes two important assumptions. One is that the expansibility of a block outside the oil leg is freely available to the oil leg. The second is that none of the fluid from a block outside the oil leg is produced. The first assumption may be eliminated if the equation is modified in having a lag factor associated with the expansibility of any block outside the oil leg.

To eliminate the assumption that no outside block fluid should be produced, the fractional-flow equation must be changed to a form which will allow for the production of these fluids when they are produced through wells in the oil-leg block. Thus, with water produced from the oil-leg block the fractional-flow equation would have to be extended to include a term which would allow for this water production. However, if the case is to be considered where there is production outside the oil leg itself, these differential forms of the depletion performance equation cannot be used unless it is possible by some other means to express the relationship between the production from any one block to any other block. This is because the effective expansibility of any block would be the total expansibility less the production rate from the block itself. Equations of the nature developed by McCord[3] for gravity segregation in Western Venezuela are necessary to allow for multi-block production when no simple ratio of producing rates between blocks can be obtained.

CONCLUSIONS

1. Muskat's depletion performance equation may be derived by considering the expansion behavior of the reservoir hydrocarbon system together with a simple fractional-flow equation.

2. Using a more extended expansion behavior for a two-block system (secondary gas cap and oil leg), a depletion performance equation may be derived for gravity segregation in a depletion-drive reservoir.

3. This method of extending the expansion behavior

term leads to a simple way of including empirically determined influx rates into the basic equation.

4. In general, depletion performance equations may be tailor-made for reservoirs by dividing the reservoir into blocks in each of which saturations may be assumed uniform, considering the expansion behavior of each block and the related flow equations, and producing an equation of the nature of a set of expansibilities multiplied by a fractional-flow equation.

NOMENCLATURE*

B_r = rock volume factor referred to initial pore volume
m_p = ratio of pore volume of primary gas cap to that of oil leg
m_s = ratio of pore volume of secondary gas cap to that of oil leg at any time
m_a = ratio of pore volume of aquifer to that of oil leg
V_p = pore volume of any block
$V_{p\cdot ol}$ = pore volume of oil leg at any time
V_{ps} = pore volume of secondary gas cap at any time

*See AIME Symbols List in *Trans.* AIME (1957) 207, 363, for other symbol definitions.

SUBSCRIPTS

m = refers to segregation variable
p = refers to primary gas cap
s = refers to secondary gas cap

ACKNOWLEDGMENT

The author wishes to thank the Mene Grande Oil Co. for permission to publish this paper, and to express appreciation to his colleagues who helped in its preparation.

REFERENCES

1. Muskat, M.: *Physical Principles of Oil Production*, McGraw-Hill Book Co., N. Y. (1949) 408.
2. Martin, J. C.: "Reservoir Analysis Based on Gravity Segregation for Pressure Maintenance Operations", *Trans.* AIME (1958) **213**, 220.
3. Terwilliger, P. L., *et al*: "An Experimental and Theoretical Investigation of Gravity Drainage Performance", *Trans.* AIME (1951) **192**, 285.
4. Stahl, O. C., *et al*: "Gravity Drainage of Liquids from Unconsolidated Wilcox Sand", *Pet. Engr.* (Jan., 1943).
5. McCord, D. R.: "Performance Predictions Incorporating Gravity Drainage and Gas-Cap Pressure Maintenance—LL-370 Area, Bolivar Coastal Field", *Trans.* AIME (1953) 198, 231. ★★★

The Material Balance as an Equation of a Straight Line

D. HAVLENA
HUDSON'S BAY OIL & GAS CO., LTD.
CALGARY, ALTA., CANADA

A. S. ODEH
MEMBER AIME
SOCONY MOBIL OIL CO., INC.
DALLAS, TEX.

ABSTRACT

The material balance equation used by reservoir engineers is arranged algebraically, resulting in an equation of a straight line. The straight line method of analysis imposes an additional necessary condition that a successful solution of the material balance equation should meet. In addition, this algebraic arrangement attaches a dynamic meaning to the otherwise static material balance equation.

The straight line method requires the plotting of one variable group vs another variable group. The sequence of the plotted points as well as the general shape of the resulting plot is of utmost importance. Therefore, one cannot program the method entirely on a digital computer as is usually done in the routine solution of the material balance equation. If this method is applied, then plotting and analysis are essential.

Only the appropriate equations and the method of analysis and interpretation with comments and discussion are presented in this paper. Illustrative field examples for the various cases treated are deferred to a subsequent writing.

INTRODUCTION

One of the fundamental principles utilized in engineering work is the law of conservation of matter. The application of this principle to hydrocarbon reservoirs for the purpose of quantitative deductions and prediction is termed "the material balance method of reservoir analysis". While the construction of the material balance equation (MBE) and the computations that go with its application are not difficult tasks, the criteria that a successful solution of the MBE should fulfill have always been a problem facing the reservoir engineer.

True and complete criteria should embody necessary and sufficient conditions. The criteria which the reservoir engineer uses possess a few necessary but no sufficient conditions. Because of this, the answers obtained from the MBE are always open to question. However, the degree of their acceptability should increase with the increase in the number of the necessary conditions that they should satisfy.

Generally, the necessary conditions commonly used are (1) an unspecified consistency of the results and (2) the agreement between the MBE results and those determined volumetrically.

This second criterion is usually overemphasized. Actually, the volumetrically determined results are based on geological and petrophysical data of unknown accuracy. In addition, the oil-in-place obtained by the MBE is that oil which contributes to the pressure-production history,[1] while the volumetrically calculated oil-in-place refers to the total oil, part of which may not contribute to said history. Because of this difference, the disagreement between the two answers might be of paramount importance, and the concordance between them should not be overemphasized as the measure of correctness of either one.

In this paper, a third necessary condition of mathematical as well as physical significance is discussed. It is not subject to any geological or petrophysical interpretation, and as such, it is probably the most important necessary condition. It consists essentially of rearranging the MBE to result in an equation of a straight line. This straight line method of the MBE solution has invalidated a few long time accepted concepts. For instance, it has always been advocated that if a water drive exists, but one neglects to take it into account in the MBE, the calculated oil-in-place should increase with time. The straight line method shows that in some cases, depending on the size of the neglected aquifer, the calculated oil-in-place might decrease with time.

The straight line method requires the plotting of a variable group vs another variable group, with the variable group selection depending on the mechanism of production under which the reservoir is producing. The most important aspect of this method of solution is that it attaches a significance to the sequence of the plotted points, the direction in which they plot, and to the shape of the resulting plot. Thus, a dynamic meaning has been introduced into the picture in arriving at the final answer. Since the emphasis of this method is placed on the interpretation of the sequence of the points and the shape of the plot, one cannot completely automate the whole sequence to obtain "the best value" as normally done in the routine application of the MBE. If one uses the straight line method, then plotting and analysis *are musts*.

The straight line method was first recognized by van Everdingen, et al,[2] but for some reason it was never fully exploited. The advantages and the elegance of this method can be more appreciated after a few cases are carefully treated and worked out by it.

SOLUTION OF THE MATERIAL BALANCE EQUATION

SATURATED RESERVOIRS

The MBE for saturated reservoirs written in AIME symbols is

Original manuscript received in Society of Petroleum Engineers office Feb. 4, 1963. Revised manuscript received May 22, 1963. Paper presented at the U. of Oklahoma-SPE Production Research Symposium, April 29-30, 1963, in Norman, Okla.

[1]References given at end of paper.

$$N_p[B_t + B_g(R_p - R_{si})] + W_p - W_i - GiBig$$
$$= N\left[(B_t - B_{ti}) + \frac{B_{ti}}{1 - S_w}(c_f + S_w c_w)\Delta p + \frac{m B_{ti}}{B_{gi}}(B_g - B_{gi})\right] + W_e \quad . \quad . \quad . \quad . \quad . \quad . \quad . \quad (0)$$

The left hand side of Eq. 0 represents the net production in reservoir barrels and will be denoted by F. On the right hand side, the first term includes, respectively, the expansion of the oil E_o, the rock and connate water $E_{f,w}$, and the free gas E_g. The second term represents the water influx which is given by[3,4]

$$W_e = C\Sigma\Delta pQ(\Delta t_D)$$

For saturated reservoirs, one normally neglects the rock and water expansion $E_{f,w}$. Thus, Eq. 0 becomes

$$F = NE_o + Nm\frac{B_{ti}}{B_{gi}}E_g + C\Sigma\Delta pQ(\Delta t_D) \quad . \quad . \quad (0a)$$

Eq. 0a is the expanded form of the MBE, where the three mechanisms of production, i.e., oil expansion, $E_o = (B_t - B_{ti})$, gas expansion, $E_g = (B_g - B_{gi})$ and water drive are included. Absence of one or two of the above mechanisms requires deletion of the appropriate terms from the equation.

In the figures that follow, the sequence of the individual plotted points, calculated for increasing cumulative production, will be indicated by an arrow.

No Water Drive, No Original Gas Cap

$$F = NE_o \quad . \quad . \quad . \quad . \quad . \quad . \quad . \quad . \quad . \quad . \quad . \quad . \quad (1)$$

A plot of F vs E_o should result in a straight line going through the origin with N being the slope, Fig. 1. It should be noted that the origin is a *must* point; thus, one has a fixed point to guide the straight line plot.

No Water Drive, A Known Gas Cap

$$F = N(E_o + m\frac{B_{ti}}{B_{gi}}E_g) \quad . \quad . \quad . \quad . \quad . \quad . \quad . \quad (1a)$$

A plot of F vs $(E_o + m\frac{B_{ti}}{B_{gi}}E_g)$ should result in a straight line going through the origin with a slope of N.

No Water Drive, N and m are Unknown

The appropriate MBE is written in two forms so as to result in two methods of solution, Eqs. 2a and 2b.

$$\frac{F}{E_o} = N + G\frac{E_g}{E_o} \quad . \quad . \quad . \quad . \quad . \quad . \quad . \quad . \quad . \quad . \quad . \quad (2a)$$

where $G = Nm\frac{B_{ti}}{B_{gi}}$ = the original gas-cap gas in scf. A plot of $\frac{F}{E_o}$ vs $\frac{E_g}{E_o}$ should result in a straight line with N being the Y intercept and G being the slope, Fig. 2a.

$$F = N\left(E_o + m\frac{B_{ti}}{B_{gi}}E_g\right) \quad . \quad . \quad . \quad . \quad . \quad . \quad . \quad . \quad (2b)$$

Assume an m and plot F vs $\left(E_o + m\frac{B_{ti}}{B_{gi}}E_g\right)$. If the assumed m is correct, the plot will be a straight line going through the origin with N being the slope. If the assumed m is too small the line will go through the origin but will curve upward. If the assumed m is too large the line will go through the origin but will curve downward (Fig. 2b). Several values of m are assumed until the straight line going through the origin plot is satisfied.

As the reader will appreciate, the solution (Eq. 2b) is a more powerful method than the one in Eq. 2a since it specifies that the line must go through the origin. However, for checking purpose it is recommended that both methods be used in every case.

Water Driven Reservoirs, Two Unknowns

Water Drive, No Original Gas Cap:

$$\frac{F}{E_o} = N + C\frac{\Sigma\Delta pQ(\Delta t_D)}{E_o} \quad . \quad . \quad . \quad . \quad . \quad . \quad . \quad . \quad (3a)$$

Assume an aquifer configuration, an $\frac{r_e}{r_w}$ and a dimensionless time Δt_D. Calculate $\Sigma\Delta pQ(\Delta t_D)$ and plot $\frac{F}{E_o}$ vs $\frac{\Sigma\Delta pQ(\Delta t_D)}{E_o}$. If the assumed aquifer and dimensionless

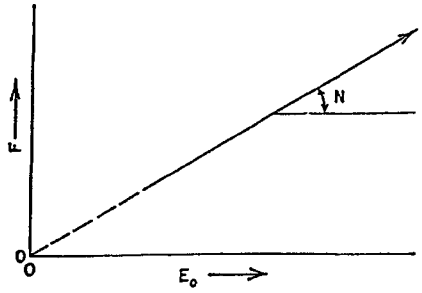

FIG. 1—F vs E_o

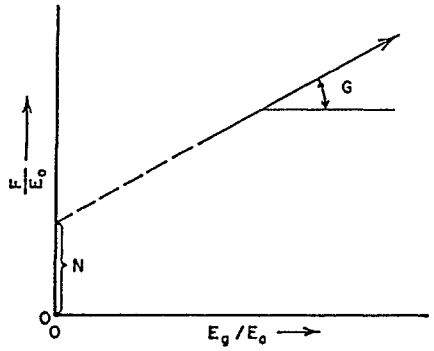

FIG. 2A—$\frac{F}{E_o}$ vs $\frac{E_g}{E_o}$

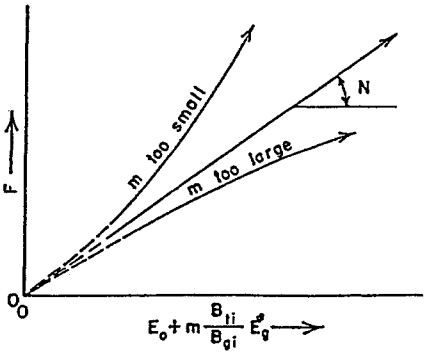

FIG. 2B—F vs $(E_o + m\frac{B_{ti}}{B_{gi}}E_g)$

ume are correct, the plot will be a straight line with N being the Y intercept and C being the slope.

Four other different plots beside the straight line may result. These are a complete scatter, a line curved upward, a line curved downward, and an S-shaped curve (Fig. 3a).

Complete random scatter of the individual points indicates that the calculations and/or the basic data are in error. A systematically upward or downward curved line suggests that the $\Sigma\Delta pQ(\Delta t_D)$ is too small or too large, respectively. This means that the assumed $\frac{r_e}{r_w}$ and/or the Δt_D are, respectively, too small or too large. An S-shaped curve indicates that a better fit could be obtained if a linear water influx is assumed.

The sequence of the plotted points as indicated by the arrow of Fig. 3a will persist as long as the aquifer behaves like an infinite one. This is particularly applicable for infinite or fairly large aquifers. In this case, non-steady state water influx calculations are a must. On the other hand, if one suspects the presence of a small aquifer, in which steady-state depletion type flow would obtain in a short time after production commences, then, it is better to start with the case shown in Eq. 3b.

After satisfactory values for $\frac{r_e}{r_w}$ and for Δt_D are chosen, the results can be refined by applying the standard deviation test suggested by van Everdingen, et al.[2] The most probable values for N and C will be those corresponding to the dimensionless time which gives the minimum standard deviation, σ min.

In some reservoirs the standard deviation σ plotted vs log Δt_D will not give a sharp minimum but will be "dish-shaped". This phenomenon usually results from the fact that the particular reservoir is insensitive to the changes of Δt_D. The establishment of the most probable value of Δt_D becomes, in such a case, only of academic interest.

An additional criterion used to judge the most probable values for N and C is called the consistency test, which is described in the following. Several Δt_D values around the minimum point of the standard deviation plot are read. For every chosen Δt_D, N and C as functions of real time are calculated. Plots of N vs real time and C vs real time are constructed, and by means of the least square method, the best straight line is drawn through the points of every plot. The slopes of the N and C straight lines are then calculated and plotted vs their corresponding Δt_D values on a common graph paper. The intersection of the two plots gives the most probable value for the Δt_D. Theoretically, the two plots should intersect at a value of zero slope. This is true because if the correct $\frac{r_e}{r_w}$ and Δt_D are chosen, and if the field data are correct, then N and C should not vary with time, i.e., the N-time plot as well as the C-time plot should result in a zero slope.

As it is evident from the foregoing, there are two basic sources of errors, systematic and random, which could prevent the obtention of a straight line when Eq. 3a is applied. Proper statistical analysis could indicate which source causes the linearity of the plot predicted by Eq. 3a not to be satisfied. In addition, statistical methods[1,2] could be used in the consistency test to determine for a preassigned degree of probability the confidence band for the calculated values of N and C.

In many large fields it is often found that an infinite linear water drive satisfactorily describes the production-pressure behavior of the said fields. For a unit pressure drop, the cumulative water influx in an infinite linear case is simply proportional to $\sqrt{t}$ and does not require the estimation of a dimensionless time. Thus, the summation term in Eq. 3a becomes $\Sigma\Delta p_n\sqrt{t - t_n}$. Because of this, it is suggested to try first the infinite linear case to determine if a successful solution could be obtained. However, even in such a case, the confidence band should be evaluated as a numerical aid in judging the acceptability of N and C.

Very Small Aquifer: In this case the water influx W_e could be represented by either

$$W_e = \Sigma\Delta pQ(\Delta t_D)$$

or by the approximate but simpler equation

$$W_e = C'\Delta p'$$

where $\Delta p' = p_i - p$, $C' = Wc_w$, W is the water volume in the aquifer and the assumption is made that a steady-state depletion condition obtains. The MBE becomes

$$\frac{F}{E_o} = N + C'\frac{\Delta p'}{E_o} \quad \ldots\ldots\ldots\ldots \quad (3b)$$

A plot of $\frac{F}{E_o}$ vs $\frac{\Delta p'}{E_o}$ should result in a straight line with N being the Y intercept and C' being the slope. The points will plot *backwards* as shown in Fig. 3b.

The reversal in the sequence of points is based on the fact that E_o increases faster than $\Delta p'$. Thus, $\frac{\Delta p'}{E_o}$ decreases as the pressure decreases. Since C', the water influx constant, is always positive and is given by the slope of the

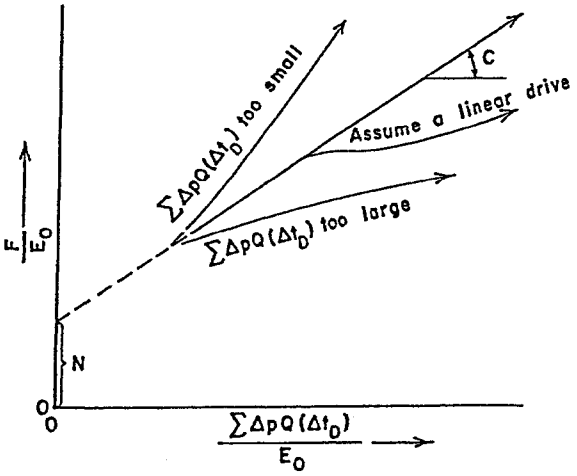

FIG. 3A—$\frac{F}{E_o}$ vs $\frac{\Sigma\Delta pQ(\Delta t_D)}{E_o}$

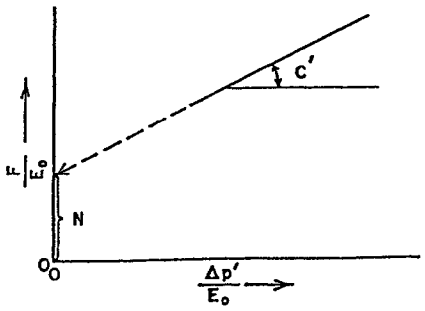

FIG. 3B—$\frac{F}{E_o}$ vs $\frac{\Delta p}{E_o}$

straight line plot, then of necessity $\frac{F}{E_o}$ should also decrease as the pressure decreases. Therefore, the points *must move in a backward sequence.*

Thus, in this case, if one neglects to take into account the water influx when performing the MBE calculations, the resulting $\frac{F}{E_o}$ which is equal to the apparent N will decrease with time.

In practical application it is often found that such a steady-state water influx sets in after a certain period of time, the length of which depends mainly on the size of the aquifer. In such a case, the plotted points, representing the early period of reservoir history during which the non-steady state water influx prevails, will plot in a forward sequence as in Fig. 3a. However, when the effect of the boundary becomes appreciable, the plotted points will reverse the sequence and plot backwards.

Sometimes, an appreciable change in the exploitation policy of the reservoir might temporarily reverse the sequence. Even in such a case the points must remain on a straight line if the correct parameters were assumed.

Having determined C', one can calculate the amount of water W contained within the aquifer since $C' = Wc_w$.

Water Drive, A Known Gas Cap:

$$\frac{F}{E_o + m\frac{B_{ti}}{B_{gi}}E_g} = N + C\frac{\Sigma\Delta pQ(\Delta t_D)}{E_o + m\frac{B_{ti}}{B_{gi}}E_g} \quad . \quad . \quad (3c)$$

A plot of the left hand side of Eq. 3c vs the variable term of the right hand side should result in a straight line if the correct aquifer and dimensionless time are assumed. If the line is not straight, then what was discussed in Eq. 3a under saturated reservoirs section applies also here.

Very Small Aquifer, A Known Gas Cap:

$$\frac{F}{E_o + m\frac{B_{ti}}{B_{gi}}E_g} = N + C'\frac{\Delta p'}{E_o + m\frac{B_{ti}}{B_{gi}}E_g} \quad . \quad . \quad (3d)$$

A plot of the left hand side of Eq. 3d versus the C'—term should result in a straight line. The points will plot backwards as shown in Fig. 3b.

Before closing the water drive section, it must be pointed out that it is not necessary to know the dimensionless time and/or the $\frac{r_e}{r_w}$ of the system. Any assumed values that satisfy the linearity of the plot are acceptable solutions. Thus, it is possible, at least theoretically, to find more than one set of aquifer properties which give a solution. However, the N's and W_e's evaluated for such cases would be identical.

In addition to the fact that too large $\frac{r_e}{r_w}$ or Δt_D will bend the line downward, interference between the reservoirs will result in the same effect. Thus, if interference is suspected, one must correct for it before applying the straight line criteria. The straight line equation to be plotted in such a case is

$$\frac{F + \text{Correction for interference}}{E_o} = N + C\frac{\Sigma\Delta pQ(\Delta t_D)}{E_o}$$

Refs. 5 and 6 outline a method for calculating the interference correction factor.

Water Drive, Original Gas Cap and N Are Unknown

Eq. 0a is differentiated with respect to pressure and the resulting equation is used with Eq. 0a to elminate m. The final equation is rearranged to give

$$\frac{Fb' - F'b}{E_o b' - E_o' b} = N + \frac{C}{E_o b' - E_o' b}\left[b'\Sigma\Delta pQ(\Delta t_D) - b\left(\Sigma\Delta pQ(\Delta t_D)\right)'\right] \quad . \quad . \quad . \quad . \quad . \quad . \quad . \quad . \quad . \quad . \quad . \quad (4)$$

where $b = \frac{B_{ti}}{B_{gi}}E_g$. The primes denote derivatives with respect to pressure.

Thus, a plot of the left hand side of Eq. 4 vs the C—term of the right hand side should result in a straight line with N being the Y intercept and C being the slope, provided the correct aquifer is chosen. When N and C are determined, then Eq. 0a is used to solve for m as a function of real time. The best value of m is then calculated by least squares.

For greater accuracy the derivatives of the summation term $\Sigma\Delta pQ(\Delta t_D)$ should be evaluated by using the derivatives of the $Q(t_D)$ function with the corresponding pressure drops.[8]

UNDERSATURATED RESERVOIRS

No Water Drive

$$N_p B_o = NB_{oi}\frac{(S_o c_o + S_w c_w + c_f)\Delta p'}{1 - S_w} \quad . \quad . \quad . \quad . \quad (5)$$

A plot of $N_p B_o$ vs $\frac{B_{oi}\Delta p'}{1 - S_w}(S_o c_o + S_w c_w + c_f)$ should result in a straight line going through the origin similar to Fig. 1 with N being the slope. $\Delta p' = p_i - p$.

With Water Drive

$$\frac{N_p B_o + W_p - W_i}{\frac{B_{oi}\Delta p'}{1 - S_w}(S_o c_o + S_w c_w + c_f)} = N + c\frac{\Sigma\Delta pQ(\Delta t_D)}{\frac{B_{oi}\Delta p'}{1 - S_w}(S_o c_o + S_w c_w + c_f)} \quad . \quad . \quad . \quad . \quad (6)$$

The procedure is similar to that given in Eq. 3a under saturated reservoirs section. A plot of the left-hand side of Eq. 6 vs the C—term of the right-hand side should result in a straight line with N being the Y intercept and C being the slope. If the plot is not straight, refer to the discussion under Eq. 3a.

GAS RESERVOIRS

No Water Drive

$$G_p B_g = GE_g \quad . \quad . \quad . \quad . \quad . \quad . \quad . \quad . \quad . \quad . \quad . \quad . \quad (7)$$

A plot of $G_p B_g$ vs E_g should result in a straight line going through the origin, similar to Fig. 1 with G being the slope.

With Water Drive

$$\frac{G_p B_g + W_p - W_i}{E_g} = G + C\frac{\Sigma\Delta pQ(\Delta t_D)}{E_g} \quad . \quad . \quad (8)$$

A plot of $\frac{G_p B_g + W_p - W_i}{E_g}$ vs $\frac{\Sigma\Delta pQ(\Delta t_D)}{E_g}$ should result

in a straight line with G being the Y intercept and C being the slope. The procedure of the analysis is identical with that advanced in Eq. 3a of the saturated reservoirs section. If the aquifer is very small, then Eq. 3b applies.

DISCUSSION

The straight line method of solving the material balance equation differs from the commonly used one, in that it imparts a dynamic meaning to the individual points. The usual method considers each calculated point separately or some averaging technique, whereas the straight line method stresses the dynamic sequence of the plotted points and the shape of the resulting plot. Because of this, plotting and analyzing the calculated points are of utmost importance for an intelligent interpretation.

Although it is theoretically possible to solve by the straight line method for all the cases treated in this paper, the authors have met only limited success in Cases 2 and 4 under the saturated reservoirs section. This is so, because whenever a gas cap is to be solved for, an exceptional accuracy of basic data, mainly pressures, is required. Furthermore, the presence of the derivatives with respect to pressure in Case 4 adds more to the necessity of exceptionally accurate data.

The rest of the cases, especially when water drive exists, have been tested on many field examples with remarkable success. The shape of the resulting plot and usual sequence of the plotted points have been of great help in gaining understanding to the problem at hand.

Often it is found that the points calculated for the early history do not conform with the latter points. This is caused either by inaccuracy of the early average production-pressure-PVT data or because pressure-production effect has not yet been felt by all the active oil-in-place. In such cases these early points should not be considered in drawing the best straight line. Moreover, once the points to be excluded are decided upon, the same points must be excluded from all subsequent analyses.

In conclusion, it should be stressed that the straight line requirement does not suffice to prove the uniqueness of the solution, but is only one of the conditions that a satisfactory solution should meet. The quantity and quality of the derived information will depend on the quantity and quality of the data; and last but not least, on the experience, judiciousness, and ingenuity of the analyst.

ACKNOWLEDGEMENT

The material presented in this paper represents the contribution of many people, especially Van Everdingen, et al., who first recognized the straight line concept. Full credit it due them. Part of this work was done while the authors were employed by Mobil Oil Co. de Venezuela. Gratitude is expressed to J. Jones-Parra of that company for useful criticism. The authors would like also to thank the management of Socony Mobil Oil Co., Inc. for permission to publish this paper.

REFERENCES

1. Schilthuis, R. J.: "Active Oil and Reservoir Energy", *Trans.*, AIME (1936) **148**, 33.
2. van Everdingen, A. F., Timmerman, E. H. and McMahon, J. J.: "Application of the Material Balance Equation to a Partial Water-Drive Reservoir", *Trans.*, AIME (1953) **198**, 51.
3. Hurst, W. and van Everdingen, A. F.: "The Application of the Laplace Transformation to Flow Problems in Reservoirs", *Trans.*, AIME (1949) **186**, 305.
4. Chatas, A. T.: "A Practical Treatment of Nonsteady-State Flow Problems in Reservoir Systems", *Pet. Engr.* (1953) **25**, No. 6, 13.
5. Mortada, M.: "A Practical Method for Treating Oil Field Interference in Water-Driven Reserves", *Trans.*, AIME (1955) **204**, 217.
6. Robinson, M.: "Pressure Interference Correction to the Material Balance Equation for Water-Drive Reservoirs Using a Digital Computer", *Trans.*, AIME (1958) **213**, 418.
7. Simon, L. E.: *An Engineer's Manual of Statistical Methods*, John Wiley and Sons, Inc., New York.
8. Deming, W. E.: *Statistical Adjustment of Data*, John Wiley and Sons, Inc., New York. ★★★

The Material Balance as an Equation of a Straight Line—Part II, Field Cases

D. HAVLENA
A. S. ODEH
MEMBER AIME

HUDSON'S BAY OIL AND GAS CO., LTD.
CALGARY, ALTA.
SOCONY MOBIL OIL CO.
DALLAS, TEX.

ABSTRACT

The use of the straight-line method of solving the material balance equation is illustrated by means of six field cases. Also, the application of statistical criteria to arrive at the most probable answer is shown. The theory underlying the straight-line method of solution and the applicability of the statistical criteria was presented in a previous paper.[1]

The field cases include saturated and undersaturated oil reservoirs with and without water drive. The aquifers discussed are: limited radial, infinite radial, very small aquifer and infinite linear. The field cases also include a gas reservoir producing under water drive.

INTRODUCTION

In a previous paper,[1] the authors presented the theory underlying the solution of the material balance as an equation of a straight line. The appropriate equations for various material balance cases as well as the methods of analysis and interpretation with comments and discussion were also included.

To illustrate the various theoretical cases treated previously, five field cases are analyzed in this paper by employing the straight-line method of solving the material balance equation (MBE) and one example previously published is referred to. The use of statistical criteria to arrive at the most probable answer is also shown.

All the field examples presented, except Case 2, are excerpts from complete reservoir studies. To illustrate the method, only sections specifically dealing with the material balance principles are included. Additional geologic information and basic data are reported to better acquire an understanding of the cases and thus to better follow the reasoning that suggested the successful application of the straight-line method of solving the MBE. The six cases are: (1) saturated reservoir, small gas cap, limited aquifer; (2) saturated reservoir, very small gas cap, infinite aquifer; (3) undersaturated-saturated reservoir, very small aquifer; (4) highly undersaturated reservoir, no water drive; (5) high undersaturated one-well reservoir, limited aquifer; and (6) gas reservoir, infinite linear aquifer.

Original manuscript received in Society of Petroleum Engineers office Feb. 17, 1964. Revised manuscript received May 25, 1964.

[1]References given at end of paper.

WATER DRIVE, A KNOWN GAS CAP

THE D_4 SAND, GUICO FIELD, VENEZUELA

The D_4 sand, which was discovered in 1943, is presently in a depleted state. Since its discovery it has produced under water drive, gas-cap-gas expansion, and solution gas drive. In Nov., 1947, water injection was initiated to arrest further pressure decline.

When discovered, the D_4 sand was a saturated reservoir with a gas cap/oil zone volume ratio m estimated volumetrically at 0.0731, an average permeability of 500 md, a porosity value of 25 per cent, and an oil viscosity at reservoir conditions of 0.3 cp. The volumetrically determined stock-tank oil initially in place was 23.1 million bbl. The volumetrically weighted physical data and production data available until Nov., 1953 are reported in Table 1.

In Ref. 1, the effects on the straight-line plot of various values of r_e/r_w for a constant Δt_D, or of various dimensionless times for a constant r_e/r_w, were theorized and were illustrated in Fig. 3A of that reference. In this field case, the previously theoretically predicted effects are established. Thus, the MBE calculations using Eq. 3c of Ref. 1 were performed for various r_e/r_w and dimensionless time values. Eq. 3c of Ref. 1 is:

$$\frac{F}{E_o + m\frac{B_{oi}}{B_{gi}}E_g} = N + C\,\frac{\Sigma\Delta pQ(\Delta t_D)}{E_o + m\frac{B_{oi}}{B_{gi}}E_g}$$

where F=net production in reservoir barrels, $E_o = B_t - B_{oi}$, and the other symbols conform to AIME standards.

In Fig. 1, three MBE plots are shown. The plot for

TABLE 1—PRESSURE-PRODUCTION-INJECTION HISTORY AND PVT DATA—THE D_4 SAND, GUICO FIELD, VENEZUELA

Date	Pressure (psig)	Cum. Oil Produced N_p (MM bbl)	Cum. GOR R_p (cu ft/bbl)	Cum. Water Produced W_p (MM bbl)	Cum. Water Injected W_i (MM bbl)	Total Formation Volume Factor B_t	Gas Formation Volume Factor $B_g \times 10^2$
10-7-43	2055	0	—	—	—	1.5166	1.2217
4-30-45	1964	1.383	970	—	—	1.5451	1.2835
9-30-45	1924	2.087	971	—	—	1.5623	1.3130
2-28-46	1897	2.861	966	—	—	1.5730	1.3337
5-31-46	1879	3.400	960	—	—	1.5808	1.3480
7-31-46	1846	3.770	952	0.001	—	1.5957	1.3745
4-30-47	1814	5.203	913	0.024	—	1.6107	1.4017
6-30-47	1799	5.494	909	0.028	—	1.6179	1.4143
9-30-47	1781	5.944	904	0.042	—	1.6270	1.4302
4-30-48	1778	7.967	916	0.013	0.478	1.6285	1.4330
5-31-49	1760	8.907	927	0.130	0.864	1.6376	1.4498
10-31-49	1750	9.555	939	0.222	1.124	1.6429	1.4590
6-30-50	1738	10.520	952	0.322	1.674	1.6491	1.4703
2-28-51	1736	11.655	956	0.442	2.238	1.6502	1.4723
6-30-51	1764	12.188	959	0.489	2.459	1.6355	1.4440
11-30-51	1734	12.790	963	0.557	2.752	1.6513	1.4742
1-31-52	1729	13.022	970	0.603	2.875	1.6541	1.4792
5-31-52	1704	13.463	984	0.717	3.159	1.6681	1.5040
11-30-52	1719	14.081	997	0.893	3.610	1.6597	1.4890
6-30-53	1747	14.651	1001	0.932	4.253	1.6446	1.4618
11-30-53	1722	15.092	1005	0.966	4.699	1.6380	1.4860

$r_e/r_w = 15$ and $t_D = 0.3t$ results in a line curving upward. This indicates that the latter values of the $\Sigma\Delta pQ(\Delta t_D)$ are too small relative to the early values. By examining the van Everdingen-Hurst $Q(t_D)$ function vs t_D for an $r_e/r_w = 15$ and for a closed exterior boundary, one notices that the maximum rate of increase in $Q(t_D)$ occurs for $100 \leq t_D \leq 500$. For $t_D > 500$ the $Q(t_D)$ vs t_D plot starts to level off and reaches its steady-state values at $t_D \simeq 1{,}000$. For the dimensionless time $t_D = 0.3t$ that was used, most of the points fell in the range $t_D > 500$. This resulted in a too slow rate of increase of $\Sigma\Delta pQ(\Delta t_D)$ as is evident in Fig. 1. To correct for this, one must decrease t_D. This was done and a $t_D = 0.078t$ resulted in a straight-line plot and an oil-in-place value of about 27 million STB.

In this case it was necessary to decrease t_D to correct for the upward bending. In other cases, depending on the shape of the $Q(t_D)$ vs t_D plot of interest, it may be necessary to increase t_D for the same condition. One must examine carefully the $Q(t_D)$ vs t_D plot of interest to determine if t_D should be increased or decreased to straighten out the MBE plot.

To show the effect of r_e/r_w for a constant t_D, several values of r_e/r_w were assumed. The calculations were performed for a $t_D = 0.3t$. The effect of increasing r_e/r_w is to increase the latter values of $\Sigma\Delta pQ(\Delta t_D)$ faster than the early values, which ultimately results in downward bending of the MBE plot, as in Fig. 1.

It must be noted that various combinations of r_e/r_w and t_D might satisfy the straight-line requirement imposed on the successful solution. However, to obtain the most probable value for N, the aquifer configuration, and t_D and r_e/r_w when applicable, one must resort to the statistical criteria advocated in Ref. 1. These criteria were not applied in this field case as they are illustrated fully in other cases and because the interest in this field case was mainly to show the effect of Δt_D and r_e/r_w values on the predicted straight-line plot.

A summary of the calculations is given in Table 2. The starting point of these calculations was April 30, 1947, when the reservoir pressure had declined by about 200 lb. However, the reference point for the water-influx calculations was the discovery date, Oct., 1943.

STURGEON LAKE SOUTH D-3 POOL, CANADA

This field example was reported in detail in the *Journal of Canadian Petroleum Technology*.[2] In the study, complete data both in numerical and graphical form are presented. The material balance as an equation of a straight line is applied, and the use of the consistency test and the determination of the confidence band for a pre-assigned degree of probability are fully illustrated.

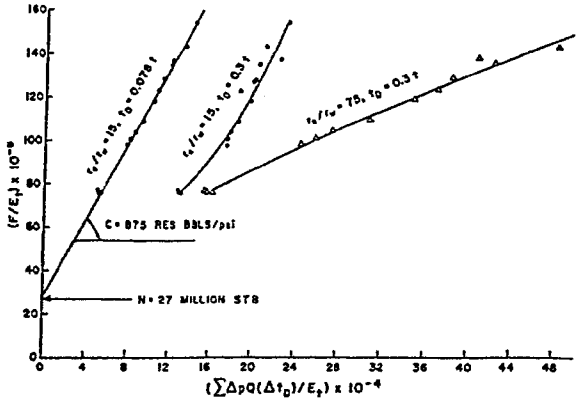

FIG. 1—D_4 SAND, GUICO FIELD.

WATER DRIVE, VERY SMALL AQUIFER, THE L-2b RESERVOIR, NORTH OSCUROTE, VENEZUELA

GENERAL DESCRIPTION

This dipping (3 to 5°) sand reservoir is limited at its updip side by an extensive fault of some 300 ft displacement and at both edges by minor faults which are more or less perpendicular to the main fault. The sand is fairly silty, and rather poorly sorted with numerous discontinuous shale breaks. It is composed of several lenticular bodies, a few of which are continuous through the entire investigated area. The reservoir was discovered in 1953, and in 1958 it was exploited by a total of 24 successful producers. The reservoir thickness ranged between 15 and 25 ft, and from numerous core analyses the following average properties were established: porosity = 18 per cent, connate-water saturation = 24 per cent, permeability = 580 md, and the stock-tank oil initially in place = 747 bbl/acre-ft. The volumetrically calculated stock-tank oil initially in place ranged between 30.6 and 37.2 million bbl depending on the location of the original oil-water contact, which was estimated to be between 9,050 and 9,100 ft subsea.

By June, 1960, cumulative oil production amounted to 5.54 million STB. The maximum number of wells producing at any particular month was 15, which was attained in 1956. Since that time, the number of producers diminished as additional wet wells were shut in. Thus, the instantaneous monthly water production was maintained at less than 10 per cent while the cumulative water cut reached 6.5 per cent in 1960. The cumulative gas-oil ratio increased slowly and surpassed the solution gas-oil ratio of 705 by only 60 cu ft/bbl.

Due to the advancing water table, a variable pressure datum corresponding to the volumetric midpoint of the oil leg was used. This procedure resulted in a 120-ft upward change in the reference pressure datum during the productive life of the field. Average reservoir pressures were always referred to the proper datum. The original pressure at the oil-water contact was evaluated from data reported on low structural wells. The original pressures used in this study were 3,909 and 3,985 psig for the oil reservoir and the oil-water contact, respectively. The bubble-point pressure was 3,765 psig at the original datum of 8,975 ft subsea. B_t was equal to

TABLE 2—MBE CALCULATIONS, THE D_4 SAND, GUICO FIELD, VENEZUELA

Pressure (psig)	E_t*	$F=(Np^{**}+W_p-W_i)$ (MM bbl)	$(F/E_t)10^{-6}$	$[\Sigma\Delta pQ(\Delta t_D)/E_t] \times 10^{-6}$ $r_e/r_w=15$ $t_D=0.078t$	$[\Sigma\Delta pQ(\Delta t_D)/E_t] \times 10^{-6}$ $r_e/r_w=15$ $t_D=0.3t$	$[\Sigma\Delta pQ(\Delta t_D)/E_t] \times 10^{-6}$ $r_e/r_w=75$ $t_D=0.3t$
1814	0.1104	8.499	76.98	5.17	12.88	15.48
1799	0.1188	8.987	75.65	5.24	12.91	15.71
1781	0.1293	9.747	75.38	5.42	13.16	16.34
1778	0.1311	12.782	97.50	7.86	17.53	24.41
1760	0.1417	14.200	100.21	8.22	17.56	25.85
1750	0.1478	15.340	103.79	8.66	17.96	27.55
1738	0.1551	16.801	108.32	9.41	18.59	30.48
1736	0.1563	18.397	117.70	10.42	19.64	34.44
1764	0.1391	19.002	136.61	12.22	22.41	40.82
1734	0.1576	20.113	127.62	11.34	20.14	38.42
1729	0.1609	20.615	128.12	11.37	19.98	38.87
1704	0.1771	21.716	122.62	10.81	18.65	37.14
1719	0.1674	22.573	134.84	12.15	20.44	42.41
1747	0.1498	22.937	153.12	14.27	23.10	50.88
1722	0.1654	23.644	142.95	13.37	21.06	48.37

*$E_t = \frac{mB_{ti}(B_g - B_{gi})}{B_{gi}} + (B_t - B_{ti}),\ m = 0.0731$

**$B_t + (R_p - R_{si})B_g$ $R_{si} = 900$ cu ft/bbl

$$1.42\left[\frac{3{,}779-p}{\alpha p+\beta p^2+\gamma p^3}+1\right]$$

where $\alpha = 2.34212$, $\beta = 0.25542 \times 10^{-3}$ and $\gamma = 0.05047 \times 10^{-6}$.

MATERIAL BALANCE CALCULATIONS

From pressure vs production plot, cumulative production before reaching the bubble-point pressure was estimated. This amount in reservoir barrels was subtracted as a constant from the cumulative net production F in all subsequent MBE calculations which were referred to the bubble-point pressure.

Fig. 2 gives the plot of a depletion-type MBE, $F = NE_o$, as shown in Eq. 1, Ref. 1. The early part of the plot, up to Point 5 corresponding to June, 1956, results in a straight line going through the origin. Beyond that date the points deviate from the straight line.

This behavior is easily explained if a very small aquifer exists. In this case[1]

$$F - \text{const} = NE_o + W_eE_{w,f}$$

where W_e is the aquifer water volume in reservoir barrels, and $E_{w,f}$ is the total water and rock expansion. The PVT properties for this reservoir show that E_o approximately varies linearly with p for $3{,}380 \leq p \leq 3{,}765$. The pressure in June, 1956, was 3,360. Thus, for this range of pressure E_o per unit pressure change is nearly constant. Since $E_{w,f}$ is also constant for all pressure ranges, then up to June, 1956, the MBE can be written as

$$F - \text{const} = (N + aW_e)E_o$$

where $a = \frac{E_{w,f}}{E_o}$. A plot of $(F - \text{const})$ vs E_o should result in a straight line with a slope equal to $(N + aW_e)$.

For $p < 3{,}380$, the relation between E_o and pressure begins to deviate considerably from linear and the above MBE equation does not hold. Thus, the points will deviate from the straight line, as Fig. 2 shows.

Because of the above behavior and because of the steady and rather large decline in pressure, the presence of a very small aquifer was suspected. Consequently Eq. 3b of Ref. 1 was used. [$F/E_o = N + C'(\Delta p'/E_o)$, where $\Delta p' = p_i - p$ and $C = Wc_{w,f}$]. It resulted in Fig. 3. As predicted by this equation the plot resulted in a straight line moving in a backward sequence with time. Point 1 corresponds to June, 1955, and Point 20 corresponds to June, 1960. The intersection of the straight line with the ordinate gave an original oil-in-place value of 32.6 million STB.

CALCULATION OF AQUIFER SIZE

A depletion-type MBE of the following form was employed: $F - \text{const} = N(E_o + nB_wE_{w,f})$ where $n = W/N$, B_w is the initial water formation volume factor, and $E_{w,f}$, the total water and rock expansion, is equal to $c_{w,f}\Delta p'$. W is the aquifer size in stock-tank barrels.

A plot of $(E_o + nB_wE_{w,f})$ vs $(F - \text{const})$ should result in a straight line going through the origin if the correct value for n is assumed. Such a straight line was obtained for a value of n of 14.2 and is shown in Fig. 4. Thus, the aquifer contained about 0.5 billion bbl of water.

The aquifer size could also be calculated from the slope of the straight-line plot of Fig. 3, which is equal to $Wc_{w,f}$. This was done and the value of 0.5 billion bbl of water was verified.

APPLICATION OF STATISTICAL CRITERIA

To check the above solutions, the standard deviation and consistency tests were applied. These tests are illustrated fully in Sturgeon Lake South D-3 reservoir, referred to previously. Therefore they will not be discussed in detail here. However, the results of the statistical investigation showed that a bubble-point pressure of 3,760 would have been a better choice than 3,765. The new bubble point pressure (3,760) resulted in an initial oil-in-place of 32.8 million STB. The standard deviation was 0.06 million STB, and the slope of the straight line of the consistency test plot for a four-year period (July 1, 1956, to June 30, 1960) was 2,560 STB/month. The confidence band for a probability range of 75 to 90 per cent was ± 1.2 million STB, and for a probability range of 95 to 100 per cent was ± 1.7 million STB.

DETERMINATION OF THE ORIGINAL OIL-WATER CONTACT

Three positions for the original oil-water contact were assumed. These were 9,100, 9,072 and 9,050 ft sub-

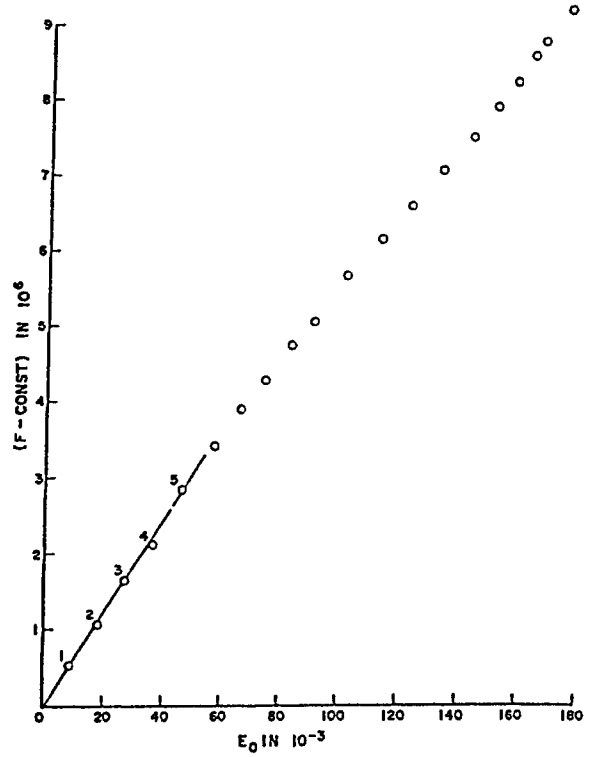

FIG. 2—L-2b RESERVOIR, OIL EXPANSION VS NET PRODUCTION.

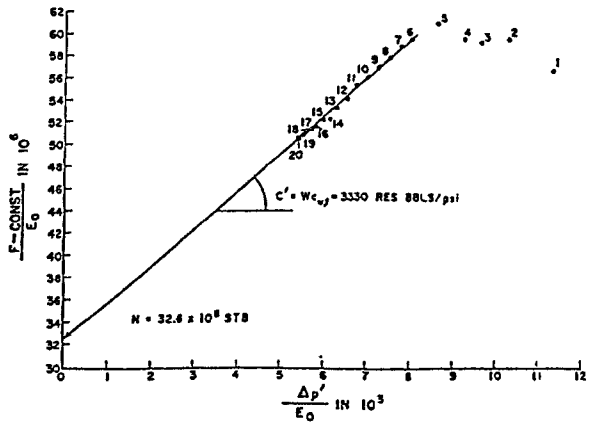

FIG. 3—L-2b RESERVOIR, SMALL AQUIFER PLOT.

sea. The position of the oil-water contact as a function of time was determined from production data by assuming that in a well the instantaneous produced per cent water in total fluid is equal to the flooded-out productive interval divided by the total productive interval expressed in per cent. This assumption clearly neglects coning.

Having determined the position of the oil-water contact with time, the flooded-out volume as a function of time for the three assumed values of the original position of the oil-water contact were calculated and plotted vs the net cumulative water influx, $We - Wp$, which was obtained from the MBE. The original oil in place was taken as 32.8×10^6 STB. This plot is shown in Fig. 5.

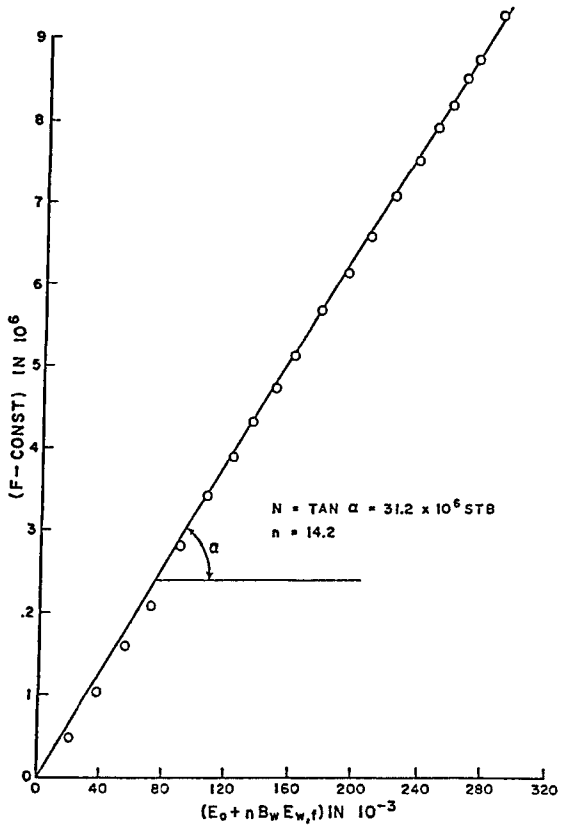

FIG. 4—L-2b RESERVOIR, NORTH OSCUROTE, DETERMINATION OF N AND AQUIFIER SIZE.

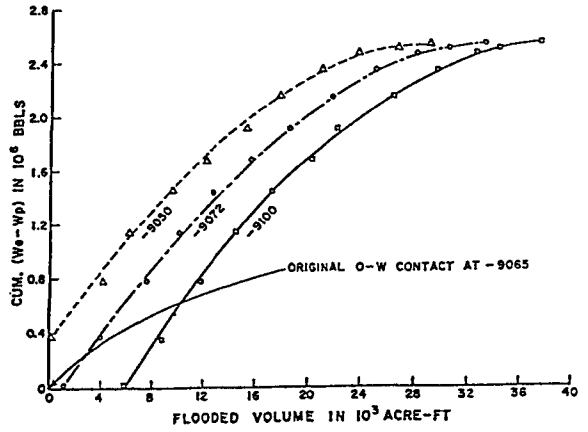

FIG. 5—L-2b RESERVOIR, DETERMINATION OF ORIGINAL POSITION OF OIL-WATER CONTACT.

If the correct position of the original oil-water contact is assumed, then the plot should show zero flooded-out volume for zero net water influx. The plot shows that this obtains for oil-water contact of 9,065 ft subsea. Thus, 9,065 ft subsea was taken as the original position of the oil-water contact. The correspondingly volumetrically determined original oil in place was 32.9 million STB, which is 0.3 per cent from the N calculated by the MBE.

UNDERSATURATED RESERVOIR, NO WATER DRIVE — ONE EXPLICIT UNKNOWN

The Virginia Hills Beaverhill Lake reservoir, located some 120 miles northwest of Edmonton in Alberta, was discovered in March, 1957, and at the end of 1961 it had been developed by 97 wells drilled on 160-acre spacing. At the present time there are about 102 producers within the field limits. The daily production rate amounts to 7,000 to 8,000 BOPD with 400 to 480 scf/bbl gas-oil ratio. By the end of Dec., 1961, the cumulative production amounted to 3.56×10^6 STB of 39° API oil and virtually no water. Tables 3 and 4, which present the solution of the MBE's, summarize also the production performance of this pool.

Detailed, foot-by-foot, petrophysical and geological evaluations on each well were made. During the subsequent well-to-well correlations of the numerous individual streaks which form the effective net pay, it was noted that, vertically, the porosity development is divisible into two units separated by a dense shaly carbonate interval varying in thickness from 2 to 10 ft. The upper zone was termed Hope Creek while the lower, thicker, porous unit was named the Main Zone.. Although both zones are being exploited as one reservoir, it was thought that for the purpose of the basic reservoir evaluation it may be advantageous to evaluate each of them separately. The reason for this approach was to avoid any eventual errors in incorrect weighting of the "average" parameters, mainly the volumetric reservoir properties and PVT's. The initial volumetric active oil in place flashed through 40 psig separator was calculated to be 74.3 and 272 million STB for the Hope Creek and Main Zone, respectively. Thus, the total Virginia Hills reservoir contained 346.3 million STB of oil.

In making the volumetric estimates of the active original oil in place only permeable intervals with connate-water saturation less than 60 per cent were considered as net pay.

The straight-line method of solving the MBE was used to answer the following questions.

1. Was the 60 per cent connate-water cut-off appropriate in defining active oil-in-place?

2. After correcting for the man-created communications (four wells were perforated through) are the two zones actually physically separated?

3. Are the two aquifers associated with the "two zones" active, and, if so, are they interconnected? Only the Main Zone is believed to be underlain by water, and Hope Creek probably has edge water.

PRESSURES AND PVT DATA

Two separate pressure datums were determined, 5,587 ft subsea for the Hope Creek and 5,617 ft subsea for the Main Zone, respectively. The individual pressures, appropriately corrected, were averaged volumetrically for each of the zones. The p_i's determined from early pressure measurements were 3,685 psig for the Main and 3,654

TABLE 3—VIRGINIA HILLS RESERVOIR, MAIN ZONE DATA

Date	No. of Producing Wells	Average* Reservoir Pressure (psig)	Estimated N_p (in 10^3)	Estimated W_p (in 10^3)	B_o (vol/vol)	$F = N_pB_o + W_p$ (in 10^3)	c_o vol/vol/psi (in 10^{-6})	$\frac{S_{oc_o} + S_{wc_w} + c_f}{1 - S_w}$** (in 10^{-6})	$\Delta p'$ (in psi)	E_t*** (in 10^{-6})
10-1-57	1	3685	0.342		1.3102	0.448	11.01	18.674	0	
1-1-58	1	3685	0.342		1.3102	0.448	11.01	18.674	0	
4-1-58	2	3680	20.481		1.3104	26 838	11.02	18.685	5	93
7-1-58	2	3680	20.481		1.3104	26.838	11.02	18.685	5	93
10-1-58	2	3680	20.481		1.3104	26.838	11.02	18.685	5	93
1-1-59	2	3676	34.750		1.3104	45.536	11.03	18.694	9	168
4-1-59	3	3667	78.557		1.3105	102.949	11.04	18.704	18	337
7-1-59	3	3667	78.557		1.3105	102.949	11.04	18.704	18	337
10-1-59	3	3667	78.557		1.3105	102.949	11.04	18.704	18	337
1-1-60	4	3664	101.846		1.3105	133.469	11.05	18.715	21	393
4-1-60	19	3640	215.681		1.3109	282.736	11.08	18.745	45	844
7-1-60	25	3605	364.613		1.3116	478.226	11.13	18.795	80	1504
10-1-60	36	3567	542.985	0.159	1.3122	712.664	11.18	18.844	118	2224
1-1-61	48	3515	841.591	0.805	1.3128	1105.646	11.26	18.924	170	3217
4-1-61	59	3448	1273.530	2.579	1.3130	1674.723	11.35	19.015	237	4506
7-1-61	59	3360	1691.887	5.008	1.3150	2229.839	11.48	19.144	325	6228
10-1-61	61	3275	2127.077	6.500	1.3160	2805.733	11.60	19.264	410	7898
1-1-62	61	3188	2575.330	8.000	1.3170	3399.709	11.86	19.524	497	9703

*p_i = 3,685
**S_{wc_w} = 0.868 × 10^{-6}, c_f = 4.95 × 10^{-6}
***$E_t = \Delta p' \frac{S_{oc_o} + S_{wc_w} + c_f}{1 - S_w}$

TABLE 4—VIRGINIA HILLS RESERVOIR, HOPE CREEK ZONE DATA

Date	No. of Producing Wells	Average* Reservoir Pressure (psig)	Estimated N_p (in 10^3)	B_o (vol/vol)	$F = N_pB_o + W_p$** (in 10^3)	c_o (vol/vol/psi) (in 10^{-6})	$\frac{S_{oc_o} + S_{wc_w} + c_f}{1 - S_w}$*** (in 10^{-6})	$\Delta p'$ (psi)	$E_t = \frac{\Delta p'}{\frac{S_{oc_o} + S_{wc_w} + c_f}{1 - S_w}}$ (in 10^{-6})
4-1-59	1	3654	9.269	1.354	12.550	11.96	20.238	0	
7-1-59	1	3654	9.269	1.354	12.550	11.96	20.238	0	
10-1-59	1	3645	15.889	1.355	21.530	11.98	20.258	9	182
1-1-60	1	3639	22.673	1.355	30.722	11.99	20.268	15	304
4-1-60	4	3620	39.562	1.355	53.606	12.02	20.298	34	690
7-1-60	6	3580	86.100	1.356	116.666	12.07	20.348	74	1505
10-1-60	10	3533	144.804	1.356	196.354	12.10	20.378	121	2465
1-1-61	18	3470	250.436	1.357	339.842	12.22	20.498	184	37771
4-1-61	25	3381	401.617	1.358	545.396	12.37	20.648	273	5637
7-1-61	25	3267	563.481	1.360	766.334	12.55	20.828	387	8060
10-1-61	32	3140	767.155	1.363	1045.632	12.74	21.019	514	10804
1-1-62	36	3008	985.403	1.365	1345.075	12.95	21.228	646	13713

*p_i = 3,654
**W_p = 0
***S_{wc_w} = 0.842 × 10^{-6}, c_f = 5.5 × 10^{-6}

psig for the Hope Creek, respectively. Average reservoir pressures at intermediate time intervals were obtained from plots of pressures vs the respective cumulative oil production.

Two subsurface Hope Creek samples and one subsurface Main Zone sample indicated that both crudes were highly undersaturated at the time of discovery, with bubble-point pressures of 1,960 and 1,792 psig, respectively. The pertinent PVT data as used in the solution of the MBE's are reported in Tables 3 and 4.

The expansion factor E_t is defined by the right-hand-side variable of Eq. 5 of Ref. 1, which is:

$$N_pB_o = NB_{oi}\frac{(S_{oc_o} + S_{wc_w} + c_f)\Delta p'}{1 - S_w}.$$

In the computations of the expansion factor the compressibility of the connate water was taken as 3.6 × 10^{-6} vol/vol/psi and the appropriate compressibilities of the rocks were obtained from the tables of Hall.[3] The average porosities and connate-water saturations for the Hope Creek were 7.58 and 23.4, and for the Main Zone were 9.25 and 24.1 per cent, respectively.

MBE CALCULATIONS

Eq. 5 of Ref. 1 was used with the appropriate production, pressure and PVT data discussed above. The computations are shown in Tables 3 and 4 and the results are presented graphically in Fig. 6.

Since all the points plotted in two separate straight lines going through the origin, it was concluded that the reservoirs were not in communication except through perforations, as indicated above. This must be true, since if there were cross flow between the two zones the points would not plot in straight lines but, instead, would bend.

From the slopes of the two straight lines the active oil in place in millions of stock-tank barrels was calculated to be 72.6 for the Hope Creek, 270.6 for the Main Zone, with 343.2 for the Virginia Hills reservoir. This compares with volumetrically determined values of 74.3, 272 and 346.3 million STB for the Hope Creek, the Main Zone and total Virginia Hills reservoir, respectively. This close agreement between the MBE results and the volumetrically determined values indicated that the 60 per cent connate-water cut-off was appropriate in defining the active oil in place. Moreover, this close agreement coupled with the fact that the points as calculated by Eq. 5 of Ref. 1 plotted in two straight lines going through the origin indicated that the reservoirs up to the end of 1961 were not producing under water drive. Thus, since the aquifers were not active, it is irrelevant as to whether they are or are not interconnected.

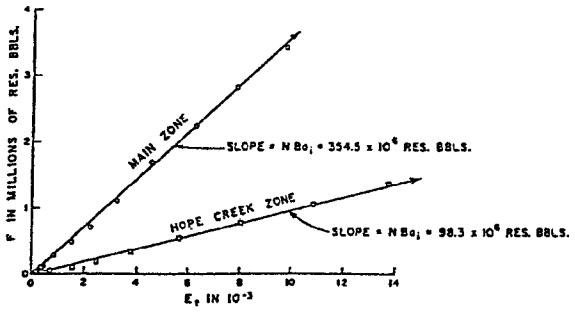

FIG. 6—VIRGINIA HILLS, BEAVERHILL LAKE RESERVOIR, DETERMINATION OF ORIGINAL OIL IN PLACE.

SPECIAL FIELD CASE
RESERVOIR X

Production from this one-well reservoir is obtained from about 15 ft of net pay which is underlain by a water table. The areal extent of this reservoir, which fringes around a granite knob of the pre-Cambrian basement, is completely unknown. The well was brought in with an initial production rate of 210 BOPD, which later increased to about 1,000 BOPD. Because of these encouraging results, several additional wells were drilled as close offsets, but despite these extensive exploration efforts, no additional producer was completed. To assist in the geological interpretation and to determine the size of this reservoir, which was impossible to estimate by volumetric methods, comprehensive reservoir and production data were collected during six years of production.

PRODUCTION, PRESSURE AND PVT DATA

Fig. 7 presents in a graphical form the six years' production-pressure performance of this interesting, but rather small, reservoir. It may be noted that the well initially produced with a 30 per cent water cut, which decreased to about 6 per cent after a cumulative oil production of about 19,000 bbl and a prolonged shut-in time of about 50 days. Afterwards, the water cut remained essentially unchanged, varying between 4 and 9 per cent. Moreover, on the basis of numerous production tests, it appears that the water cut over a wide range of production rates is rather insensitive to the rate of fluid withdrawals. Similar characteristics as discussed for the water production are exhibited also by the GOR curve (Fig. 7).

Considerable subsurface pressure measurements, at least five, of a prolonged shut-in time duration were obtained on this well. A pressure build-up test taken during the initial production test indicated that the initial reservoir pressure was 2,913 psig.

The early surface-recombined PVT sample suggested that this oil was highly undersaturated (p_b = 2,297 psig). The combined oil, rock and connate-water compressibility was calculated to be $20 \times 10^{-6} \times 1.28$, or 25.6×10^{-6} vol/vol/psi referred to stock-tank conditions through a 40 psig separator. B_{oi} was 1.28.

ORIGINAL OIL IN PLACE

By MBE

Because of the presence of the free water table and because of the repressuring of the oil reservoir by a slow water influx, as will be discussed in the following subsections on the pressure build-ups, the MBE was applied in the form of Eq. 6 of Ref. 1, which is

$$\frac{N_p B_o + W_p - W_i}{\frac{B_{oi}\Delta p'}{1 - S_w}(S_o c_o + S_w c_w + c_f)} = N + C\frac{\Sigma \Delta p Q(\Delta t_p)}{\frac{B_{oi}\Delta p'}{1 - S_w}(S_o c_o + S_w c_w + c_f)}.$$

Furthermore, because a limited aquifer was suspected as suggested by numerous close offsets (dry holes), several combinations of r_e/r_w and t_D were used. A plot of the calculations, all carried out on a digital computer, was made for each combination of r_e/r_w and t_D. An example is shown in Fig. 8. The most probable values corresponding to the minimum standard deviation and as determined by the consistency test (for details of which refer to the Sturgeon Lake South D-3 study) are shown in Table 5.

TABLE 5

Effective aquifer radius — r_e/r_w	= 8 reservoir radii
Dimensionless time — t_D	= 0.22/month
Original oil-in-place — N	= 2.15×10^6 STB
Aquifer constant — C	= 50 res. bbl/psi
Min. standard deviation — σ_{min}	= 148×10^3 STB

Using statistical methods, the confidence band for a probability of 89 to 95 per cent was calculated to be $\pm$ 0.06×10^6 STB.

If the pay thickness of 15 ft, as found in the well, were uniform, the 2.15 million STB would extend over about 400 acres. The reservoir has a weak water drive from an aquifer which apparently extends out about 8 field radii. From the constants C and t_D, and speculating on the basis of seismic and geological information that the aquifer thickness h might be about 30 ft and that the water influx is effected over π radians, the permeability k of the aquifer would be about 1.5 md. This deduction is substantiated by solution of the radial flow formula which suggested that the aquifer permeability might be about 3 md. This small permeability of the aquifer was further confirmed by core analysis made on samples obtained from the aquifer zone of the well and from offsetting dry holes. The results gave an average aquifer permeability of about 1 md.

By Pressure Build-Ups

A plot of a typical two-month pressure build-up is presented in Fig. 9. Because the production rates were usual-

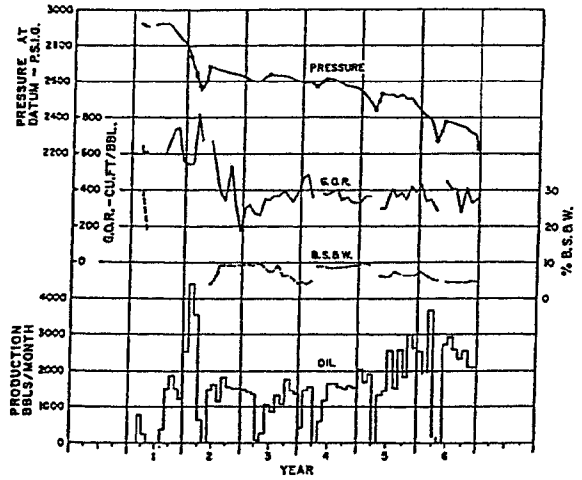

FIG. 7—RESERVOIR X, PRODUCTION PERFORMANCE VS TIME.

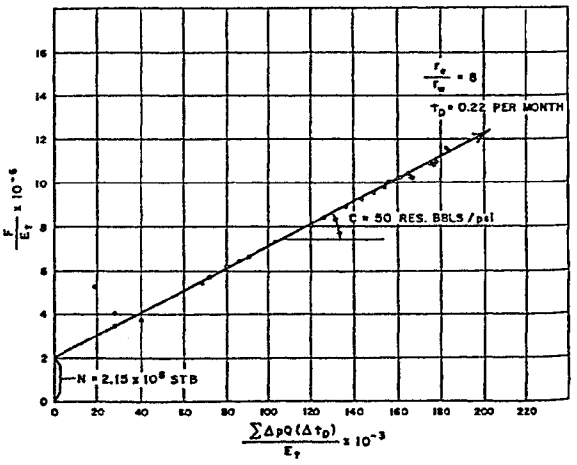

FIG. 8—RESERVOIR X, DETERMINATION OF N.

ly changed many times prior to shutting in the well, Horner's superposition approach was applied. The shut-in time in hours is given at each calculated pressure point.

Using Slope 1, which extends from 0.75 to 4 hours, of Fig. 9, a *kh* of 14,000 md-ft corresponding to a *k* of about 1 darcy was calculated. The second slope, which persisted from 4 to about 61 hours shut-in time, yields a *kh* of 2,400 md-ft corresponding to a *k* of about 160 md. Thus, the formation in the vicinity of the wellbore was more permeable than the formation away from it. The increased conductivity *kh* in the vicinity of the wellbore was probably caused by the treatment with 18 bbl (1.2 bbl/ft) of 30 per cent hydrochloric acid which was given to this well in July of its first year. The steep increase in the rate of pressure build-up, noticeable at prolonged shut-in time, probably is caused by water influx into the oil reservoir. This slow action of water drive is undoubtedly caused by the low permeability of the aquifer, as discussed in the previous subsection.

Pressures obtained from four pressure build-ups were plotted vs shut-in time on regular coordinate paper. A typical plot is given in Fig. 10. The rate of pressure increase due to water influx was constant. From the solution of the MBE as given by Fig. 8, the necessary parameters to calculate the rate of water influx were obtained. Thus, the rates of water influx during the shut-in periods and for constant rates of pressure increase were calculated and used in the following equation to calculate *N*:

$$N = \frac{\text{Rate of water influx}}{\text{Rate of pressure increase} \times \text{compressibility} \times B_{oi}}$$

Table 6 summarizes the results of the calculations. It shows that the arithmetically determined average for *N* is 2.06 × 10⁸ STB.

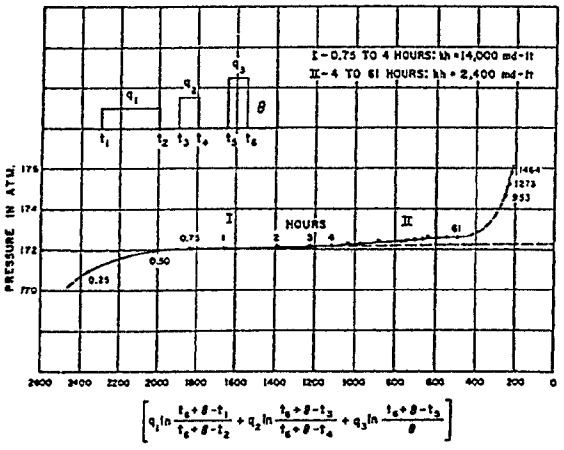

FIG. 9—RESERVOIR X, PRESSURE BUILD-UP.

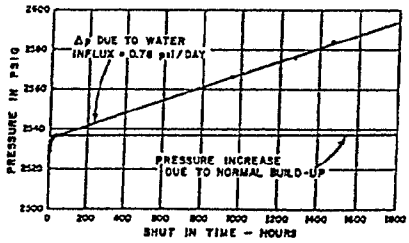

FIG. 10—RESERVOIR X, PRESSURE BUILD-UP.

TABLE 6—RESERVOIR X, DETERMINATION OF N FROM PRESSURE BUILD-UPS

Year of Survey	Rate of Water Influx (B/D) from MBE	Rate of Pressure Rise from Pressure Build-Ups psi/day	N (In 10^8 STB)
3	36.5	0.64	2.22
4	43.5	0.76 (Figure 10)	2.24
5	75.	1.70	1.72
6	105	2.00	2.05
			average 2.06

By Park Jones' Approximation

Twice during the life of the well sufficient data were obtained to attempt application of Park Jones' reservoir limit test.[4] Typical plots of pressure vs flow time are presented in Figs. 11 and 12. It was concluded that semi-steady-state conditions did not obtain at the end of the test. At that time the pressure decline was 30 psi/day. By applying Park Jones' approximation for unsteady-state flow:

$$N = \frac{2.5\,q}{c(-dp/dt)}.$$

A value of 2.1 × 10⁸ STB was obtained for the oil associated with an unsteady-state flow test of 18 hours duration.

Thus, the original oil in place as determined by MBE, from pressure build-up, and by Park Jones approximation is, respectively, (2.15 ± 0.06) × 10⁸, 2.06 × 10⁸ and 2.1 × 10⁸ STB.

SUMMARY

By using three different methods of determining *N*, a considerable amount of information was gained on this

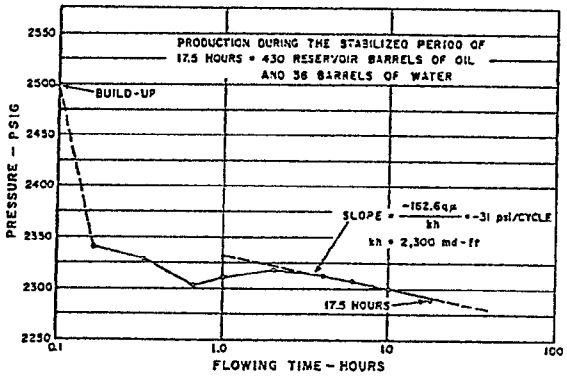

FIG. 11—RESERVOIR X, FLOW TEST.

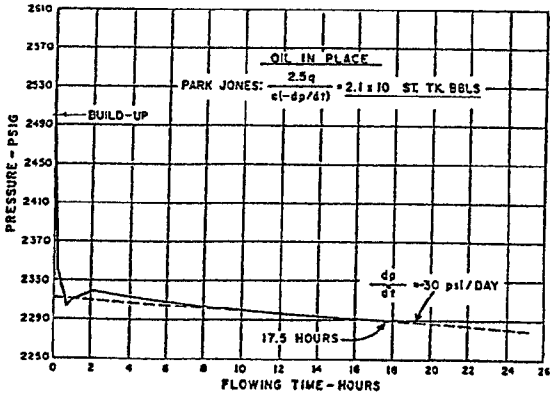

FIG. 12—DETERMINATION OF ORIGINAL OIL IN PLACE.

TABLE 7—RESERVOIR Y DATA

Time (Months)	Average Reservoir Pressure (psig)	$E_g = (B_g - B_{gi})$ (in 10^{-6} res cu ft/scf	$F = G_p B_g$ (in 10^6 res cu ft)	$\frac{\Sigma \Delta p_n \sqrt{t - t_n}}{E_g}$ (in 10^6)	F/E_g (in 10^{12})
0	2883	0.0	—		
2	2881	4.0	5.5340	0.3536	1.3835
4	2874	18.0	24.5967	0.4647	1.3665
6	2866	34.0	51.1776	0.6487	1.5052
8	2857	52.0	76.9246	0.7860	1.4793
10	2849	68.0	103.3184	0.9306	1.5194
12	2841	85.0	131.5371	1.0358	1.5475
14	2826	116.5	180.0178	1.0315	1.5452
16	2808	154.5	240.7764	1.0594	1.5584
18	2794	185.5	291.3014	1.1485	1.5703
20	2782	212.0	336.6281	1.2426	1.5879
22	2767	246.0	392.8592	1.2905	1.5970
24	2755	273.5	441.3134	1.3702	1.6136
26	2741	305.5	497.2907	1.4219	1.6278
28	2726	340.0	556.1110	1.4672	1.6356
30	2712	373.5	613.6513	1.5174	1.6430
32	2699	405.0	672.5969	1.5714	1.6607
34	2688	432.5	723.0868	1.6332	1.6719
36	2667	455.5	771.4902	1.7016	1.6937

one-well reservoir. Two of these methods, the pressure build-up and Park Jones', may not always apply. Thus, they do not have the general applicability of the MBE. However, in the case of this reservoir they resulted in satisfactory answers which may be due to the high permeability of the reservoir, to its size, and to the fact that the oil was undersaturated during the six producing years.

GAS RESERVOIR WITH WATER DRIVE RESERVOIR Y

GENERAL DESCRIPTION

This dry-gas reservoir was discovered in the late forties, and at the present time it is being exploited by about 10 wells. The reservoir is about 11 miles long and 1 to 1.5 miles wide. The productive structure is found at a depth of about 5,900 ft subsea and attains a maximum pay thickness of 440 ft. Its original gas-water contact, established by logs and tests of several wells, is placed at 6,340 ft subsea. The areal extent of the original gas-water contact covers some 16 sq. miles. The volumetric estimates of the original dry gas in place varies from 1.3 to 1.65 Tscf, depending mainly on the structural interpretation and estimates of percentage "net" hydrocarbon volume. Other minor differences in interpretation and averaging of the basic data also contribute to the above discrepancy of 27 per cent in the original gas in place.

Production, pressures and the pertinent expansion factors are presented in Table 7. For convenience, the original basic data were converted from centimeters-grams-seconds to standard U. S. units. Cumulative production is expressed in reservoir cubic feet. Since no pressures at the original oil-water table were available, the average reservoir pressures were used for the evaluation of the gas expansion factor E_g and also for calculation of the effective pressure drops which govern the calculations of the "water influx". Any error caused by this simplification should be relatively small since only the "changes" in the pressure drops are involved and the pressure equalizes relatively fast within the gas reservoir.

MATERIAL BALANCE CALCULATIONS

A summary of data and calculations is presented in Table 7. The depletion-type MBE ($G_p B_g = G E_g$, as shown in Eq. 7 of Ref. 1) was tried first. F, i.e. $G_p B_g$, was plotted vs E_g on cartesian coordinate paper. The line represented

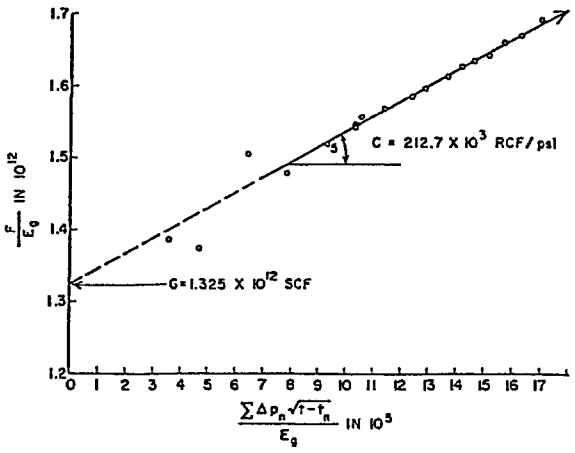

FIG. 13—RESERVOIR Y, DETERMINATION OF ORIGINAL GAS IN PLACE.

by these points curved upwards and thus did not satisfy the necessary straight-line relation.

Because of this condition, the MBE with water drive was next tried. Since an infinite linear case does not require the estimation of dimensionless time and is easy to perform, it was tried first. The results are shown in Table 7, and are illustrated in Fig. 13. The necessary straight-line relationship was evident and the solution was regarded as satisfactory. The best straight line through Points 5 to 18 was drawn by means of the least-squares method. The original gas in place was 1.325 Tscf and the standard deviation was 0.0035 Tscf. The confidence band for a probability range of 75 to 90 per cent was ± 1.4 Bscf and for a probability range of 95 to 100 per cent was ± 2.9 Bscf. The consistency-test straight-line plot resulted in a slope equal to 28.8 MMscf for two months. This very small slope of the consistency-test straight line indicated a high degree of consistency with time. Because of this, the infinite linear aquifer case was accepted and no further calculations were deemed necessary.

ACKNOWLEDGMENT

The authors would like to thank Mobil Oil Co. de Venezuela for releasing for publication the data on the Guico and North Oscurote fields; and the managements of Hudson's Bay Oil and Gas Co., Ltd., and Socony Mobil Oil Co., Inc. for permission to publish this paper.

REFERENCES

1. Havlena, D. and Odeh, A. S.: "The Material Balance as an Equation of a Straight Line", *Jour. Pet. Tech.* (Aug., 1963) 896.
2. McKibbon, J. H., Paxman, D. S. and Havlena, D.: "A Reservoir Study of the Sturgeon Lake South D-3 Pool", *Jour. Canadian Pet. Tech.* (Fall, 1963) 2, No. 3.
3. Hall, H. N.: "Compressibility of Reservoir Rocks", *Trans.*, AIME (1953) 198, 309.
4. Jones, Park: "Gulf Coast Wildcat Verifies Reservoir Limit Test", *Oil and Gas Jour.* (June 18, 1956) 184.

★★★

SPE
Society of Petroleum Engineers

SPE 21514

The Material Balance Equation for a Gas Condensate Reservoir With Significant Water Vaporization

N.V. Humphreys, Mobil E&P U.S.
SPE Member

Copyright 1991, Society of Petroleum Engineers, Inc.

This paper was prepared for presentation at the SPE Gas Technology Symposium held in Houston, Texas, January 23–25, 1991.

This paper was selected for presentation by an SPE Program Committee following review of information contained in an abstract submitted by the author(s). Contents of the paper, as presented, have not been reviewed by the Society of Petroleum Engineers and are subject to correction by the author(s). The material, as presented, does not necessarily reflect any position of the Society of Petroleum Engineers, its officers, or members. Papers presented at SPE meetings are subject to publication review by Editorial Committees of the Society of Petroleum Engineers. Permission to copy is restricted to an abstract of not more than 300 words. Illustrations may not be copied. The abstract should contain conspicuous acknowledgment of where and by whom the paper is presented. Write Publications Manager, SPE, P.O. Box 833836, Richardson, TX 75083-3836 U.S.A. Telex, 730989 SPEDAL.

ABSTRACT

In hot, high pressure gas condensate reservoirs significant vaporization of connate water can occur during depletion. As the reservoir pressure decreases, the equilibrium water vapor content of the reservoir gas increases, causing connate water within the gas-bearing portion of the reservoir to vaporize. This both increases the vapor phase pore volume of the reservoir, and decreases the hydrocarbon content of the reservoir gas. Also, condensation of liquid hydrocarbons below the dewpoint will decrease the vapor phase pore volume of the reservoir, invalidating assumptions made in a simple material balance calculation.

A modified form of the material balance equation has been developed to account for these effects. Failure to account for them can result in erroneous predictions of gas-initially-in-place, and hence reserves. It may also lead to incorrect identification of reservoir drive mechanisms.

Field examples are presented for a gas condensate reservoir below the dewpoint, and for a gas reservoir where water vaporization effects are significant.

As targets for gas reservoirs become progressively deeper, and hotter, the significance of the effects noted in this paper increases.

INTRODUCTION

The simple material balance equation for a gas reservoir assumes that the reservoir is isothermal, that no changes in rock compressibility occur during depletion, and that no phase changes occur in the reservoir as pressure declines. Under these circumstances, the standard plot of average reservoir pressure divided by gas deviation factor (at the average reservoir pressure) versus cumulative production (P/Z plot) may be used to calculate gas initially in place, and reserves.

Modifications to the basic P/Z plot to account for phase changes in the reservoir in retrograde condensate systems by means of a two-phase gas deviation factor have been presented by Craft & Hawkins (1). Changes in formation compressibility as a function of average reserve pressure, particularly for the case of over pressured formations, has been studied by Hammerlindl (3), and subsequent researchers.

In addition to phase changes occurring in the hydrocarbon phase in a reservoir due to condensation and subsequent revaporization, phase changes can occur in water present in the reservoir. These changes, caused by vaporization of connate water as reservoir pressure declines, are most pronounced in high temperature reservoirs, and can significantly affect estimates of gas-initially in place, and reserves.

As targets for gas exploration become progressively deeper, the occurrence of reservoirs where this effect is significant will increase. Generally, the effect will lead to an over estimate of gas initially in place, and reserves, if conventional analysis methods are applied

This paper will present a technique for accounting for these effects, which may also be used for analysis of gas condensate reservoirs where changes in liquid saturation occur in the reservoir.

Application of the technique will be demonstrated using two examples: one for a gas condensate reservoir where changing hydrocarbon liquid saturations occur over the reservoir life; and, a hot gas reservoir where changes in both hydrocarbon and connate water saturations occur during depletion.

References and Illustrations at end of paper.

THE PHYSICAL SYSTEM.

Consider the case of a gas reservoir above the dewpoint at discovery. At these conditions the pore space in the reservoir will be filled with hydrocarbon vapor, inert and acid gases (sometimes), water vapor, and liquid water. There will be small quantities of hydrocarbon and inert gases dissolved in the liquid water phase, and somewhat larger quantities of carbon dioxide if acid gases are present. It is assumed that the vapor phase will be water saturated.

The amount of water vapor present in the vapor phase pore volume will depend on the partial pressure of water at reservoir conditions. Because of the large surface area available for mass transfer between connate water and the vapor phase pore volume, it may reasonably be assumed that this pore volume will be saturated with water vapor. This will mean that the hydrocarbon pore volume of the reservoir is not solely a function of reservoir pore volume and water saturation. Rather, it must also be adjusted for the amount of water vapor present.

The mole (volume) fraction of the vapor phase which is water vapor can be measured experimentally; predicted using an equation of state; or, estimated from correlations. An example correlation, based on data extrapolated from Figure 15-14 of Reference 2 is presented as Figure 1. The original data data only extended to 290°F (143°C). However, the validity of the extrapolation is confirmed by new data points measured in the laboratory at 350°F (177°C) which are also shown on the figure.

It is seen that as reservoir temperature increases, the amount of water vapor present in the vapor phase pore volume becomes significant. For instance, at 6000 psia (42MPa) and 350°F (177°C), a saturated 0.6 gravity hydrocarbon gas contains about 4 mole percent water vapor. If this quantity is ignored in volumetric estimates, values of gas initially in place for the reservoir will be overestimated.

However, the most significant effect of water vapor content is when reservoir pressure declines due to production. It can be seen from Figure 1 that the water vapor content of a 0.6 gravity hydrocarbon gas at 350°F (177°C) and 1000 psia (7MPa) is 13 percent. Failure to account for this volume of water vapor can lead to significant errors in estimates of reserves. Additionally, the water vapor will be condensed in surface facilities as the saturated hydrocarbon gas is produced. Volumes of condensed water can be significant, and must be carefully discriminated from free water production if erroneous conclusions about reservoir drive mechanism are not to be made.

As the reservoir pressure decreases, above the dewpoint, the saturated water content of the hydrocarbon gas increases, and water evaporates from the liquid phase to maintain the gas phase in a saturated condition. This decreases the liquid water saturation in the pore space, and increases the mole fraction of water in the vapor phase. Additionally, some reduction in the pore volume occurs due to rock compressibility (Figure 2).

It is assumed that any vapor dissolved in connate water is negligible for the purposes of this discussion. However, if it is necessary to account for these quantities, the material balance equation may easily be modified. It will be assumed that all water transferring from the liquid to the vapor phase will come from connate water, rather than any aquifer which may exist. This is a reasonable assumption, as mass transfer is a function of surface area. The contact area between the vapor phase and any aquifer is negligible when compared with the contact area between the vapor phase and connate water. Using data presented by Collins, for specific surface area (Reference 4), it may be shown that the ratio of connate water contact area to aquifer contact area is on the order of ten million for a reservoir 100 ft (30m) thick covering an area of 5000 acres (20×10^6 m^2).

As the reservoir pressure passes through the dewpoint, hydrocarbon liquids condense. This reduces the vapor phase pore volume in the reservoir. Additionally, water will move from the liquid phase (connate water) to the vapor phase to maintain the vapor phase in a water saturated condition. For example, for a natural gas system initially at 10000 psi (70MPa), being depleted to 500 psia (3.5MPa) at 350°F (177°C), the water vapor content of the vapor phase pore volume will increase from 3 mole percent to 19 mole percent. This will have a significant, beneficial, effect on the eventual recovery of hydrocarbon gas from the reservoir.

EFFECT OF CHANGES IN PRESSURE ON PORE SPACE CONTENT

The properties of a lean condensate fluid in contact with liquid phase water, over the pressure range 200-7000 psia (1.4 - 70 MPa) are presented on Table 1. These data were obtained from data measured in a PVT cell at 350° F (177°C), smoothed using a two component equation-of-state (EOS). These data are also presented graphically on Figure 3.

It is observed that the amount of total pore space occupied by hydrocarbon gas declines from 86 percent at 7000 psia (49 MPa) to 76 percent at 1000 psia (7 MPa) and to only 29% at 200 psia (1.4 MPa). This implies both a lower value for gas initially in place, and a higher value for recovery factor, than would be expected if water vapor is neglected.

It is seen that for this fairly lean condensate fluid, the major change in pore space content is from water vaporization. However, for richer fluids, much greater volumes of liquid hydrocarbons may condense as the system pressure declines. Any effect these condensed hydrocarbons may have in slowing the vaporization of connate water by reducing contact area between the gas and water is neglected in the discussion. It is not believed that the effect of condensed hydrocarbon volumes would be significant.

In addition to affecting calculations at the reservoir level, the presence of water in the vapor phase, and changes in the vapor phase water content over time can profoundly affect the design of surface facilities. For the system shown, the water content of the saturated gas increases from 5.6 BBl/MMSCF ($2.06 \times 10^{-5} m^3/m^3$) at 7000 psia (49MPa) to 21.6 BBl/MMSCF (1.21×10^{-5} m^3/m^3) at 1000 psia (7 MPa). If the system pressure were further reduced to 200 psia (1.4MPa), the saturated water vapor content increases to 95.2 BBl/MMSCF (5.35×10^{-4} m^3/m^3). Failure to account for increasing water production with time, purely due to vaporization effects within

the reservoir, can lead to under design of facilities.

Also, it is possible for water condensed from the vapor phase in surface facilities to be incorrectly identified as produced free water. Comparison of produced water volumes with the saturated water vapor content of reservoir gas allows discrimination between condensed and produced free water volumes.

THE MATERIAL BALANCE EQUATION

The material balance equation for a volumetric gas condensate reservoir, with constant formation compressibility, where water vaporization and hydrocarbon condensation effects are accounted for is derived in Appendix A.

The conventional volumetric gas reservoir material balance equation is (Reference 5)

$$\frac{G_p}{G_i} = 1 - \frac{E}{E_i}(1-c_f\Delta P) \quad \ldots\ldots\ldots\ldots\ldots\ldots\ldots\ldots(1)$$

where
- G_i is the initial gas-in-place in the reservoir (scf) (m^3)
- G_p is the cumulative net gas production at some time, t (scf) (m^3)
- E_i is the initial gas expansion factor (scf/rcf) (m^3/m^3)
- E is the gas expansion factor at time t. E = 35.37 P/ZT (2880 P/ZT)
- c_f is the rock compressibility (vol/vol/psi) (vol/vol/MPa)
- ΔP is the pressure difference from initial conditions, at time t (psi) (MPa)
- P is the average reservoir pressure at time t (psia) (MPa)
- Z is the vapor phase gas deviation factor at time t
- T is the average reservoir temperature (°R)(°K)

The modified volumetric gas reservoir material balance equation for a reservoir with condensation and vaporization effects is

$$\frac{G_p}{G_i} = 1-\left[\frac{E}{E_i}\right]\left[\frac{1-y}{1-y_i}\right]\left[\frac{1-S_w-S_{HCL}}{1-S_{wi}}\right](1-c_f\Delta P) \quad \ldots.(2)$$

where
- y_i is the initial mole fraction of water in the vapor phase (fraction)
- y is the mole fraction of water in the vapor phase at time t (fraction)
- S_{wi} is the initial water saturation in the reservoir (fraction)
- S_w is the water saturation in the reservoir at time t (fraction)
- S_{HCL} is the liquid hydrocarbon saturation in the reservoir at time t (fraction)

The modified material balance equation is thus the conventional equation, plus two terms; one correcting for the change in water vapor content of the reservoir gas phase; and, one correcting for the change in reservoir vapor phase pore volume due to water vaporization and hydrocarbon condensation.

For the PVT data given in Table 1, the relative magnitudes of these factors are shown in Figure 4. It is observed that the term describing the change in water vapor content of the reservoir gas is the most significant of these factors. Also, a distinct break in the locus of the overall correction term occurs at the dewpoint, as hydrocarbon liquids start to condense from the gas phase.

Equation (2) may be rearranged, with substitution for E, to yield

$$\frac{P}{Z}\left[\frac{1-y}{1-y_i}\right]\left[\frac{1-S_w-S_{HCL}}{1-S_{wi}}\right][1-c_f\Delta P] = \left[\frac{P_i}{Z_iG_i}\right]G_p - \left[\frac{P_i}{Z_i}\right] \quad \ldots\ldots(3)$$

Thus, a plot of P/Z multiplied by the correction factors for vapor phase water content, and liquid saturation changes, versus net gas production will yield a straight line which will intersect the y axis at P_i/Z_i, and the x axis at G_i.

The net value of the correction factors on the left hand side of Equation (3) is normally less than one, and the overall correction becomes greater as the reservoir pressure decreases. This means that an uncorrected plot of P/Z versus G_p will tend to deviate upward from the true straight line value, with deviation increasing at higher values of G_p (lower reservoir pressure).

The effect of this is shown graphically on Figure 5. Normally, upward deviation from an initial straight line on a P/Z plot is taken as being evidence of a water drive. However, in reservoirs where the water vapor content of the vapor phase is changing with time (pressure), this need not be true.

Examining the effects of these corrections in detail, it is seen that above the dewpoint the P/Z locus first deviates upwards as a straight line. This yields overoptimistic estimates of gas-initially-in-place at early times if the correction factors are not applied. Also, because of the non-linearity of the correction terms as a function of pressure (Figure 4), the P/Z locus will tend to curve slightly upwards, which may be misinterpreted as a water drive.

As the system drops below the dewpoint, significant curvature occurs in the P/Z locus due to hydrocarbon condensation within the reservoir. At pressures close to the dewpoint, this again is likely to be misinterpreted as the presence of a water drive.

As the system pressure depletes further, the curvature of the P/Z locus decreases, as the absolute value of the correction factor decreases. Again, the initial deviation upward from a straight line, followed by lessening curvature in the P/Z locus with increasing production could be misinterpreted as a water drive. In this case, however, the aquifer volume would have to be postulated as being significantly larger than the reservoir, as a time

lag would occur between reservoir pressure drop and aquifer response.

Consequently, failure to account for water vaporization and hydrocarbon condensation effects within the reservoir will yield anomalously shaped P/Z versus G_p loci. These anomalies may lead to either overoptimistic estimates of gas initially in place, incorrect determination of reservoir drive mechanism, or a combination of these errors.

FIELD EXAMPLE: RICH GAS CONDENSATE RESERVOIR WITHOUT WATER VAPORIZATION.

Allen and Roe (Reference 6) have presented data for a rich gas condensate reservoir which was at the dewpoint at initial conditions. As the reservoir pressure depleted, significant quantities of hydrocarbon liquids condensed in the reservoir (Figure 6) occupying up to twelve percent of the pore space. With further pressure depletion, condensate revaporization occurred within the reservoir, reducing the hydrocarbon liquid saturation to about six percent at abandonment.

Due to concern over whether measured well pressures were representative of average reservoir pressures, Allen and Roe presented P/Z data for the reservoir based on both measured pressures, and average pressures back calculated from production and ultimate recovery. These are presented on Figure 7, along with P/Z data calculated using the modified material balance approach derived here.

It is observed that Allen and Roe's data plot as a curve, with early time data plotting significantly below the smooth trend of later data. This may be indicative of lack of pressure equilibration at early times, or (more likely) some inaccuracy in the measured properties of the reservoir fluid. Since the reservoir is believed to have been at its dewpoint initially, the difficulties of obtaining a representative fluid sample are apparent.

Data calculated using the modified material balance approach presented here plot as a straight line, except for very early time data. Also, this straight line does not extrapolate to the value of P_i/Z_i measured on the reservoir fluid. It is believed that the deviation of these early points is due to the very rapid change in liquid hydrocarbon saturation which occurs in other reservoir immediately below the dewpoint (Figure 6). Lack of equilibrium across the reservoir would cause significant deviation from a straight line. Additionally, as noted by Allen and Roe, uncertainty exists over the original reservoir fluid properties. It is believed these effects are responsible for the early time deviation.

However, use of the modified material balance approach yields a straight line modified P/Z plot (as opposed to Allen and Roe's more curved locus using conventional P/Z) which extrapolates to a recovery of 20.1 BSCF (569×10^6 std m^3) at an average reservoir pressure of 500 psia (3.5 MPa). Actual recovery reported by Allen and Roe at this pressure was 20.2 BSCF (572×10^6 std m^3).

It is believed that use of the modified material balance approach has successfully matched actual ultimate recovery for this retrograde gas condensate reservoir.

FIELD EXAMPLE - HOT, HIGH PRESSURE GAS CONDENSATE RESERVOIR WITH WATER VAPORIZATION

Pressure and production data for a hot (350°F, 177°C) gas condensate reservoir which was overpressured at discovery (7000 psia at 10000 ft, 49MPa at 3050m) are presented on Table 2. The properties of the reservoir fluid for this system are shown on Table 1. Water vaporization effects are known to be significant in this reservoir, as increasing mole fractions of water vapor in the produced gas stream have been observed over time.

Modified, and unmodified P/Z plots as a function of net cumulative production are shown on Figure 8. It is seen that significant curvature of the unmodified P/Z locus exists. If the data from this curve were used to estimate gas initially in place, a figure 13 percent higher than that calculated using the modified material balance method is obtained.

Additionally some curvature of the unmodified P/Z locus is apparent. This could be misinterpreted as the presence of a water drive, whereas careful gas/water contact monitoring using observation wells has shown no movement of the contact over a 2000 psi (14MPa) depletion from initial reservoir conditions.

Separate studies of this reservoir using a three dimensional fully compositional reservoir simulator, history matched by well on pressures, production, and condensate/gas ratio confirm estimates of gas initially in place, and reserves, predicted by the modified material balance method.

CONCLUSIONS

1. Hot gas reservoirs can exhibit significant changes in reservoir vapor phase pore content as a function of pressure, due to vaporization of connate water.

2. A modified form of the material balance equation has been derived for use in gas condensate reservoirs where hydrocarbon condensation and connate water vaporization effects are significant.

3. The modified form of the material balance equation can be used to predict changes in produced fluid composition as a function of production, and to accurately predict gas-initially-in place, recovery factor, and hence reserves.

4. The validity of this approach has been demonstrated by means of two field examples, one with, and one without water vaporization effects.

5. Failure to account for water vaporization effects can lead to overprediction of gas initially in place, and underprediction of recovery factor.

6. Failure to account for water vaporization effects when using the material balance equation can lead to incorrect identification of reservoir drive mechanisms.

7. Failure to account for changes in water vapor content of produced gas as reservoir pressure

depletes can cause water handling facilities to be under designed.

ACKNOWLEDGEMENTS

I would like to thank Rafi Al-Hussainy for his encouragement during the evolution of this work, and Mobil Oil Corporation for permission to publish this paper.

REFERENCES

1. CRAFT, B.C. & HAWKINS, M.F. "Applied Petroleum Reservoir Engineering" Prentice-Hall Inc. Englewood Cliffs, New Jersey (1959)

2. GAS PROCESSORS SUPPLIERS ASSOCIATION "Engineering Data Book" Tulsa, Oklahoma (1972)

3. HAMMERLINDL, D.J. "Predicting Gas Reserves in Abnormally Pressured Reservoirs" 46th Annual Fall Meeting of SPE of AIME, New Orleans (1971)

4. COLLINS, R.E. "Flow of Fluids Through Porus Materials" PennWell, Tulsa, Oklahoma (1961)

5. DAKE, L.P. "Fundamentals of Reservoir Engineering" Elsevier, Amsterdam (1978)

6. ALLEN, F.H., & ROE, R.P. "Performance Characteristics of a Volumetric Gas Condensate Reservoir" Trans. AIME, 189, (1950)

APPENDIX A

Derivation of Modified Material Balance Equation

Figure 2 shows the changes in Pore Volume (PV), Vapor Phase Pore Volume (VPPV) and Hydrocarbon Vapor Phase Pore Volume (HVPPV) at initial conditions, depletion above the dewpoint, and depletion below the dewpoint.

Defining G_i as the initial hydrocarbon gas in phase (Scf) (m^3)
E_i as the initial vapor phase (gas + water vapor) gas expansion factor (scf/rcf) (m^3/m^3)
and, other variables as defined in the body of the paper.

At initial conditions,

$$VPPV_i = PV_i\ (1 - S_{wi}) \quad \text{.....(A1)}$$

$$= HVPPV_i \frac{1}{(1-y_i)}$$

$$= \frac{G_i}{E_i} \frac{1}{(1-y_i)} \quad \text{.....(A2)}$$

and $$PV_i = \frac{G_i}{E_i} \frac{1}{(1-y_i)} \frac{1}{(1-S_{wi})} \quad \text{.....(A3)}$$

At some depleted pressure, above the dewpoint:

$$VPPV = PV_i\ (1-c_f\Delta P)\ (1-S_w)$$

$$= \frac{G_i}{E_i} \left[\frac{(1-c_f\Delta P)}{(1-y_i)}\right]\left[\frac{(1-S_w)}{(1-S_{wi})}\right] \quad \text{.....(A4)}$$

Now, defining the hydrocarbon gas remaining in the reservoir at this depleted pressure as G,

$$VPPV = \frac{G}{E} \left[\frac{1}{(1-y)}\right] \quad \text{.....(A5)}$$

Then combining equations (A4) & (A5)

$$G = G_i \left[\frac{E}{E_i}\right]\left[\frac{1-y}{1-y_i}\right]\left[\frac{1-S_w}{1-S_{wi}}\right] (1-c_f\Delta P) \quad \text{.....(A6)}$$

Defining G_p as the cumulative hydrocarbon gas production, by a material balance on the hydrocarbon gas,

$$G_p = G_i - G \quad \text{.....(A7)}$$

Then combining equations (A6) & (A7)

$$\frac{G_p}{G_i} = 1 - \left[\frac{E}{E_i}\right]\left[\frac{1-y}{1-y_i}\right]\left[\frac{1-S_w}{1-S_{wi}}\right] (1 - c_f\Delta P) \quad \text{..(A8)}$$

Equation A8 is the material balance equation above the dewpoint for a gas reservoir with significant water vaporization. Following a similar procedure, the material balance equation below the dewpoint may be shown to be

$$\frac{Gp}{G_i} = 1 - \left[\frac{E}{E_i}\right]\left[\frac{1-y}{1-y_i}\right]\left[\frac{1-S_w-S_{HCL}}{1-S_{wi}}\right] (1-c_f\Delta P) \quad \text{..(A9)}$$

TABLE 1

RESERVOIR FLUID PROPERTIES

PRESSURE [PSIA]	VAPOR PHASE Z FACTOR	MOLE % WATER [VAPOR PHASE]	VOLUME % WATER [LIQUID PHASE]	VOLUME % HYDROCARBON [LIQUID PHASE]
7000	1.104	4.10	9.97	0
6000	1.036	4.47	9.94	0
5000	0.974	4.97	9.89	0
4500	0.946	5.31	9.86	Trace
4000	0.927	5.67	9.82	0.30
3000	0.908	6.81	9.72	1.12
2000	0.911	9.08	9.54	1.40
1000	0.934	15.95	9.14	1.37
200	0.955	70.22	6.98	1.20

INITIAL RESERVOIR PRESSURE 7100 PSIA
RESERVOIR TEMPERATURE 350 F
DEWPOINT PRESSURE 4500 PSIA
INITIAL GAS MOLECULAR WEIGHT 26.1
INITIAL INERTS [CO2 + N2] 14.5 MOL %
INITIAL WATER VAPOR 4.1 MOL %

TABLE 2

PRESSURE / PRODUCTION DATA

NET CUMULATIVE GAS PRODUCTION [% GIP]	AVERAGE RESERVOIR PRESSURE [PSIA]
0	7115
0.21	7088
0.65	7020
1.27	6966
2.30	6855
3.42	6745
4.52	6622
5.68	6504
6.96	6427
8.48	6313
9.89	6203
11.45	6106
12.45	5981

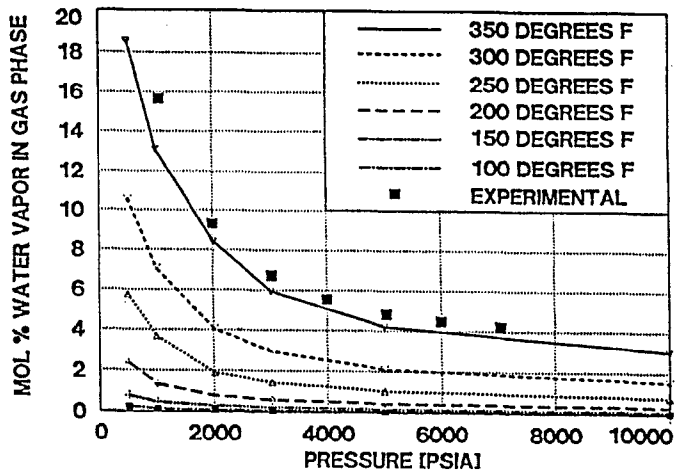

Fig. 1 – Saturated water content of a 0.6 gravity (air = 1) natural gas as a function of temperature and pressure. (After Reference 1)

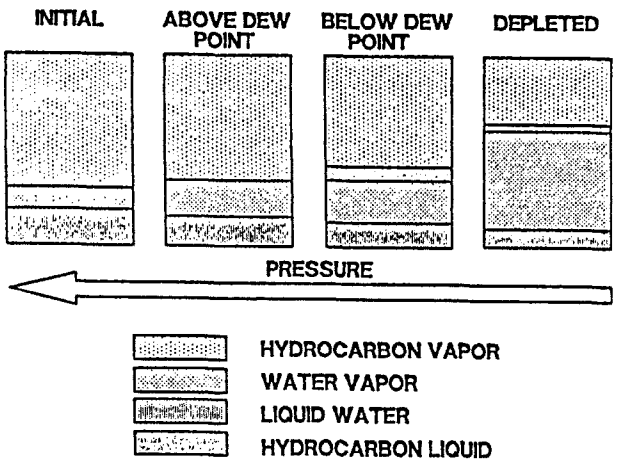

Fig. 2 – The effect of pressure on the relative proportions of pore volume occupied by different phases.

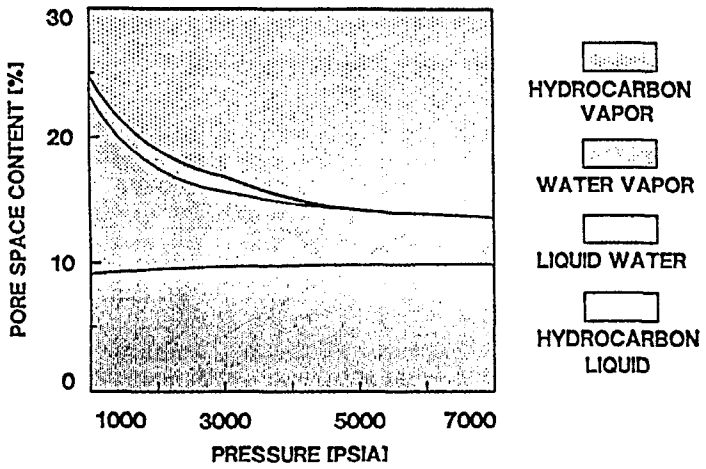

Fig. 3 – Experimental data showing the proportion of pore volume occupied by different phases as a function of pressure.

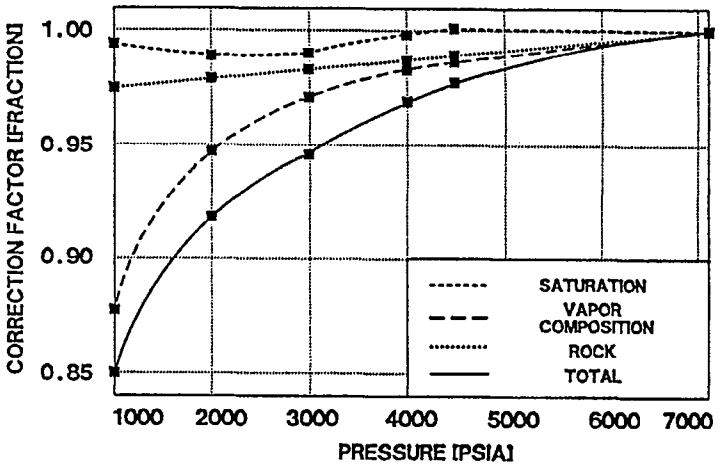

Fig. 4 – Effect of pressure on correction factors used to adjust calculated values of P/Z for condensation and vaporization.

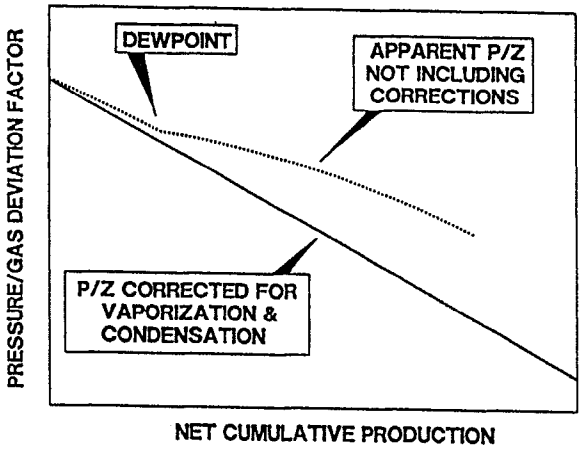

Fig. 5 – Effect of vaporization and condensation on a P/Z plot.

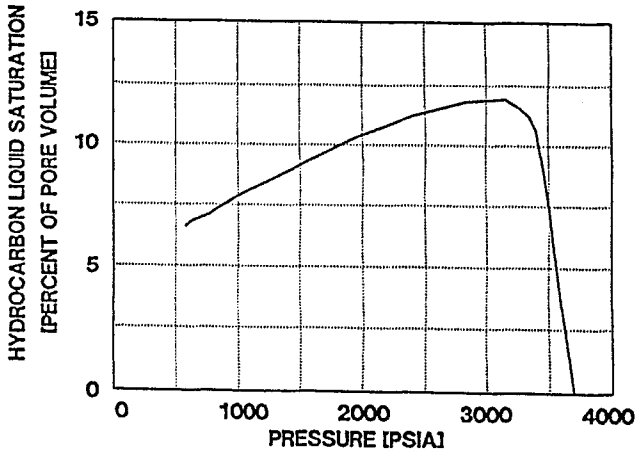

Fig. 6 – Volumes of hydrocarbon liquids condensed as a function of pressure (After Reference 6).

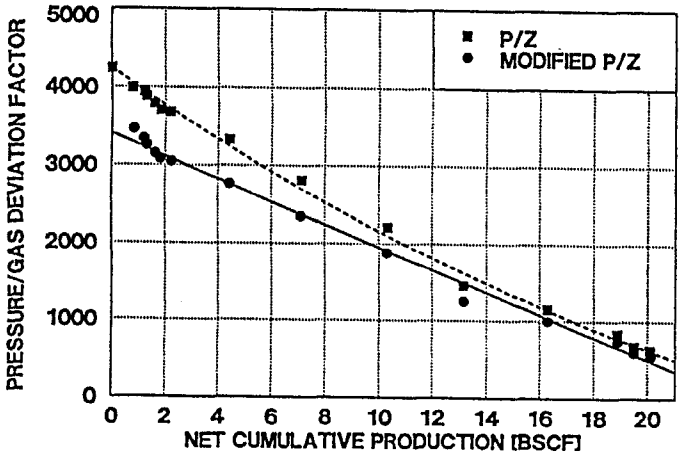

Fig. 7 – Effect of correcting for hydrocarbon condensation on a P/Z plot (Data from Reference 6).

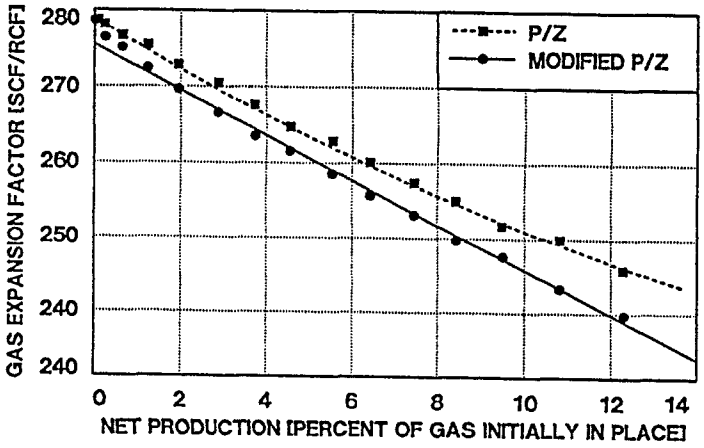

Fig. 8 – Effect of correcting for water vaporization and hydrocarbon condensation on a P/Z plot.

Application of a General Material Balance for High-Pressure Gas Reservoirs

Michael J. Fetkovich, SPE, Dave E. Reese, SPE, Phillips Petroleum Co., and C.H. Whitson, SPE, Norwegian U. of Science and Technology

Summary

This paper presents the derivation of a general gas material balance that has particular application to high-pressure gas reservoirs, [both normal pressured and overpressured (geopressured)]. Its main application is to calculate original gas in place and assist in calculating remaining recoverable reserves from pressure/production data.

The form of the material-balance equation is $(p/z)[1 - \bar{c}_e(p)(p_i - p)] = (p/z)_i(1 - G_p/G)$, which includes a pressure-dependent cumulative effective compressibility term $\bar{c}_e(p)$ that is defined in terms of the following reservoir parameters: pore compressibility, water compressibility, gas solubility, and total water associated with the gas reservoir volume. "Associated" water includes connate water, water within interbedded shales and nonpay reservoir rock, and any limited aquifer volume. $\bar{c}_e$ physically represents the cumulative change in hydrocarbon pore volume (PV) caused by compressibility effects and encroaching water.

High pressure gas reservoirs typically have concave downward p/z vs. G_p plots which may result in serious overestimation of original gas in place and remaining recoverable reserves. The proposed form of the gas material balance equation provides a method to linearize the p/z vs. G_p plot, and thereby predict the true original gas in place. A method is suggested to determine initial gas in place by analyzing the behavior of cumulative effective compressibility backcalculated from pressure/production data. The $\bar{c}_e(p)$ function determined by this procedure, or estimated from logs and geological maps when sufficient production data is not available, is then used to forecast pressure/cumulative behavior. Two field examples are provided showing the application of the material balance equation to high pressure gas reservoirs.

Introduction

High pressure gas reservoirs experiencing depletion drive typically have downward curving p/z vs. G_p behavior. Incorrect extrapolation of early depletion data may result in serious overestimation of original gas in place and remaining reserves.

Bruns *et al.*[1] work in 1965 was a result of a field study conducted on a large moderately overpressured gas reservoir in the Texas Gulf Coast area. Investments were made, and never needed, based on linear extrapolation of the early field p/z vs. G_p performance to an apparent original gas in place that was later found to be overstated by about 200 Bscf. Fig. 5 in Ref. 1 (Run 20) shows the concave downward curvature typical for the pressure response of a limited external aquifer system that simulated the reservoir's response.

This type of "limited" aquifer behavior, where pressure in the reservoir and aquifer are virtually equal, led to the derivation of a general material balance for high pressure gas reservoirs (see Appendix, Ref. 2). The derivation includes pressure-dependent rock and water compressibility (with gas evolving from solution). All water and rock volumes associated with the reservoir and available for expansion, including a limited aquifer volume, were included in a cumulative effective compressibility term $\bar{c}_e(p)$. Rock and water compressibilities were defined to account for cumulative changes in volume to be multiplied by the cumulative pressure drop $(p_i - p)$; instantaneous compressibilities are not used at all. The final form of the material balance is similar to that published by Ramagost and Farshad,[3] except that they considered $\bar{c}_e$ as a constant. The general gas material balance as presented in this paper defines a cumulative effective compressibility $\bar{c}_e(p)$ as a function of pressure.

Copyright 1998 Society of Petroleum Engineers

Original SPE manuscript received for review 11 March 1997. Revised manuscript received 24 November 1997. Paper peer approved 9 December 1997. Paper (SPE 22921) first presented at the 1991 SPE Annual Technical Conference and Exhibition held in Dallas, 6-9 October.

Literature Review

Harville and Hawkins[4] and Hammerlindl[5] attribute the concave downward shape of p/z vs. G_p curves obtained in abnormally pressured gas reservoirs entirely to pore collapse and formation compaction. No definition of pore collapse is given in Ref. 4, but a plot of backcalculated PV change indicated a system compressibility change from 28×10^{-6} psi^{-1} at initial pressure to about 6×10^{-6} psi^{-1} at low pressures. This magnitude of PV change implies associated water volume. The decreasing "system" compressibility is expected for an overpressured reservoir with pressure-dependent PV compressibility, and based on results presented in this paper pore collapse is not a necessary condition for such behavior.

The Anderson "L" reservoir performance presented by Duggan[6] shows curved p/z vs. G_p field behavior which was primarily attributed to shale water influx with no evidence of reservoir pore compaction. The water influx drive mechanism was supported by the fact that several wells watered out. Wallace[7] also concluded that shale water influx is an important drive mechanism in abnormally pressured gas reservoirs. Bass[8] discounts shale water influx, and attributes curved p/z vs. G_p behavior to peripheral water influx from a limited aquifer and formation compaction treated with a constant PV compressibility c_f. For a limited aquifer, Bass defines a term F_p as the ratio of peripheral water PV to the PV of gas-bearing rock.

Roach[9] and Ramagost and Farshad[3] both use the term $p/z[1 - c_e(p_i - p)]$ for geopressured and abnormally pressured gas reservoirs. Both authors consider c_e a constant and they consider the Anderson "L" example.

Bernard[10] does not accept the rock collapse theory as the cause for overpressured p/z vs. G_p behavior, concluding that water influx is the basic drive mechanism. He also uses $p/z[1 - c(p_i - p)]$ where c is a "catch-all" term for treating the effects of rock and water compressibility, a small steady-state acting aquifer, and steady state shale water influx. He further states that the term c is almost impossible to quantify in terms of reservoir properties.

Begland and Whitehead,[11] Prasad and Rogers,[12] and Wang and Teasdale[13] all present studies of overpressured gas reservoirs based on computer models. Refs. 11 and 12 treat c_f and c_w as functions of pressure, including the effect of solution gas in the water. External water sources are also included in Refs. 12 and 13. The differential forms of the material balance used in these references correctly apply instantaneous compressibility in a history-matching approach to determine initial gas in place. A direct plot of $(p/z)[1 - \bar{c}_e(p_i - p)]$ vs. G_p was not made because the $\bar{c}_e$ term had not been defined.

Poston and Chen[14] analyzed several abnormally pressured gas reservoirs, and recognized that calculated values of $c_e > 30 \times 10^{-6}$ psi^{-1} required to linearize the material-balance plot reflected the influence of water influx.

Bourgoyne[15] demonstrates that reasonable values of shale permeability and compressibilities treated as a function of pressure can be used to match abnormal gas reservoir performance behavior. He points out, however, that determining k and c_f of the shale necessary for modeling this behavior is practically impossible.

Ambastha[16] uses Bourgoyne's general material-balance equation to develop a graphical matching technique based on a constant effective compressibility c_e. The example given in that paper shows a lack of uniqueness in determining initial gas in place.

General Material Balance

The general form of the gas material balance is

$$\frac{p}{z}[1-\bar{c}_e(p)(p_i-p)]=\left(\frac{p}{z}\right)_i-\frac{(p/z)_i}{G}\left[G_p-G_{inj}+W_pR_{sw}+\frac{5.615}{B_g}(W_pB_w-W_{inj}B_w-W_e)\right], \quad \ldots\ldots(1)$$

which reduces to

$$\frac{p}{z}[1-\bar{c}_e(p)(p_i-p)]=\frac{p}{z_i}-\left(\frac{p_i/z_i}{G}\right)G_p \quad \ldots\ldots(2)$$

when water terms and gas injection are neglected. The cumulative effective compressibility term $\bar{c}_e(p)$ is pressure-dependent, consisting of a cumulative PV compressibility $\bar{c}_f(p)$, cumulative total water compressibility $\bar{c}_{rw}(p)$, and the total pore and water volumes associated (i.e., in pressure communication) with the gas reservoir,

$$\bar{c}_e(p)=\frac{S_{wi}\bar{c}_{rw}(p)+\bar{c}_f(p)+M[\bar{c}_{rw}(p)+\bar{c}_f(p)]}{1-S_{wi}}. \quad \ldots\ldots(3)$$

The formation and total water compressibility terms $\bar{c}_f$ and $\bar{c}_{rw}$ account for cumulative changes in volume from initial pressure to the current pressure.

The interbedded nonpay volume and limited aquifer contributions to pressure support are quantified in terms of the M ratio,

$$M=\frac{V_{pNNP}+V_{pAQ}}{V_{pR}}. \quad \ldots\ldots(4)$$

An important aspect of the material balance for high-pressure gas reservoirs is that the gas in solution in the connate and associated water provide both pressure support and additional gas available for production. The level of pressure support provided by the evolved solution gas depends on the level of depletion, and it is shown that this support is significant below about 1,500 psia. The solution gas available for production also depends on the level of depletion, i.e., how much of the original solution gas has evolved $[R_{sw}(p_i) - R_{sw}(p)]$ and the quantity of this gas that is mobile.

The term G is used for the initial free gas in place, and it is this quantity that will be determined from the material balance plot given by Eq. 2 when extrapolated to $(p/z)[1-\bar{c}_e(p_i-p)]=0$. This condition is reached at a pressure when $1-\bar{c}_e(p)(p_i-p)=0$, and not when $p=0$, i.e., additional gas may be produced after G_p reaches original free gas in place G. At pressures where G_p exceeds G the corrected p/z term $(p/z)[1-\bar{c}_e(p_i-p)]$ becomes negative. If reservoir pressure could be brought to standard conditions ($p = p_{sc}$) the total gas would be G plus the total solution gas in place G_s, $(G+G_s)$.

The effect of connate water saturation S_{wi} and M are important to the magnitude of $\bar{c}_e$. With typical values of $\bar{c}_f = c_{fi} = 4\times10^{-6}$ psi^{-1} and $\bar{c}_{rw} = c_{wi} = 3\times10^{-6}$ psi^{-1} for a high-pressured gulf coast sandstone reservoir, the cumulative effective compressibility is initially $\bar{c}_e = 7.5\times10^{-6}$ psi^{-1} for $S_{wi}=35\%$ and $M=0$; and $\bar{c}_e = 15\times10^{-6}$ for $S_{wi}=35\%$ and $M=1$. Fig. 1 shows the percentage of true original free gas in place that would be overestimated by extrapolating early p/z vs. G_p data, indicating that the overestimation is greater for larger initial pressure and higher $\bar{c}_e$ values at initial conditions. For an initial pressure of 10,000 psia and a $\bar{c}_e = 10\times10^{-6}$ psi^{-1} the extrapolation of early data gives an estimate of G that is about 25% higher than the true original free gas in place. The sections below discuss the calculation of $\bar{c}_f(p)$ and $\bar{c}_{rw}(p)$ functions.

Cumulative PV Compressibility $\bar{c}_f$. The material balance presented in this paper uses a cumulative PV compressibility $\bar{c}_f$ defined as

$$\bar{c}_f(p)=\frac{1}{V_{pi}}\left[\frac{V_{pi}-V_p(p)}{p_i-p}\right]. \quad \ldots\ldots(5)$$

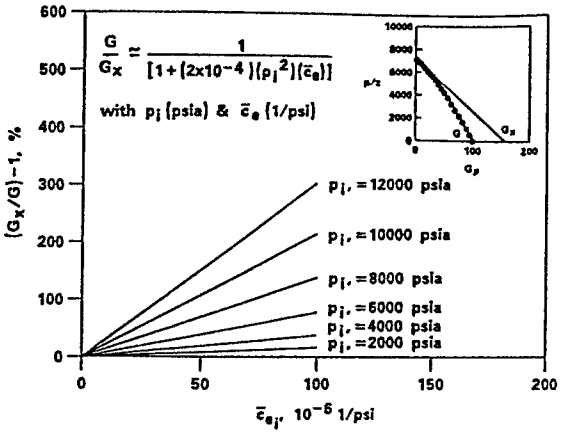

Fig. 1—Effect of p_i and $\bar{c}_e$ on overestimating G.

The term in brackets is the slope of the chord from the initial condition (p_i, V_{pi}) to any lower pressure (p, V_p), as shown in Fig. 2. This implies that $\bar{c}_f$ is a function of both pressure and the initial condition. The instantaneous PV compressibility c_f is defined as

$$c_f(p)=\frac{1}{V_p}\frac{\partial V_p}{\partial p} \quad \ldots\ldots(6)$$

and is only a function of pressure. At initial pressure the two PV compressibilities are equal: $\bar{c}_f(p_i) = c_f(p_i)$. The instantaneous compressibility function $c_f(p)$ should be used in reservoir simulation and differential forms of the material balance, while the cumulative compressibility function $\bar{c}_f(p)$ must be used with forms of the material balance that apply the cumulative pressure drop $(p_i - p)$, i.e., p/z vs. G_p plots.

The pressure dependence of $\bar{c}_f$ is best determined by special core analysis under appropriate reservoir conditions. Table 1 summarizes the calculation of $\bar{c}_f$ as a function of pressure using laboratory data for a gulf coast sandstone. Fig. 3 shows how c_f and $\bar{c}_f$ vary as a function of pressure for this overpressured reservoir rock.

In the absence of pore collapse $\bar{c}_f$ is always greater than or equal to c_f. The cumulative PV compressibility remains higher than the instantaneous compressibility because of an averaging effect that reduces the pressure dependence of $\bar{c}_f$ compared with c_f. An important consequence of this behavior is that a rock exhibiting large PV change because of a high level of overpressure will initially have and maintain a high cumulative compressibility $\bar{c}_f$ as shown in Fig. 3.

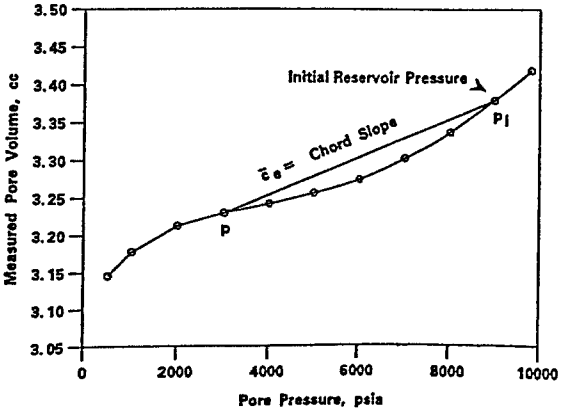

Fig. 2—Cumulative PV compressibility as a chord slope.

TABLE 1—CALCULATION OF PORE VOLUME COMPRESSIBILITY FROM LABORATORY DATA

Reported Laboratory Data					Calculations for p_i = 9,800 psia			
p_o (psia)	V_{p_o} (cm³)	V_{p_i} (cm³)	ϕ (%)	c_f	p (psia)	$p_i - p$ (psi)	$V_{pi} - V_p$ (cm³)	$\bar{c}_f$ Eq. 5
200.0	3.420	20.530	16.70	16.50	9,800	0	0.000	16.50
1,000.0	3.379	20.489	16.49	13.70	9,000	800	0.041	14.99
2,000.0	3.337	20.447	16.32	11.40	8,000	1,800	0.083	13.48
3,000.0	3.303	20.413	16.18	9.10	7,000	2,800	0.117	12.22
4,000.0	3.276	20.386	16.07	6.90	6,000	3,800	0.144	11.08
5,000.0	3.257	20.367	15.99	5.00	5,000	4,800	0.163	9.93
6,000.0	3.243	20.353	15.93	3.80	4,000	5,800	0.177	8.92
7,000.0	3.230	20.340	15.88	4.10	3,000	6,800	0.190	8.17
8,000.0	3.213	20.323	15.81	7.30	2,000	7,800	0.207	7.76
9,000.0	3.177	20.287	15.70	16.80	1,000	8,800	0.243	8.07
9,500.0	3.144	20.254	15.50	25.80	500	9,300	0.276	8.68

All compressibilities in 10^{-6} psi^{-1}.

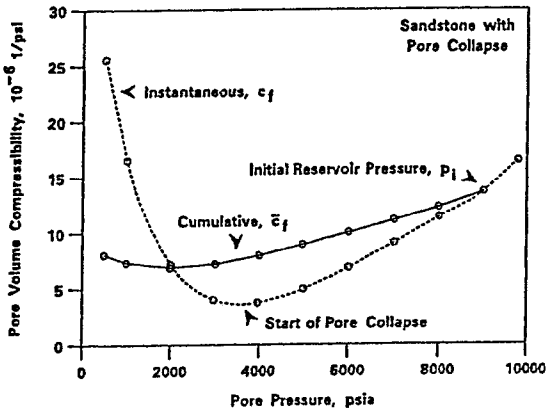

Fig. 3—Cumulative and instantaneous c_f vs. p for a sandstone with pore collapse.

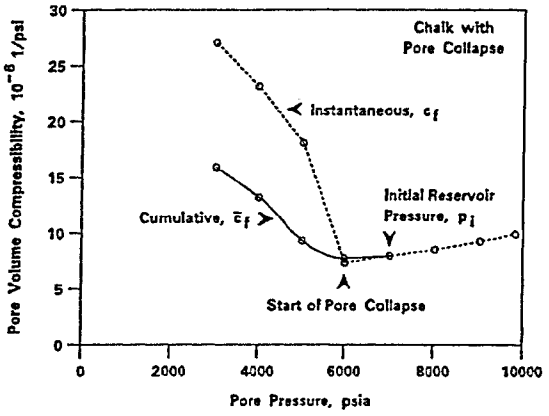

Fig. 4—Cumulative and instantaneous c_f vs. p for a chalk with pore collapse.

Pore collapse is defined as the condition when a rock's instantaneous PV compressibility starts to increase at decreasing reservoir pressure. Pore collapse provides greater pressure support when collapse occurs at a high pressure. However, pore collapse is not reflected by the $\bar{c}_f(p)$ function and will not therefore be seen on the p/z vs. G_p plot at the pressure when pore collapse occurs. In fact, pore collapse may not be identifiable at all on the cumulative compressibility term. For example, the gulf coast sandstone in Fig. 3 exhibits pore collapse at 4,000 psia (about 5,000 psi less than initial pressure p_i). Despite the increase in c_f from 4 to 25 × 10^{-6} psi^{-1} in the pressure range 4,000 to 1,000 psia, the change in $\bar{c}_f$ over the same pressure range is almost insignificant. Fig. 4 shows a North Sea chalk sample from a reservoir with initial pressure of 7,000 psia exhibiting pore collapse at 6,000 psia. Here the effect pore collapse is greater, causing $\bar{c}_f$ to increase from 6 to 20 × 10^{-6} psi^{-1} in the pressure range from 6,000 to 2,000 psia. In general, however, pore collapse in and of itself does not have a significant effect on the p/z vs. G_p plot.

In the absence of laboratory data, PV compressibilities can be estimated from correlations presented by Hall[17] and by Von Gonten and Choudhary.[18] Hall's correlation (his Fig. 2) gives instantaneous PV compressibility as a function of porosity, i.e., there is no pressure dependence. Von Gonten develops correlations for instantaneous PV compressibility c_f as a function of net overburden pressure (p_o), where p_o equals the overburden gradient times depth minus reservoir pressure.

Cumulative Total Water Compressibility $\bar{c}_{tw}$. The pressure support provided by water is made up of two components. First, the water expansion with decreasing pressure, and second, the release of solution gas and its expansion. The total or composite compressibility effect is expressed as

$$\bar{c}_{tw}(p) = \frac{1}{B_{tw}(p_i)} \frac{B_{tw}(p) - B_{tw}(p_i)}{p_i - p} \quad \ldots\ldots\ldots\ldots\ldots\ldots (7)$$

in terms of the total water formation volume factor B_{tw},

$$B_{tw}(p) = B_w(p) + \frac{[R_{swi} - R_{sw}(p)]B_g(p)}{5.615}. \quad \ldots\ldots\ldots\ldots\ldots (8)$$

Fig. 5 shows typical behavior for B_w and B_{tw} as a function of pressure; the figure also shows the behavior of $\bar{c}_{tw}(p)$ where it is seen that little increase occurs before a pressure of about 1,500 psia, and that, at pressures below 1,000 psia, there is a significant increase in $\bar{c}_{tw}$ with a limiting relationship $\bar{c}_{tw} \propto 1/p$ at low pressures,

$$\bar{c}_{tw}(p \to 0) \equiv \left[\frac{1}{5.615} \frac{Tp_{sc}}{T_{sc}} \frac{R_{swi}}{p_i B_{twi}}\right] \frac{1}{p} \quad \ldots\ldots\ldots\ldots\ldots (9)$$

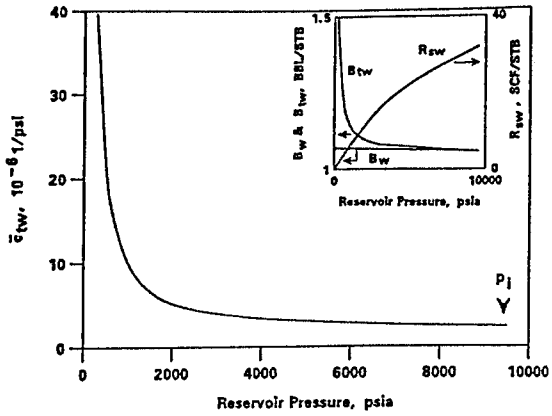

Fig. 5—Cumulative total water compressibility, $\bar{c}_{tw}$, vs. p.

Specifically at standard conditions (p_{sc}), $\bar{c}_{tw}$ is given by

$$\bar{c}_{tw}(p_{sc}) = \left[\frac{1}{5.615}\frac{T}{T_{sc}}\frac{R_{swi}}{p_i B_{wti}} - \frac{1}{p_i}\right]. \quad \ldots\ldots\ldots\ldots\ldots\ldots (10)$$

To calculate $\bar{c}_{tw}$, values of B_w, R_{sw}, and B_g are tabulated with pressure as shown in Table 2. These properties can be obtained from correlations at pressures less than about 10,000 psia and 300°F. At more extreme conditions of pressure and temperature, and for gases with high concentrations of nonhydrocarbons CO_2, N_2, and H_2S, we have used the Peng-Robinson[19] equation of state with volume translation and binary interaction coefficients that are dependent on both temperature and salinity.[20]

Another approach for high pressures is simply to extrapolate B_w linearly and R_{sw} with a flattening curvature toward a constant value. Nonhydrocarbons can be treated by evaluating R_{sw} of each component separately at its partial pressure, and summing the values for all soluble components,

$$[R_{sw}(p)]_{TOTAL} = \sum_j [R_{sw}(y_j p)], \quad \ldots\ldots\ldots\ldots\ldots\ldots (11)$$

where y_j is the reservoir gas mole fraction of Component j. Typically the only components with appreciable solubility are methane, CO_2, and H_2S.

TABLE 2—COMPARISON OF c_f FOR NORMAL PRESSURE AND OVERPRESSURED CONDITIONS

Sample	Initial Porosity (%)	Normal Pressure c_{fi} (psi^{-1})	Over-Pressured c_{fi} (psi^{-1})
Gulf coast sandstones			
Sample 1	13	4.8	6.4
Sample 2	20	4.4	16.5
North Sea chalk			
Sample 9 (pore collapse)	32	18.3	7.9
Sample 10 (pore collapse)	30	20.1	7.4
Von Gonten			
Sample 9A	11	3.0	6.0
Sample 4A	22	4.6	9.2
Sample 7A	26	5.9	7.2
Sample 3A	28	8.6	10.6
Sample 6A	25	7.8	8.6

Normal Pressured is 0.5 psi/ft × Depth; Overpressured is 0.8 psi/ft × Depth. Depth Used is 10,000 ft.

Associated Water Volume Ratio M. The total compressibility effect on the gas material balance depends on the magnitudes of rock and total water compressibilities and on the total pore and water volumes in pressure communication with the gas reservoir (including connate water and the PV within the net pay).

Associated water and PVs external to the net pay include nonnet pay (NNP) such as interbedded shales and dirty sands, plus external water volume found in limited aquifers. Including these water volumes in reservoir simulation is referred to as using a "gross" model. In the proposed material balance equations this associated volume is expressed as a ratio relative to the PV of the net pay reservoir,

$$M = M_{NNP} + M_{AQ}, \quad \ldots\ldots\ldots\ldots\ldots\ldots (12)$$

where

$$M_{NNP} = \frac{V_{pNNP}}{V_{pR}} \quad \ldots\ldots\ldots\ldots\ldots\ldots (13)$$

and

$$M_{AQ} = \frac{V_{pAQ}}{V_{pR}}. \quad \ldots\ldots\ldots\ldots\ldots\ldots (14)$$

In the simplest case when $M = 0$, there will be pressure support only from connate water and the net pay PV. This is equivalent in simulation to building a net model. The cumulative effective compressibility term $\bar{c}_e$ will then be expected to have values ranging from 7 to 15 × 10^{-6} psi^{-1} for normal-pressure reservoirs, where the larger values will generally result from high connate water saturation.

Net pay compressibility effects alone can cause noticeable curvature in the p/z vs. G_p plot with potential overestimation of initial free gas in place (G) (see Fig. 1).

M_{NNP}. The nonnet pay water volume ratio M_{NNP} comprises interbedded reservoir PV, including shales and poor quality rock, that are assumed to be completely filled with water. With this definition M_{NNP} can be written in terms of the net to gross ratio R_{NG} defined as

$$R_{NG} = \frac{h_R}{h_R + h_{NNP}} = \frac{h_R}{h_t}. \quad \ldots\ldots\ldots\ldots\ldots\ldots (15)$$

Accounting for different porosities in the net pay and nonnet pay M_{NNP} is given by

$$M_{NNP} = \frac{(\overline{\phi hA})_{NNP}}{(\overline{\phi hA})_R} = \frac{\phi_{NNP}}{\phi_R}\left(\frac{1 - R_{NG}}{R_{NG}}\right). \quad \ldots\ldots\ldots\ldots\ldots\ldots (16)$$

Properties and thicknesses of the net pay and nonnet pay are readily available from log analysis.

M_{AQ}. Aquifers with sufficient permeability and limited areal extent can be treated as part of the total cumulative compressibility term. The water volume ratio of the aquifer M_{AQ} can be determined using geological maps and well control to define areal extent, and electric logs to define the gas/water contact. In general, M_{AQ} is defined as

$$M_{AQ} = \frac{(\overline{\phi hA})_{AQ}}{(\overline{\phi hA})_R}, \quad \ldots\ldots\ldots\ldots\ldots\ldots (17)$$

and for a radial aquifer geometry quantified in terms of the aquifer to reservoir radius r_{AQ}/r_R, the aquifer volume ratio can be expressed

$$M_{AQ} = \frac{(\overline{\phi h})_{AQ}}{(\overline{\phi h})_R}\left[\left(\frac{r_{AQ}}{r_R}\right)^2 - 1\right]. \quad \ldots\ldots\ldots\ldots\ldots\ldots (18)$$

Bruns *et al.*[1] show that limited aquifers with r_{AQ}/r_R ratios up to 5 have the same p/z vs. G_p behavior for permeabilities 100 md and higher. This implies that the transient effects in the aquifer have

negligible effect on reservoir performance and the aquifer can be treated as part of the cumulative effective compressibility term. Values of M_{AQ} used in the definition of $\bar{c}_e$ may be as high as 25, $[M_{AQ} \sim (r_{AQ}/r_R)^2 - 1]$, in reservoirs with moderate permeability. With higher permeabilities, limited aquifers can include r_{AQ}/r_R ratios greater than 5 and still be treated as part of the cumulative effective compressibility term.

When the aquifer is sufficiently large and requires treatment with either superposition or the Schilthius infinite aquifer model, the $\bar{c}_e$ term should still be used, but it will only contain the effect of net pay and nonnet pay volumes; i.e., $M = M_{NNP}$.

Cumulative Effective Compressibility $\bar{c}_e$. Total cumulative effective compressibility represents all available pressure support from rock and water. The equation for $\bar{c}_e$ is

$$\bar{c}_e(p) = \frac{S_{wi}\bar{c}_{rw}(p) + \bar{c}_f(p) + M[\bar{c}_{rw}(p) + \bar{c}_f(p)]}{1 - S_{wi}} \quad \ldots\ldots\ldots (19)$$

For a specific reservoir a family of $\bar{c}_e(p)$ curves can be generated for several M values. These curves will have specific characteristics depending on the pressure dependence of rock and water compressibilities. The $\bar{c}_{rw}(p)$ curves are relatively constant at high pressure, increasing slightly as pressure decreases, then rising sharply at low pressure around 1,000 psia. Typically, a constant PV compressibility c_f can be assumed and the $\bar{c}_e(p)$ curves will then have the same character as the $\bar{c}_{rw}(p)$ curve. Fig. 6 illustrates an example of $\bar{c}_e(p)$ curves at various M ratios for a typical gulf coast reservoir with $p_i = 9{,}000$ psia, $T = 200°F$, $\gamma_g = 0.7$ (air = 1), and a constant $\bar{c}_f = 3.2 \times 10^{-6}$ psi^{-1}.

For overpressured reservoirs exhibiting a pressure-dependent $\bar{c}_f(p)$, the family of $\bar{c}_e(p)$ curves at high pressures will tend to decrease with depletion. In the absence of pore collapse $\bar{c}_f(p)$ decreases to a constant value at lower pressure and the $\bar{c}_e(p)$ curves at lower pressure are dominated by the increasing $\bar{c}_{rw}(p)$ function. If pore collapse occurs, but not early in depletion, the pore collapse is almost insignificant because the $\bar{c}_f(p)$ function does not start increasing until low pressures because it represents a cumulative PV change, and, when the $\bar{c}_f(p)$ function finally starts to increase it will be masked by the $\bar{c}_{rw}(p)$ function which is increasing as $1/p$. Fig. 7 illustrates this point for a gulf coast overpressured reservoir with $p_i = 9{,}000$ psia, $T = 300°F$, and $\gamma_g = 0.71$ (air = 1). Although pore collapse occurs at approximately 3,500 psia (Fig. 3), $\bar{c}_f$ does not start increasing until 2,000 psia. The increase is insignificant relative to the increase in $\bar{c}_{rw}(p)$ at lower pressures.

The next example is a North Sea chalk (Fig. 4) that shows pore collapse at a pressure only 1,000 psi below initial pressure of 7,000 psia. The $\bar{c}_f(p)$ function increases almost simultaneously with instantaneous c_f, and the effect of $\bar{c}_f(p)$ on $\bar{c}_e(p)$ is shown in Fig. 8. Although $\bar{c}_f(p)$ has an impact on $\bar{c}_e(p)$ at moderate and high pressures for this example, the $\bar{c}_{rw}(p)$ function still dominates the behavior of $\bar{c}_e(p)$ at pressures less than 1,500 psia.

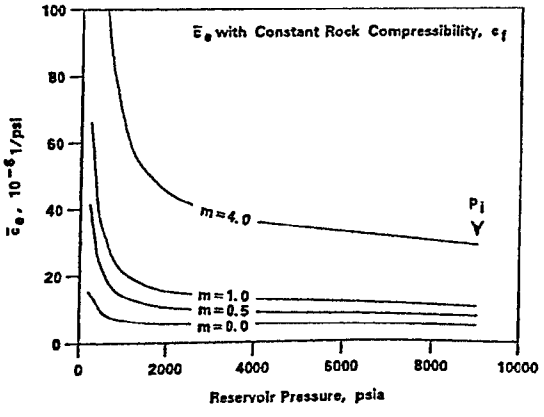

Fig. 6—Cumulative effective compressibility vs. p at various M ratios.

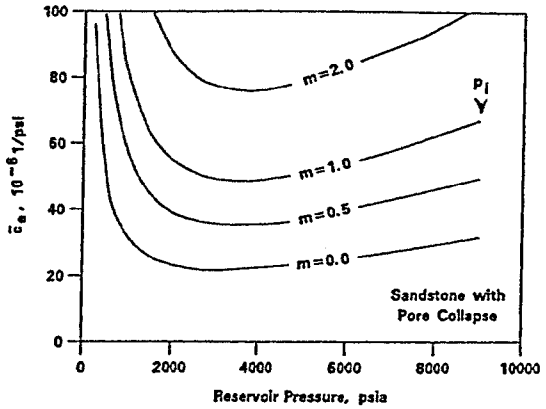

Fig. 7—Cumulative effective compressibility vs. p for a sandstone w/pore collapse.

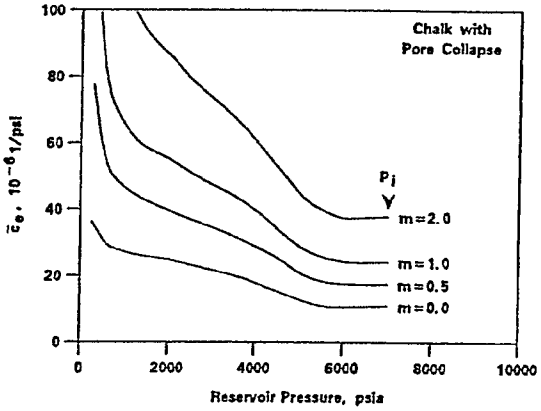

Fig. 8—Cumulative effective compressibility vs. p for a chalk w/pore collapse.

Estimating Gas-in-Place. A method is proposed for estimating the initial (free) gas in place G based on historical pressure/cumulative data. The procedure also determines the water volume ratio M and the $\bar{c}_e(p)$ function. First, a plot of p/z versus cumulative gas production G_p should have the characteristic concave downward shape of a high-pressure reservoir influenced by associated water and PV compressibility.

A range of values for G should then be assumed, with the largest value based on an extrapolation of the early depletion data, and the lowest value being somewhat larger than the current G_p. For an assumed value of G, calculate for each measured p/z and G_p data the $\bar{c}_e$ value from the rearranged material balance, Eq. 2,

$$(\bar{c}_e)_{\text{backcalculated}} = \left[1 - \frac{(p/z)_i}{(p/z)}\left(1 - \frac{G_p}{G}\right)\right]\frac{1}{(p_i - p)} \quad \ldots\ldots\ldots (20)$$

At this point, a plot can be made of backcalculated $\bar{c}_e$ as a function of pressure given the assumed G. Using reservoir rock and water properties, a family of $\bar{c}_e(p)$ curves at various M values can be generated independently to match against the backcalculated $\bar{c}_e$ values. The data should honor the shape and magnitude of one $\bar{c}_e(p)$ curve, where this match yields G, the M value, and a $\bar{c}_e(p)$ function that can be used to forecast future p/z vs. G_p behavior. This procedure gives a sound physical significance to the estimation of G as opposed to a pure statistical best fit that may lead to unrealistic

solutions. The Field Examples section discusses criteria for matching field data, and the expected behavior of $\bar{c}_e(p)$.

Characteristics of p/z vs. G_p Plots for High-Pressure Reservoirs

PV reduction, water expansion, and solution gas evolution, expressed in terms of $\bar{c}_e(p)$ in the general material balance equation, provide pressure support for all reservoirs during depletion. The reservoir does not have to be overpressured or geopressured. The term $\bar{c}_e(p)(p_i - p)$ determines whether the conventional p/z vs. G_p plot yields a straight line. For most low-pressure reservoirs this term is small and is often neglected because a straight-line p/z vs. G_p plot is obtained. Reservoirs undergoing depletion with initial pressure exceeding 5,000 psia are automatically candidates for being treated with the complete material balance equation.

Fig. 9 presents three generated p/z vs. G_p curves for a gulf coast overpressured sandstone reservoir using $M = 0$ (i.e., $\bar{c}_e(p) = [\bar{c}_f(p) + S_{wi}\bar{c}_{rw}(p)]/(1 - S_{wi})$. Curve A accounts for PV reduction, including pore collapse at about 4,000 psia. Curve B uses the same $\bar{c}_f(p)$ function as Curve A down to 4,000 psia (where pore collapse occurs) and thereafter uses a constant instantaneous compressibility of 4×10^{-6} psi^{-1}. Plots of p/z vs. G_p for A and B are almost identical, showing only a slight separation at pressures less than 3,500 psia. This clearly shows the limited effect of pore collapse on the p/z vs. G_p plot when collapse occurs late in depletion. Curve C assumes that the initial PV compressibility of 13×10^{-6} psi^{-1} remains constant throughout depletion. The difference between the two p/z vs. G_p Curves A and C is a result of the actual decrease in PV compressibility. Including an external water volume quantified with $M = 2$ produces more curvature in the p/z vs. G_p plots, but the separation between curves with and without pore collapse is still very small (not shown).

Another example relates to a North Sea chalk reservoir where pore collapse occurs just below initial pressure. Fig. 10 presents generated p/z vs. G_p plots for $M = 0$ with pore collapse (Curve A) and with no pore collapse (Curve B). The effect of pore collapse is more significant than in the previous example because it occurs at a relatively high pressure.

Field Examples

Ellenburger Gas Reservoir. This field example is for a normal pressured (0.5 psi/ft) 1,600-ft-thick, dry gas reservoir with initial reservoir pressure of 6,675 psia at 200°F. Average porosity is about 5% with connate water saturation in the pay of about 35%. Permeability is high because of an extensive microfracture system that results in a high degree of interwell pressure communication and almost instantaneous pressure buildup to static conditions. Initial CO_2 concentration was about 28 mol%, and a gradual increase in CO_2 concentration to 31 mol% at the present time has been

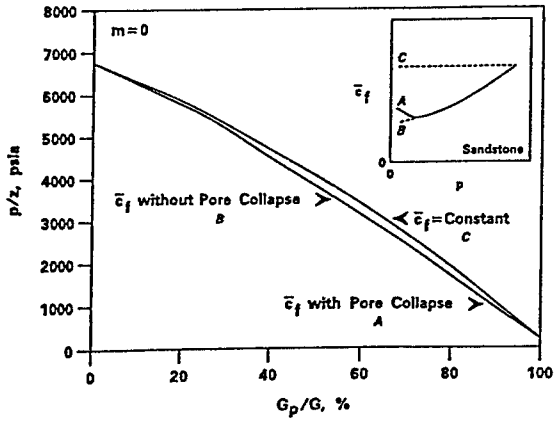

Fig. 9—Effect on p/z vs. G_p with and without pore collapse, sandstone.

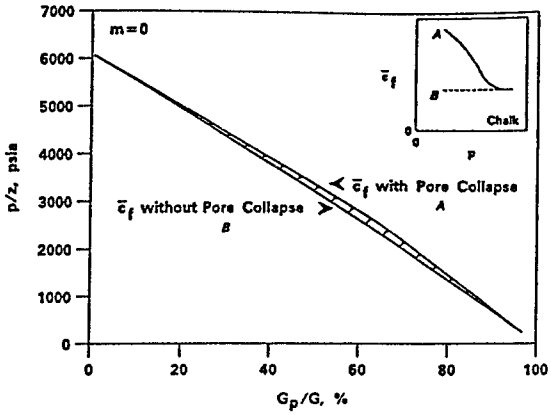

Fig. 10—Effect on p/z vs. G_p with and without pore collapse, chalk.

observed. The reservoir has produced about 3.1 Tscf, and currently has an average fieldwide bottomhole pressure of approximately 1,000 psia. The p/z vs. G_p plot shows a characteristic concave downward behavior, with an initial gas in place estimate of more than 4.4 Tscf using early data (Fig. 11). The p/z vs. G_p data at low pressures has started flattening.

The procedure outlined earlier for determining initial free gas in place G was used for this reservoir. Fig. 12 shows a plot of backcalculated $\bar{c}_e$ vs. pressure for a range of G from 3.0 Tscf to 3.6 Tscf. Another plot of $\bar{c}_e(p)$ was generated independently from rock and fluid properties by use of an equation of state for several values of M with $S_{wi} = 0.35$, $\bar{c}_f = 6.5 \times 10^{-6}$ psi^{-1} (from Hall[17]), and $\bar{c}_{rw}(p)$. Fig. 13 shows the best-fit of data on the $\bar{c}_e(p)$ curve for $M = 3.3$, corresponding to an initial free gas in place $G = 3.15$ Tscf.

The total water volume including connate and associated waters is given by

$$W = \frac{1}{5.615}\frac{GB_{gi}}{B_{twi}}\frac{(S_{wi} + M)}{(1 - S_{wi})}, \quad \ldots\ldots\ldots\ldots\ldots\ldots\ldots\ldots\ldots\ldots (21)$$

which yields 8.45(10^9) STB. The initial solution gas in place G_s is equal to W times the initial solution gas/water ratio R_{swi},

$$G_s = WR_{swi}. \quad \ldots\ldots\ldots\ldots\ldots\ldots\ldots\ldots\ldots\ldots\ldots\ldots\ldots\ldots (22)$$

Because of the high CO_2 concentration in this reservoir, the solution gas/water ratio (R_{swi} = 67.5 scf/STB) is about three times larger than for hydrocarbon gas systems. This yields a solution gas in place of $G_s = 0.55$ Tscf and a total initial gas in place of $G + G_s = 3.70$ Tscf. Fig. 11 shows the p/z vs. G_p forecast using the M value determined from the match to calculate the $\bar{c}_e(p)$ function from S_{wi}, M, $\bar{c}_f$, and $\bar{c}_{rw}(p)$. Also shown on this figure is the plot of $(p/z)[1 -$

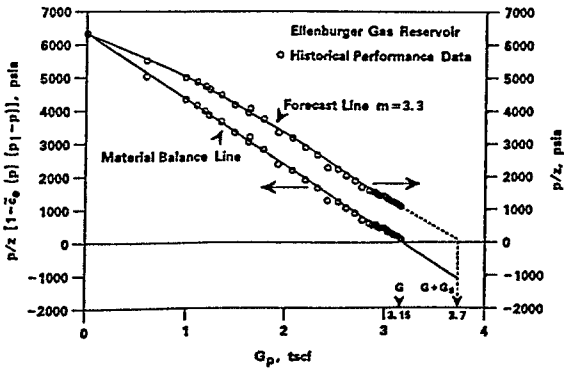

Fig. 11—Pressure vs. cumulative production, Ellenburger gas reservoir.

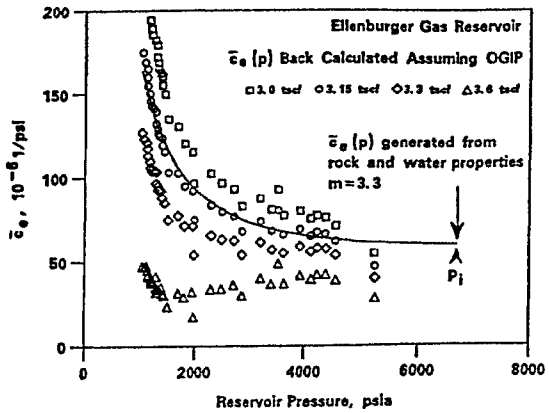

Fig. 12—Backcalculated $\bar{c}_e$ vs. p at various original gas in place (OGIP) values, Ellenburger gas reservoir.

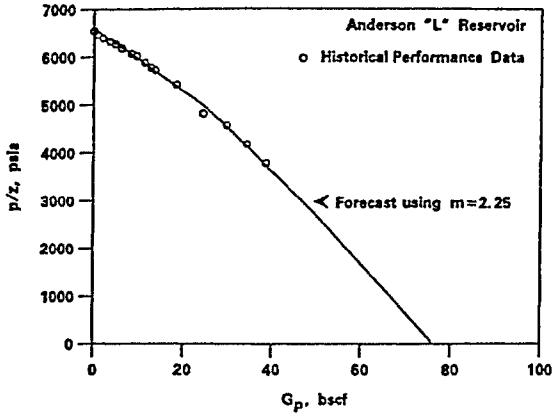

Fig. 14—p/z vs. cumulative production, Anderson "L" reservoir.

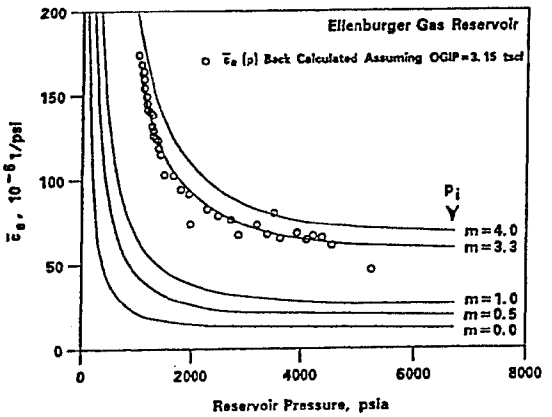

Fig. 13—Matching backcalculated $\bar{c}_e$ to generated $\bar{c}_e$ curves, Ellenburger gas reservoir.

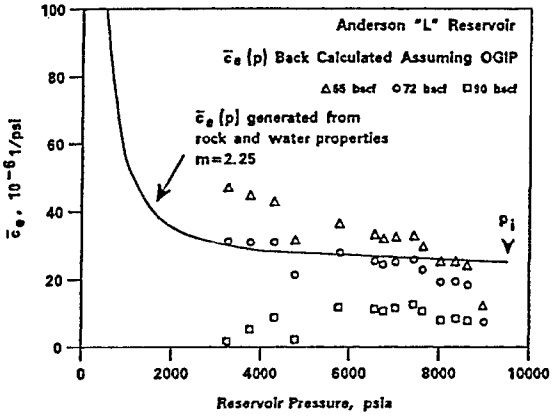

Fig. 15—Backcalculated $\bar{c}_e$ vs. p at various OGIP, Anderson "L" reservoir.

$\bar{c}_e(p)(p_i - p)$] vs. G_p for historical performance data and for the forecast, where it is seen that the current cumulative gas produced equals the original free gas in place.

The associated water volume given by $M = 3.3$ consists of nonnet pay and an external limited aquifer. Log analysis indicates a net-to-gross ratio $R_{NG} = 0.5$, $\phi_R = 0.05$, and $\phi_{NNP} = 0.03$, yielding $M_{NNP} = 0.6$. External water is known to exist but has not been mapped because of lack of well control. The calculated aquifer water volume ratio $M_{AQ} = 2.7$ (3.3 − 0.6), or an equivalent $r_{AQ}/r_R = 1.9$, seems reasonable for a limited aquifer.

Anderson "L". This reservoir has been studied by several authors and it is perhaps the best recognized example of a high-pressure gas reservoir with concave downward $p/z - G_p$ behavior (Fig. 14). The reservoir was abandoned after producing 55 Bscf, but pressure tests of public record were discontinued after 40 Bscf had been produced.

Different analyses by other authors have indicated original free gas in place between 65 to 75 Bscf. Fig. 15 shows backcalculated $\bar{c}_e$ vs. pressure for values of G equal to 65, 72, and 90 Bscf. The 72 Bscf volume is chosen based on a best-fit match with the $\bar{c}_e(p)$ function calculated using $M = 2.25$, $S_{wi} = 0.35$, $\bar{c}_f = 3.2 \times 10^{-6}$ psi^{-1}, and a $\bar{c}_{nw}(p)$ function from equation of state results. Although the first four data do not fall on the slightly increasing $\bar{c}_e(p)$ curve, data at pressures below this value do follow the trend down to the last pressure datum near 3,000 psia.

The 90 Bscf estimate produces unrealistically low $\bar{c}_e$ values, lower than would be calculated using the net reservoir PV and connate water compressibilities. The lowest estimate of 65 Bscf gives a shape for $\bar{c}_e(p)$ that cannot be accounted for using normal $\bar{c}_f(p)$ and $\bar{c}_{nw}(p)$ functions.

The forecasted p/z vs. G_p performance (Fig. 14) is calculated with the match determined above. Total gas in place of is 76 Bscf, which includes 72 Bscf of original free gas plus 4 Bscf of solution gas.

Conclusions

1. A general form of the material balance equation for gas reservoirs has been presented. This equation has particular application to high-pressure reservoirs. A cumulative effective compressibility term $\bar{c}_e(p)$ has been defined in terms of pressure-dependent PV and total water cumulative compressibilities, $\bar{c}_f(p)$ and $\bar{c}_{nw}(p)$, and the total volume of water associated with the net pay reservoir expressed as a ratio M.

2. The general material balance equation applies to all high-pressure reservoirs, both normal pressured and abnormally pressured (overpressured and geopressured).

3. The effect of a limited aquifer can be included as part of the M term for most depletion-type reservoirs. Using the water volume ratio M in the cumulative effective compressibility term, together with normal values of $\bar{c}_f$ and $\bar{c}_{nw}$, explains the "large" $\bar{c}_e$ values commonly reported for high-pressure gas reservoirs when linearizing the material balance equation. In fact, large values of $\bar{c}_e$ backcalculated from field performance data indicate that associated water influx is a dominant drive mechanism.

4. Only cumulative compressibilities ($\bar{c}_f$ and $\bar{c}_{nw}$) can be used in the general gas material balance equation because they are applied

against the cumulative pressure drop ($p_i - p$) in p/z vs. G_p plots. A method is given for calculating cumulative total water and PV compressibility $\bar{c}_{tw}(p)$ and $\bar{c}_f(p)$.

5. A method is proposed for estimating the original free gas in place from production data. This method uses backcalculated cumulative effective compressibility $\bar{c}_e$ which is plotted against pressure and compared with expected $\bar{c}_e(p)$ behavior calculated solely from rock and water properties for a range of values of the associated water volume ratio M.

6. Pore collapse, in and of itself, does not contribute significantly to pressure support in overpressured gas reservoirs. In fact, pore collapse has little effect unless it occurs early in depletion at a relatively high pressure. The effect of pore collapse, if present, is a positive effect and tends to flatten the p/z vs. G_p curve, not bending the curve downward as has been implied by others.

7. Gas found initially in solution in the connate and associated water is an important component of pressure support late in depletion (below 1500 psia) and may contribute additional producible volumes of gas. Typically, the solution gas in place G_s represents 2 to 10% of the original free gas in place, the value depending primarily on total water volume $(M + S_{wi})/(1 - S_{wi})$ and the initial solution gas/water ratio R_{sw_i}. Gas reservoirs with high CO_2 concentration (>20 mol%) can have even higher solution gas in place, G_s.

Nomenclature

A = area, ft^2 [m^2]
B = formation volume factor, reservoir per standard volume
c = instantaneous compressibility, 1/psi [1/kPa]
$\bar{c}$ = cumulative compressibility, 1/psi [1/kPa]
G = original free gas-in-place, Bscf [std m^3]
G_p = cumulative gas production, Bscf [std m^3]
G_s = initial solution gas in place, Bscf [std m^3]
G_x = early overestimate of G, Bscf [std m^3]
G_{inj} = cumulative gas injection, Bscf [std^3]
h = thickness, ft [m]
M = volume ratio, dimensionless
R_{NG} = net to gross ratio, dimensionless
p = reservoir pressure, psia [kPa]
p_i = initial reservoir pressure, psia [kPa]
p_o = net overburden pressure, psia [kPa]
r_R = radius of reservoir, ft [m]
r_{AQ} = radius of aquifer, ft [m]
R_{sw} = solution gas water ratio, scf/STB [std m^3/m^3]
S_{wi} = initial water saturation, fraction
T = reservoir temperature, °R [K]
V = volume, ft^3 [m^3]
V_p = PV, cm^3 and ft^3 [m^3]
V_b = bulk volume, cm^3 [m^3]
W = total water in place, bbl [m^3]
W_e = cumulative water influx, bbl [m^3]
W_{inj} = cumulative water injection, bbl [m^3]
W_p = cumulative water production, bbl [m^3]
z = gas compressibility factor, dimensionless
ϕ = porosity, fraction

Subscripts

A = associated water
AQ = limited aquifer
e = effective
f = PV ("formation")
g = gas
t = gross interval thickness
i = initial
inj = injection
NNP = nonnet pay
R = reservoir
sc = standard conditions
tw = total water
w = water

Acknowledgments

We thank the management of Phillips Petroleum Co. for permission to publish this paper. We also acknowledge Fred Kent for work done on the Ellenburger example.

References

1. Bruns, J.R., Fetkovich, M.J., and Meitzen, V.C.: "The Effect of Water Influx on p/z-Cumulative Gas Production Curves," *JPT* (March 1965) 287.
2. Fetkovich, M.J., Reese, D.E., and Whitson, C.H.: "Application of a General Material Balance for High-Pressure Gas Reservoirs," paper SPE 22921 presented at the 1991 SPE Annual Technical Conference and Exhibition, Dallas, 6–9 October.
3. Ramagost, B.P. and Farshad, F.F.: "p/z Abnormal Pressured Gas Reservoirs," paper SPE 10125 presented at the 1981 SPE Annual Technical Conference and Exhibition, San Antonio, Texas, 5–7 October.
4. Harville, D.W. and Hawkins, M.F. Jr.: "Rock Compressibility and Failure as Reservoir Mechanisms in Geopressured Gas Reservoirs," *JPT* (December 1969) 1528.
5. Hammerlindl, D.J.: "Predicting Gas Reserves in Abnormally Pressured Reservoirs," paper SPE 3479 presented at the 1971 SPE Annual Meeting, New Orleans, 3–6 October.
6. Duggan, J.O.: "The Anderson "L"—An Abnormally Pressured Gas Reservoir in South Texas," *JPT* (February 1971) 132.
7. Wallace, W.E.: "Water Production From Abnormally Pressured Gas Reservoirs in Louisiana," *JPT* (August 1968) 969.
8. Bass, D.M.: "Analysis of Abnormally Pressured Gas Reservoirs With Partial Water Influx," paper SPE 3850 presented at the 1972 SPE Abnormal Subsurface Pressure Symposium, Baton Rouge, Louisiana, 15–16 May.
9. Roach, R.H.: "Analyzing Geopressured Reservoirs—A Material Balance Technique," paper SPE 9968 available from SPE, Richardson, Texas (August 1981).
10. Bernard, W.J.: "Gulf Coast Geopressured Gas Reservoirs: Drive Mechanism and Performance Prediction," paper SPE 14362 presented at the 1985 SPE Annual Technical Conference and Exhibition, Las Vegas, Nevada, 22–25 September.
11. Begland, T.F. and Whitehead, W.R.: "Depletion Performance of Volumetric High Pressured Gas Reservoirs," *SPERE* (August 1989) 279; *Trans.*, AIME, 287.
12. Prasad, R.K. and Rogers, L.A.: "Superpressured Gas Reservoirs: Case Studies and a Generalized Tank Model," paper SPE 16861 presented at the 1987 SPE Annual Technical Conference and Exhibition AIME, Dallas, 27–30 September.
13. Wang, B. and Teasdale, T.S.: "GASWAT-PC: A Microcomputer Program for Gas Material Balance With Water Influx," paper SPE 16484 presented at the 1987 SPE Petroleum Industry Applications of Microcomputers, Del Lago on Lake Conroe, Montgomery Texas, 23–26 June.
14. Poston, S.W. and Chen, H.Y.: "Case History Studies: Abnormal Pressured Gas Reservoirs," paper SPE 18857 presented at the 1989 SPE Productions Operations Symposium, Oklahoma City, Oklahoma, 13–14 March.
15. Bourgoyne, A.T. Jr.: "Shale Water as a Pressure Support Mechanism in Gas Reservoirs Having Abnormal Formation Pressure," *J. Pet. Sci.* (1990) 3, 305.
16. Ambastha, A.K.: "Analysis of Material Balance Equations for Gas Reservoirs," paper CIM/SPE 90-36 presented at the 1990 CIM/SPE International Technical Meeting, Calgary, Alberta, Canada, 10–13 June.
17. Hall, H.N.: "Compressibility of Reservoir Rocks," *Trans.*, AIME (1953) 198, 309.
18. Von Gonten, W.D. and Choudhary, B.K.: "The Effect of Pressure and Temperature on Pore-Volume Compressibility," paper SPE 2526 presented at the 1969 SPE Annual Meeting, Denver, Colorado, 28 September–1 October.
19. Peng, D.-Y. and Robinson, D.B.: "A New Two-Constant Equation of State," *Ind. Eng. Chem. Fund.* (1976) No. 1, 59.
20. Soreide, I. and Whitson, C.H.: "Peng-Robinson Predictions for Hydrocarbons, CO_2, and H_2S With Pure Water and NaCl Brine," *Fluid Phase Equilibria* (1992) 77, 217.

Appendix A—Derivation of General Gas Material Balance

The derivation that follows is based on the following assumptions:

1. Any pressure change caused by production or injection into the reservoir will be felt immediately throughout the total system including (a) *net pay reservoir* (R); (b) *nonnet pay* (NNP), including interbedded shales and poor quality rock assumed to be 100% water-saturated; and (c) *limited aquifer* (AQ), when present, also assumed to be water-saturated. The nonnet pay and aquifer volumes are referred to as "associated" water volumes and both contribute to water influx during depletion.
2. Simple modifications to the material balance equations can be made to generalize for nonnet pay that has an initial free gas saturation.
3. All water in the system is initially saturated with solution gas.

Practically, the assumption of equal pressure throughout the system is reasonable, and any transient effects caused by a large aquifer may be treated by a conventional water influx term (W_e) as shown below.

For the sake of brevity we have chosen to omit explicit reference to pressure dependence—i.e., $\bar{c}_e$, $\bar{c}_f$, and $\bar{c}_{tw}$ should actually read $\bar{c}_e(p)$, $\bar{c}_f(p)$, and $\bar{c}_{tw}(p)$.

Derivation. The volumetric balance at any pressure states that the total PV ($V_{pR} + V_{pA}$) equals the net reservoir PV occupied by gas and water ($V_{gR} + V_{wR}$) plus the associated (nonnet pay and aquifer) PV which also is occupied by gas and water ($V_{gA} + V_{wA}$):

$$(V_{pR} + V_{pA}) = (V_{gR} + V_{wR}) + (V_{gA} + V_{wA}). \quad \text{.....(A-1)}$$

The net-pay reservoir PV V_{pR} is given by the initial volume V_{pRi} less the change in PV ΔV_{pR},

$$V_{pR} = V_{pRi} - \Delta V_{pR}, \quad \text{.....(A-2)}$$

$$V_{pRi} = V_{gRi} + V_{wRi}, \quad \text{.....(A-3)}$$

$$V_{pRi} = GB_{gi} + \frac{GB_{gi}}{1 - S_{wi}} S_{wi},$$

and

$$\Delta V_{pR} = \frac{GB_{gi}}{1 - S_{wi}} \bar{c}_f(p_i - p); \quad \bar{c}_f = (\bar{c}_f)_R, \quad \text{.....(A-4)}$$

yielding

$$V_{pR} = GB_{gi} + \frac{GB_{gi}}{1 - S_{wi}} S_{wi} - \frac{GB_{gi}}{1 - S_{wi}} \bar{c}_f(p_i - p). \quad \text{.....(A-5)}$$

PV of the associated rock is given by the initial PV less the change in PV, i.e.,

$$V_{pA} = \frac{GB_{gi}}{1 - S_{wi}} M - \frac{GB_{gi}}{1 - S_{wi}} M\bar{c}_f(p_i - p). \quad \text{.....(A-6)}$$

The net reservoir gas volume is given by the sum of unproduced free gas, gas released from solution, and any injected gas,

$$V_{gR} = (V_{gR})^{\text{Unproduced}}_{\text{Free Gas}} + (V_{gR})^{\text{Released}}_{\text{From Solution}} + (V_{gR})_{\text{Injected}}, \quad \text{....(A-7)}$$

resulting in

$$V_{gR} = [G - (G_p - W_pR_{sw})]B_g + \frac{GB_{gi}}{1 - S_{wi}} \frac{S_{wi}}{B_{wi}} (R_{swi} - R_{sw}) \frac{B_g}{5.615} + G_{inj}B_g. \quad \text{.....(A-8)}$$

pressure/volume/temperature properties B_g and R_{sw} are evaluated at current reservoir pressure. Value G_p for a gas condensate is the wet gas volume calculated by adding separator gas to liquid condensate converted to an equivalent surface gas volume. Also, the two-phase Z-factor must be used to calculated B_g for gas condensate reservoirs. Strictly speaking the cumulative water production term W_p represents "free" water production and not the water condensed out of solution from the produced gas wellstream.

The gas volume in the associated PV is a function of the amount of gas that has come out of solution,

$$V_{gA} = \frac{GB_{gi}}{1 - S_{wi}} M \frac{1}{B_{wi}} (R_{swi} - R_{sw}) B_g \frac{1}{5.615}. \quad \text{.....(A-9)}$$

The water volume in the net-pay reservoir equals the unproduced initial water plus injected water plus water encroachment from an external aquifer,

$$V_{wR} = (V_{wR})_{\text{Unproduced}} + (V_{wR})_{\text{Injected}} + [(V_{wR})_{\text{Encroachment}}], \quad \text{.....(A-10)}$$

yielding

$$V_{wR} = \left(\frac{GB_{gi}}{1 - S_{wi}} \frac{S_{wi}}{B_{wi}} B_w - \frac{W_pB_w}{5.615} \right) + 5.615W_{inj}B_w + 5.615W_e. \quad \text{.....(A-11)}$$

The aquifer encroachment term W_e represents any external water volume that is not already included in the M term. Later in the derivation, we show the conditions required so that water encroachment (treated rigorously by the method of superposition) can be included as part of the M term used in the cumulative effective compressibility $\bar{c}_e$.

The water volume in the associated PV is given by simple expansion,

$$V_{wA} = \frac{GB_{gi}}{1 - S_{wi}} M \frac{1}{B_{wi}} B_w \quad \text{.....(A-12)}$$

Inserting the appropriate equations above in Eq. A-1, rearranging, and grouping terms yields,

$$G(B_g - B_{gi}) + \frac{GB_{gi}}{1 - S_{wi}} \left\{ S_{wi} \left[\frac{(B_w + ((R_{swi} - R_{sw})B_g)/5.615)}{B_{wi}} - \frac{B_{wi}}{B_{wi}} \right] + \bar{c}_f(p_i - p) + M \left[\frac{(B_w + ((R_{swi} - R_{sw})B_g)/5.615)}{B_{wi}} - \frac{B_{wi}}{B_{wi}} \right] + M\bar{c}_f(p_i - p) \right\} = (G_p - W_pR_{sw} - G_{inj})B_g + 5.615 \left(W_p - W_{inj} - \frac{W_e}{B_w} \right) B_w. \quad \text{.....(A-13)}$$

Defining the total water/gas formation volume factor B_{tw},

$$B_{tw} \equiv B_w + \frac{(R_{swi} - R_{sw})B_g}{5.615}. \quad \text{.....(A-14)}$$

Noting that $B_{twi} = B_{wi}$, and defining the cumulative total water/gas compressibility $\bar{c}_{tw}$,

$$\bar{c}_{tw} \equiv \frac{(B_{tw} - B_{twi})}{B_{twi}} \frac{1}{(p_i - p)} \quad \text{.....(A-15)}$$

Now, defining a cumulative effective compressibility $\bar{c}_e$,

$$\bar{c}_e \equiv \frac{S_{wi}\bar{c}_{tw} + \bar{c}_f + M(\bar{c}_{tw} + \bar{c}_f)}{1 - S_{wi}} \quad \text{.....(A-16)}$$

gives

$$G(B_g - B_{gi}) + GB_{gi}[\bar{c}_e(p_i - p)] = B_g\left[G_p - G_{inj} + W_pR_{sw} + \frac{5.615}{B_g}(W_pB_w - W_{inj}B_w - W_e)\right]. \quad \text{(A-17)}$$

Dividing through by GB_{gi} and expressing $B_g = (p_{sc}/T_{sc})(zT/p)$ gives the final form of the material balance

$$\frac{p}{z}[1 - \bar{c}_e(p_i - p)] = \left(\frac{p}{z}\right)_i\left\{1 - \frac{1}{G}\left[G_p - G_{inj} + W_pR_{sw} + \frac{5.615}{B_g}(W_pB_w - W_{inj}B_w - W_e)\right]\right\}. \quad \text{(A-18)}$$

The p/z vs. cumulative plot, including all terms, would consider $(p/z)[1 - \bar{c}_e(p_i - p)]$ vs. the entire production/injection/encroachment term Q

$$\frac{p}{z}[1 - \bar{c}_e(p_i - p)] = \left(\frac{p}{z}\right)_i - \frac{(p/z)_i}{G}Q, \quad \text{(A-19)}$$

with

$$Q = G_p - G_{inj} + W_pR_{sw} + \frac{5.615}{B_g}(W_pB_w - W_{inj}B_w - W_e), \quad \text{(A-20)}$$

where the intercept is given by $(p/z)_i$ and the slope equals $(p/z)_i/G$. Setting $G_{inj} = W_{inj} = W_p = W_e = 0$ gives the common form of the gas material balance,

$$\frac{p}{z}[1 - \bar{c}_e(p_i - p)] = \left(\frac{p}{z}\right)_i\left(1 - \frac{G_p}{G}\right). \quad \text{(A-21)}$$

Treating Limited Aquifers in $\bar{c}_e$ Term. The material balance thus far has considered any associated water volume expressed in terms of the M parameter. In fact M may include a limited aquifer with up to 25 times the reservoir PV for a system permeability greater than about 100 md, and even larger aquifer volumes for higher permeabilities. The condition that determines when a limited aquifer can be treated as part of the $\bar{c}_e$ term is outlined below. We start with the general material-balance equation including a water encroachment term W_e and a $\bar{c}_e$ term that considers only nonnet pay.

$$\frac{p}{z}[1 - \bar{c}_e(p_i - p)] = \left(\frac{p}{z}\right)_i\left(1 - \frac{G_p}{G} + 5.615\frac{W_e}{GB_g}\right) \quad \text{(A-22)}$$

and

$$\bar{c}_e = \frac{S_{wi}\bar{c}_w + \bar{c}_f + (V_{pNNP}/V_{pR})(\bar{c}_w + \bar{c}_f)}{1 - S_{wi}}. \quad \text{(A-23)}$$

The water encroachment term calculated by superposition is expressed,

$$W_e = B\sum_j Q_D(\Delta t_j)_D\Delta p_j, \quad \text{(A-24)}$$

where $Q_D(t_D)$ is the dimensionless cumulative influx given as a function of dimensionless time t_D and aquifer to reservoir radius $r_D = r_{AQ}/r_R$. Value Δp_j is given by $p_j - p_{j-1}$ (in the limit for small time steps), and $\Delta t_j = t - t_{j-1}$. Assuming that permeability is reasonably high and the ratio r_{AQ}/r_R is not too large, Q_D for the smallest time step will approach the limiting value Q_D^{∞}, and the summation can be closely approximated by

$$\sum_j Q_D(\Delta t_j)_D\Delta p_j \approx Q_D^{\infty}(p_i - p), \quad \text{(A-25)}$$

giving a simple expression for W_e that is independent of time and only dependent on reservoir pressure,

$$W_e = BQ_D^{\infty}(p_i - p); \quad W_e(\text{bbl}) \quad \text{(A-26)}$$

$$B = \frac{2\pi}{5.615}\phi r_R^2 h(\bar{c}_{tw} + \bar{c}_f),$$

$$Q_D^{\infty} = \frac{1}{2}\left[\left(\frac{r_{AQ}}{r_R}\right)^2 - 1\right]. \quad \text{(A-27)}$$

Expressing W_e in terms of aquifer PV V_{pAQ},

$$W_e = \pi(r_{AQ}^2 - r_R^2)\phi h(\bar{c}_{tw} + \bar{c}_f)(p_i - p);$$

and

$$W_e(\text{ft}^3) = V_{pAQ}(\bar{c}_{tw} + \bar{c}_f)(p_i - p). \quad \text{(A-28)}$$

The material-balance equation can then be written

$$\frac{p}{z}[1 - \bar{c}_e(p_i - p)] = \left(\frac{p}{z}\right)_i\left(1 - \frac{G_p}{G}\right) + \left(\frac{p}{z}\right)_i\frac{W_e}{GB_g}5.615 \quad \text{(A-29)}$$

and simplified in a form where the $\bar{c}_e$ term includes the aquifer contribution to pressure support,

$$\left(\frac{p}{z}\right)_i\frac{W_e}{GB_g} = \left(\frac{p}{z}\right)_i\frac{W_e}{G}\frac{T_{sc}}{P_{sc}T}\frac{p}{z} = \frac{p}{z}\frac{W_e}{GB_{gi}};$$

$$GB_{gi} = V_{pR}(1 - S_{wi}) = \frac{p}{z}\frac{V_{pAQ}(\bar{c}_{tw} + \bar{c}_f)(p_i - p)}{V_{pR}(1 - S_{wi})}. \quad \text{(A-30)}$$

Rearranging, we arrive at the general form of the material balance (without water production and gas/water injection terms):

$$\frac{p}{z}[1 - \bar{c}_e(p_i - p)] = \left(\frac{p}{z}\right)_i\left(1 - \frac{G_p}{G}\right), \quad \text{(A-31)}$$

where

$$\bar{c}_e = \frac{S_{wi}\bar{c}_w + \bar{c}_f + ((V_{pNNP}/V_{pR}) + (V_{pAQ}/V_{pR}))(\bar{c}_w + \bar{c}_f)}{1 - S_{wi}} \quad \text{(A-32)}$$

$$M \equiv \frac{V_{pNNP} + V_{pAQ}}{V_{pR}} = \frac{V_{pA}}{V_{pR}}, \quad \text{(A-33)}$$

and

$$\bar{c}_e = \frac{S_{wi}\bar{c}_{tw} + \bar{c}_f + M(\bar{c}_{tw} + \bar{c}_f)}{(1 - S_{wi})}. \quad \text{(A-34)}$$

SI Metric Conversion Factors

°F	(°F−32)/1.8	= °C
in.³	× 1.638 706 E+01	= cm³
ft³	× 2.831 685 E−02	= m³
psi	× 6.894 757 E+00	= kPa

SPEJ

Michael J. Fetkovich is a Phillips Fellow Emeritus in the Reservoir & Production Technology Branch, Research & Services Div. of Corporate Technology, Phillips Petroleum Co. in Bartlesville, Oklahoma. He holds a BS degree in petroleum and natural gas

engineering from the U. of Pittsburgh and a Dr.Ing. degree from the Norwegian Inst. of Technology. A Distinguished Member, Fetkovich received the 1993 Lester C. Uren Award and the 1989 Reservoir Engineering Award and served as Distinguished Lecturer during 1977–78. **David E. Reese** is a Senior Staff Associate Reservoir Engineer in Phillips' Reservoir & Production Technology Branch, Research & Services Div. of Corporate Technology, working in the areas of gas reservoir engineering, gas and gas-condensate simulation, and decline-curve analysis. He also teaches an industry short course on decline-curve analysis. Reese holds a BS degree in petroleum engineering and an MS degree in petroleum management, both from the U. of Kansas. A 1994–95 Distinguished Lecturer, he is currently serving on the Editorial Review Committee, Gas Reservoir Engineering Reprint Committee, and the Low Permeability Meeting Program Committee. He has served on the Gas Technology Symposium Program Committee, and Annual Meeting Technical committees. **Curtis H. Whitson** is Professor of petroleum engineering at the Norwegian U. of Science and Technology, Trondheim. He also consults, develops software, and teaches industry coursesthrough his own company, Pera A/S. Whitson holds a BS degree in petroleum engineering from Stanford U. and a Dr.techn. degree from Norwegian Inst. of Technology. Coauthor of the book *Well Performance* and of the SPE monograph *Phase Behavior*, he also served on the Editorial Review Committee and on the Reservoir Simulation Symposium Program Committee.


Fetkovich


Reese


Whitson